FORENSICASIA

THE ASIAN FORENSIC SCIENCES NETWORK NEWSLETTER | ISSUE 16 | OCTOBER 2026

Celebrating Our Community, Shaping Our Future

FROM THE AFSN PRESIDENT

Every milestone achieved by the Asian Forensic Sciences Network (AFSN) is, above all, a reflection of its people. It is through the dedication of our member institutes, the generosity of our volunteers, and the unwavering commitment of forensic professionals across Asia that our network continues to grow and thrive. As we celebrate our achievements, we also look ahead with confidence, embracing new opportunities to strengthen collaboration and shape the future of forensic science.

I would like to take this opportunity to give a special tribute to Dr Lui Chi Pang of HSA, Singapore for his unwavering dedication, exceptional vision, and professionalism in transforming ForensicAsia into a respected platform for sharing scientific knowledge, highlighting the achievements of our member institutes, and strengthening communication across the AFSN community since 2018. Under his leadership, ForensicAsia has continued to grow in both quality and influence, marked by initiatives such as the introduction of the Best Paper Award and a valuable collaboration with the Forensic Science and Technology journal. His legacy will continue to inspire future generations, and we wish him every success, good health, and fulfilment in his well-deserved retirement.

"Our greatest strength lies not in numbers alone, but in the collective expertise, dedication, and spirit of collaboration that unite us across Asia"

This year has been one of meaningful milestones for the Asian Forensic Sciences Network (AFSN). As we celebrate our growing community of 90 member institutes, we are reminded that our greatest strength lies not in numbers alone, but in the collective expertise, dedication, and spirit of collaboration that unite us across Asia.

The success of AFSN has always been driven by its people. I extend my sincere appreciation to our Board Members, Working Group Chairs and Vice Chairs, the Secretariat, and all representatives from our member institutes whose dedication, expertise, and willingness to share knowledge continue to shape our organisation. Your contributions have enabled AFSN to flourish as a respected regional network that promotes scientific excellence, professional development, and meaningful collaboration across borders.



As our community continues to grow, it is equally important that we recognise those whose exceptional service has helped build the foundation of AFSN. Our commitment to recognising excellence is reflected in the introduction of the AFSN Distinguished Service Award, honouring individuals whose outstanding service has shaped the growth and success of our network. At the same time, the establishment of the Artificial Intelligence Committee marks an exciting step forward as we embrace emerging technologies and prepare our community for the evolving landscape of forensic science. Together, these initiatives reflect AFSN's commitment to honouring our achievements while investing in our future.

I warmly invite all members to join us at the AFSN Annual Meeting and Symposium in Xiamen, China, from 2-6 November 2026. Our annual gathering provides an invaluable opportunity to strengthen partnerships, exchange ideas, and

Ts. ChM. Nor Aidora Saedon, President, Asian Forensic Sciences Network

explore innovations that will continue to advance forensic science throughout the region. I look forward to welcoming many of you there.

As you turn the pages of this edition, I hope you will find guidance in the articles, insights, and accomplishments shared by our colleagues throughout the region. Together, they remind us that while our expertise may span many disciplines and our institutes may be separated by geography, we are united by a common purpose that is to advance forensic science in the pursuit of truth and justice.

The President

FROM THE EDITOR

Welcome to the 16th issue of ForensicAsia, a newsletter that brings AFSN news and technical content together in one place.

ForensicAsia exists for the forensic science community in Asia to stay connected. As the field continues to evolve rapidly with new technology and techniques, our annual meetings, together with this publication, helps us grow together as practitioners and keep forensic science moving forward.

This issue curates a selection of current forensic science practices and real-world casework. Technical papers explore advances in the field and workflow automation in sperm detection, gunshot residue analysis, urine testing, and DNA analysis. Other articles cover methodological development in toxicology and drug analysis, including quality control and isotope-based approaches to drug quantitation. The case studies highlight emerging drug trends, unusual concealment methods, and a regional cyanide mass poisoning incident.

My heartfelt thanks go to authors who contributed to the issue, as well as guest editors and the editorial team for their dedicated review of each submission. I would like to acknowledge and extend special thanks to our former Editor, Dr Lui Chi Pang, for his dedication and outstanding work he had done in leading the editorial team for the past nine years.

Finally, I would like to thank you for being part of this community. This community exists because of your individual participation and collective collaboration. I hope you find this issue – and its refreshed look, engaging and inspiring.

Lim Thiam Bon
Editor

EDITORIAL CONTRIBUTION

Editorial Advisors:
Ts. ChM. Nor Aidora Saedon
Department of Chemistry
Malaysia

Dr Weerakit Harnpaniphan
Central Institute of Forensic Science
Thailand

Dr Angeline Yap
Health Sciences Authority
Singapore

Editor:
Mr Lim Thiam Bon
Health Sciences Authority
Singapore

Guest Editors:
Prof Jose A Lorente
University of Granada
Spain

Prof Alastair Ross
Monash University
Australia

Dr Barbara Remberg
International Narcotics Control Board Secretariat (SINCB)

Dr Vanitha Kunalan
Department of Chemistry
Malaysia

Mr PG Mohd Helmy Bin PG Haji Rabaha
Department of Scientific Services
Brunei Darussalam

Dr Guo Hongling
Dr Ren Xin Xin
Dr Wang Chong
Mr Zhang Guangfeng
Institute of Forensic Science
China

Ms Lee Kang Hua
Ms Leong Wai Ying
Mr Liu Jing
Dr Lui Chi Pang
Dr Ong Mei Ching
Mr Phua Zai Rong
Dr Thong Zhonghui
Dr Xie Huifang
Dr Yao Yi Ju
Health Sciences Authority
Singapore

Editorial Assistants:
Ms Belinda Chiam
Ms Grace Law
Ms Kwang Jia Yi
Ms Lau Yen Hui
Ms Nadia Wong
Ms Tan Joo Chin
Health Sciences Authority
Singapore

For enquiries, feedback or contribution of articles, please email to AFSN_ForensicAsia@hsa.gov.sg.

IN THIS ISSUE

Members' News

4 UP DNA Analysis Laboratory: 30 Years of Science in the Service of Society

6 A New Virtual Anatomy Center in Suzhou Public Security Bureau: Transforming Forensic Investigations

7 Development of Forensic Science Capacity at LPC-PCIC, Timor-Leste: Challenges, Routine Casework Experience, and Pathway Towards ISO/IEC 17025

9 Maintaining Forensic Quality Standards in Sri Lanka: Experiences of the Government Analyst's Department in Implementing ISO/IEC 17025:2017

New AFSN Member

11 Advancing Public Safety Through Science: An Introduction to the Police Advanced Institute of Science and Technology (PAIST), Korean National Police University

International Scene

12 From Camp Crame to the World

Technical Paper

DNA

14 Generating Investigative Leads from Forensic DNA Data: Mapping Y-STR Profiles to Ancestral Haplogroups

18 Optimization of Sperm Separation Parameters in Differential Extraction Using the EZ2 DNA Investigator Sep&Prep Kit

22 Enhancing Forensic Sperm Detection Using Motorized Microscope and Deep Learning Improving Accuracy and Efficiency Through Automated Imaging and Neural Network Optimization

25 Streamlining Forensic DNA Analysis: A Strategic Approach to Laboratory Automation

29 Frequency of Y-Chromosomal Short Tandem Repeats in the Sri Lankan Population Using PowerPlex® Y23 System

Illicit Drugs

32 Evaluation of Carbon-13 Isotope for Mitigating Detector Saturation in Quantitation of Methamphetamine, MDMA and Ketamine in Hair

36 Application of Fortified Hair as Quality Control Sample in Multi-drug Analysis

Criminalistics

40 Optimization and Stability Assessment of SEM-EDS Parameters for High-Throughput Automated iGSR Analysis

43 Simplified Urine Detection Workflow for Stained Fabrics

Case Study

DNA

47 A Rare Case of Heteropaternal Superfecundation: A Case Study from Sri Lanka

49 The Protection of Children from Sexual Offences (POCSO) Act and the Case Scenario in Forensic Science Laboratory, Delhi, India

Illicit Drugs

52 Uncovering MDMB-4en-PINACA in "Tuklaw" Cigarette Sticks: Evidence of Synthetic Cannabinoid Adulteration

56 Persistence of MDMB-4en-PINACA in Indonesia's Illicit Drug Market: Evidence of Continued Supply and Local Synthesis from MDMB-INACA

60 Forensic Profiling of Synthetic Drugs in the Republic of Uzbekistan

63 Cocaine Trafficking Using Counterfeit Coffee Beans: A Case Study from Hong Kong

Toxicology

65 Acute Cyanide Poisoning in Multiple Related and Unrelated Victims: A Seven-Case Forensic Report from Sri Lanka

AFSN Member Institution

68 Listing of AFSN Member Institutes (As of September 2026)

UP DNA Analysis Laboratory: 30 Years of Science in the Service of Society

Maria Corazon A. De Ungria
DNA Analysis Laboratory, University of the Philippines Diliman Quezon City, Philippines
Email: madeungria@up.edu.ph

Quezon City, Philippines - 8 June 2026 - The DNA Analysis Laboratory (DAL) of the Natural Sciences Research Institute (NSRI), University of the Philippines, Diliman, celebrates its 30th anniversary, marking three decades of pioneering work in forensic DNA science and human genetics in the Philippines (Figure 1).



Figure 1. Members of the DNA Analysis Laboratory, Natural Sciences Research Institute (NSRI), University of the Philippines Diliman.

Established on 16 May 1996, DAL was the country's first forensic DNA laboratory, created by a joint effort between the government and the national university. At a time when DNA forensics was still emerging globally, the laboratory's founding vision placed molecular science at the forefront of human identification - a critical component in the pursuit of justice.

That vision was championed by Dr. Saturnina C. Halos, who transformed an existing plant genetic engineering laboratory into a facility dedicated to human DNA analysis. Through sustained engagement with local and international partners, she secured the support needed to establish the country's first operational DNA forensic unit.

In its initial years, the laboratory faced significant administrative challenges, resulting in several changes in leadership. Stability was achieved on 19 February 1999, with the appointment of Maria Corazon A. De Ungria as Head of the Laboratory, a position she still holds. Under her leadership, DAL has grown into a nationally recognized institution, integrating scientific rigor, ethical responsibility, and public service in its work.

From Foundations to National Impact

In its early years, DAL focused on building infrastructure and developing expertise with only two permanent junior scientists and three temporary staff. Despite these limitations, the young team actively sought support from external partners, including the European Union, the British Embassy, the World Bank, the Royal Society of London, the Philippine Department of Science and Technology, and the Philippine Council for Health Research and Development. These collaborations enabled the laboratory to pursue critical research areas, notably DNA mixture analysis for sexual assault investigations [1] and humanitarian identification of human remains, including disaster victim identification and support for families affected by extrajudicial killings [2].

Staff were trained in emerging DNA technologies and core forensic practices - documentation, chain of custody, and secure evidence storage - essential for credible expert testimony in court [3]. The laboratory shifted from capacity building to casework, supporting investigations involving paternity disputes, sexual assault, and the identification of human remains. DAL's research-led approach aligned scientific inquiry with national needs to develop and validate protocols suited to local conditions, ensuring biological evidence - from degraded samples to complex DNA mixtures - is analyzed with rigor and is legally defensible.

From the outset, the laboratory recognized the need for population reference databases [4]. In an archipelago of 7,641 islands with more than 110 Indigenous Cultural Communities/Indigenous Peoples (ICCs/IPs) and numerous mainstream populations, patterns of geographic isolation and genetic diversity necessitated careful, inclusive representation [5]. DAL researchers engaged communities and government agencies, including the National Commission on Indigenous Peoples, the Office for Southern Cultural Communities, and the Ministry for Indigenous Peoples Affairs, inviting representative volunteers to partner with the laboratory and ensuring all human populations, regardless of size or location, are respectfully included in the expanding Philippine Reference Database [6].

Advancing Science, Strengthening Justice

Beyond individual cases, DAL has played a key role in shaping the broader forensic landscape in the Philippines. Its work has contributed to the drafting, application, and understanding of the Rule on DNA Evidence [7], strengthening the use of DNA as objective evidence in courts of law. Through sustained partnerships with hospitals, law enforcement agencies, and academic institutions, the laboratory continues to advance the standardization of practices in evidence collection, handling, and analysis.

Regionally, DAL helped foster forensic DNA collaboration in Southeast Asia. In May 2005, it organized one of the first meetings of forensic researchers from Southeast Asia in Manila alongside the Indo-Pacific Association of Law, Medicine and Science meeting, catalyzing further regional engagement. In 2006, the Health Sciences Authority in Singapore hosted a similar gathering, and in 2007 delegates formed the Regional East Asia Forensic DNA Workgroup in Malaysia; this group was later integrated into the Asian Forensic Sciences Network as its DNA Working Group, strengthening regional cooperation in forensic DNA science and promoting shared standards, training, and research across Asia.

Building the Future of Forensic Science

On 19 May 2026, in partnership with Manila HealthTek, the laboratory launched the first Filipino Sexual Assault Investigation Kit (SAI.Kit) [8]. This innovation is the result of more than 25 years of research, validation, and refinement of prototype kits developed by the team. Working closely with the Child Protection Network, the SAI.Kit has already been used in over 250 sexual assault cases involving child patients. It has proven to be a valuable tool for medical practitioners, supporting clinical examinations and the proper collection of biological samples for downstream DNA profiling (Figure 2). The commercial launch of the SAI.Kit at NSRI, where much of the scientific thinking, testing, prototype assembly, and validation were undertaken by several generations of researchers, all working toward one purpose: to help identify perpetrators through DNA evidence recovered from the victim's body (Figure 3). The SAI.Kit exemplifies science, perseverance, compassion, and an unwavering commitment to survivors through objective, and evidence-based investigation.

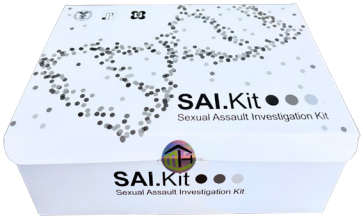


Figure 2. The Sexual Assault Investigation Kit (SAI. Kit), developed through the collaboration of the DNA Analysis Laboratory and Manila HealthTek.



Figure 3. Signing of the Commercial Licensing Agreement for the Sexual Assault Investigation Kit (SAI.Kit) between the University of the Philippines and Manila HealthTek.

On 20 and 21 May, the celebration continued with a two-day webinar themed "Science in the Service of Society: DAL's 30 Years of Forensic and Population Genetics in Action", drawing more than 200 participants to reflect on the past, examine current challenges, and envisage the future of DNA science in the Philippines. DAL's expansion into population genetics and genomics has deepened understanding of Filipino genetic diversity [9, 10] and advances in technologies and protocols now enable scientists to identify human sources of biological samples and evaluate family relationships across extended pedigrees, provided samples are properly collected, handled, and preserved.

From its beginnings as a modest laboratory with an ambitious vision, the DNA Analysis Laboratory has grown into a national leader in forensic science. Its journey demonstrates how sustained investment in research, people, and purpose can build institutions that serve not only science, but also society. As it enters its fourth decade, DAL continues to strengthen its research programs, expand DNA databases, and build international collaborations. Its work remains guided by a commitment to ethical practice, scientific excellence, and public service.

References

1. *Delfin FC, et al.,Y-STR analysis for detection and objective confirmation of child sexual abuse. Int J Legal Med, 2005. 119(3): p. 158-63.*
2. *Calacal GC, et al., Identification of exhumed remains of fire tragedy victims using conventional methods and autosomal/Y-chromosomal short tandem repeat DNA profiling. Am J Forensic Med Pathol, 2005. 26(3): p. 285-91.*
3. *De Ungria, MCA, DNA evidence in paternity cases. Philippine Law Journal, 2005. 80(2): p. 227-235.*
4. *De Ungria, MCA, et al.,Allele frequencies of 19 STR loci in a Philippine population generated using AmpFISTR multiplex and ALF singleplex systems. Forensic Sci Int, 2005. 152(2-3): p. 281-4.*
5. *Delfin FC, The Population history of the Philippines: A genetic overview. Philippine Studies: Historical and ethnographic viewpoints, 2015. 63(4): p. 449-476.*
6. *Rodriguez JJRB. et al., Ethical challenges in genetic research among Philippine indigenous peoples: Insights from fieldwork in Zamboanga and the Sulu Archipelago. Frontiers in Genetics, 2022. 13: p. 901515.*
7. *Philippines Supreme Court, Rule on DNA evidence, A.M.n. 06-11-5-SC, Editor. 2007, Lexpertbooks: Manila. p. 10 p.*
8. *De Ungria, MCA, et al., The development of a Local sexual assault investigation kit: The Philippine experience. Acta Medica Philippina, 2022. 56(15): p. 32-41.*
9. *Salvador JM, et al., Filipino DNA variation at 36 Y-chromosomal Short Tandem Repeat (STR) marker units. Phil J Science, 2019. 148(S1): p. 43-52.*
10. *Salvador JM, et al., Filipino DNA variation at 12 X-chromosome short tandem repeat markers. Forensic Sci Int Genet, 2018. 36: p. e8-e12.*

A New Virtual Anatomy Center in Suzhou Public Security Bureau: Transforming Forensic Investigations

Lijun Yang*, Jun Chu, Dong Gao, Ruhua Zhou and Min Li
Criminal Science and Technology Research Institute of Suzhou Public Security Bureau, China
**Email: 544270655@qq.com*

In March 2026, the Virtual Anatomy Center of Suzhou Public Security Bureau was officially commissioned. The Center has introduced advanced virtual-imaging CT equipment from Neusoft Medical, with technical specifications at an international advanced level. It has also adopted leading domestic cadaver-imaging equipment from Dian Company. By combining CT and AI technology, the Center achieves non-invasive, efficient, precise and traceable digital autopsies comprehensively upgrading forensic identification and criminal technology capabilities. It can empower criminal investigation in the following ways:



The Virtual Anatomy Center of Suzhou Public Security Bureau

Enhance identification accuracy and resolve complex cases

Virtual anatomy technology can non-invasively obtain deep-level information, revealing the entire body's skeletal and visceral injuries, hemorrhage, gas distribution, and ballistic or sharp-instrument trajectories without damaging the corpses. It addresses challenges that traditional autopsies struggle with, such as closed injuries, high falls, gunshot wounds, drowning and mechanical asphyxia. This technology can automatically mark injuries, reconstruct the temporal sequence of injuries and preserve trace evidence (bloodstains, hair, fibers) without disruption, reducing subjective error. The evidence is more objective and quantifiable, facilitating secondary examination and traceability.

Improve efficiency and support rapid case resolution

Virtual anatomy technology has brought about a qualitative improvement in post-mortem speed. Traditional autopsies typically take 2-3 hours, while microscopic pathological examination can take 5 to 7 days. With virtual autopsy, scanning can be completed in 30 minutes and a preliminary report generated quickly. Imaging data can be processed collaboratively across regions in real time, enabling cloud-based data sharing. Experts can conduct remote consultations and real-time annotation, quickly solving difficult issues in forensic death cause identification. This technology further enhances efficiency in cross-city and cross-provincial case collaboration.

Strengthen rule-of-law preservation and reduce public opinion risks

Virtual anatomical imaging data can be permanently preserved and are completely objective avoiding the limitation of traditional autopsy that "once dissected, the remains cannot be re-examined". This supports judicial disputes and retrial needs, reducing the need for repeated identifications and petitions. By avoiding invasive autopsy in some cases, the Center reduces family resistance and the dilemma of "seeking the truth while refusing autopsy". This approach is particularly applicable to cases of unnatural deaths, accidents and mass incidents, significantly improving stability, reducing disputes and increasing handling efficiency.

Prioritize strengthening the police with technology and empower AI data

With the widespread application of virtual anatomy technology, forensic imaging big data can be generated, providing training data for AI-based cause-of-death diagnosis, intelligent injury recognition and case correlation analysis. This promotes the transformation of forensic medicine from empirical judgment to digital, intelligent decision-making. Virtual anatomical imaging datasets can be integrated into smart policing and criminal technology analysis systems, becoming core technical support for handling homicide cases, abnormal deaths and major accidents.

Virtual anatomy technology represents a digital revolution in forensic medicine for public security: it enables non-invasive preservation of remains, rapid case conclusions, precise determination of cause of death, traceable data, more efficient collaboration and greater public acceptance. It comprehensively enhances case investigation, legal protection and social governance capabilities.

Development of Forensic Science Capacity at LPC-PCIC, Timor-Leste: Challenges, Routine Casework Experience, and Pathway Towards ISO/IEC 17025

Monica Menezes
Polícia Científica de Investigação Criminal, Timor-Leste
Email: gmonicaalda@gmail.com

Introduction

Forensic science plays a critical role in supporting criminal justice systems by providing objective, scientific evidence for investigations and prosecutions. In developing and post-conflict countries, establishing and strengthening forensic laboratory capacity is particularly challenging due to limitations in infrastructure, human resources, and access to international standards.

The Polícia Científica de Investigação Criminal (PCIC) is the national criminal investigation authority in Timor-Leste. Within PCIC, the Laboratório de Polícia Científica (LPC) conducts forensic examinations and provides expert opinions to support law enforcement and judicial authorities. Since becoming a member of the Asian Forensic Sciences Network (AFSN) in 2017, LPC-PCIC has expanded its disciplines, strengthened human capacity, and progressively adopted quality-based practices.

Background and Historical Evolution

LPC-PCIC operates as the central forensic laboratory under PCIC, ensuring technical oversight and scientific integrity. Since its inception in 2015, the institution's backbone was built through a strategic partnership with the Polícia Judiciária (PJ) of Portugal. The PJ was instrumental in the professional qualification of our staff, providing rigorous training for both investigators and forensic experts in Portugal.

The laboratory has evolved from foundational services into a multi-disciplinary institution with the following sectoral timeline:

- 2015: Crime Scene Investigation (CSI / Sektor TKP) and Judicial Identification & Fingerprints (Lofoscopia).
- 2016: Physico-Document Examination (Questioned Documents) and Ballistics.
- 2022: Digital Forensics.
- 2025: Biology (DNA Profiling).
- In Development: Toxicology (Current collection and initial testing are supported by PJ-Portugal and POLRI for advanced analysis).

Technical Infrastructure and International Cooperation

LPC-PCIC's technical capacity is supported by modern instrumentation, including:

- CSI: Two mobile laboratories and specialized transport.
- Ballistics: Comparative microscopy for firearm analysis (Figure 1).
- Document Examination: VSC 8000 for handwriting and document security analysis.
- Digital Forensics: XRY and X-Ways for data acquisition.
- Biology: Genetic analyzer for DNA profiling (Figure 2).



Figure 1. Comparative examination of ballistic bullets conducted in the Ballistics Laboratory.



Figure 2. Genetic Analyzer for DNA laboratory, supported by China.

Strategic Partnerships:

To solidify its regional integration, LPC-PCIC formalized key agreements:

- March 26, 2025: MoU with the Indonesian National Police (POLRI) for technical exchange (Figure 3).
- August 2025: Strategic cooperation with the Australian Federal Police (AFP) and TLPDP, focusing on infrastructure and digital forensic upgrades (Figure 4).
- PJ-Portugal: Continued reliance for advanced Handwriting Examination and specialized toxicology support.



Figure 3. Signing of the Memorandum of Understanding (MoU) between the PCIC of Timor-Leste and the Indonesian National Police (POLRI).



Figure 4. Signing of the Memorandum of Understanding (MoU) between the Australian Federal Police (AFP) and the PCIC of Timor-Leste.

Impact of AFSN Membership (Since 2017)

The AFSN has been a major catalyst for LPC-PCIC's growth. Beyond knowledge transfer through Workgroups, the network helped overcome a critical hurdle:

- Logistics. Through AFSN, we identified reliable distributors for reagents, equipment, and consumables—a vital step for our institutional development.

Selected Routine Casework: Digital Forensics

Digital forensics is increasingly vital. All examinations comply with legal authorization and strict chain-of-custody.

- Workflow: Receipt and registration → Preservation and acquisition (using write-blockers) → Examination and analysis → Impartial reporting.
- Quality is maintained through examiner accountability and adherence to forensic principles, despite limited automation.

Challenges in Forensic Practice

Operating in a post-conflict context presents unique constraints:

- Infrastructure: Difficulty in securing high-purity reagents and Certified Reference Materials (CRMs).
- Human Resources: Balancing recruitment with the need for highly specialized training.
- Backlog Management: Managing time-sensitive demands with meticulous scientific requirements.

Pathway Towards ISO/IEC 17025 Accreditation

LPC-PCIC's strategic goal is ISO/IEC 17025 accreditation. Preparatory steps include:

- SOP Harmonization: Standardizing protocols based on international training.
- Documentation: Robust case record management and traceability.
- Proficiency Testing: Future participation in external tests through AFSN.
- Quality Culture: Implementing a "Plan-Do-Check-Act" (PDCA) framework under centralized leadership.

Conclusion

The journey from 2015 to the present day demonstrates the resilience of LPC-PCIC. From our foundational training in Portugal to our active role in AFSN, we are committed to providing Timor-Leste with a justice system rooted in scientific truth. Accreditation will be the ultimate validation of our reliability in the regional legal landscape.

Acknowledgements

The author wishes to acknowledge the support of the Polícia Judiciária of Portugal, the Indonesian National Police (POLRI), the Australian Federal Police (AFP), the TLPDP and AFSN for their enduring contribution to Timor-Leste's forensic development.

Maintaining Forensic Quality Standards in Sri Lanka: Experiences of the Government Analyst's Department in Implementing ISO/IEC 17025:2017

M. Eranthi Jalika Seneviratne*, Ilmini Janaki Ambepitiya and W. Sammani Heshala Kumari Jayawansha
Government Analyst's Department, Sri Lanka
**Email: eranthijs@gmail.com*

Introduction

The Government Analyst's Department (GAD) is the central forensic laboratory in Sri Lanka and consists of nine specialized laboratories functioning under forensic science and food science divisions. The Toxicology, DNA and Serology, Narcotics, Examination of Questioned Documents, Ballistics and Firearms, Explosives and Fire, and Forensic Miscellaneous laboratories function under the Forensic Division while the Liquor and Food laboratories function under the Food Division. As the primary government institution responsible for forensic analysis, the Department plays a vital role in supporting the criminal justice system by providing scientifically reliable and legally defensible results [1].

To ensure reliability, consistency, and international acceptance of forensic results, the GAD operates in alignment with ISO/IEC 17025:2017, the international standard for the competence of testing and calibration laboratories [2]. The Department first obtained accreditation through the Sri Lanka Accreditation Board (SLAB) in 2016 and later transitioned to ISO/IEC 17025:2017 in 2019, and is currently accredited for 37 test methods [3,4]. Although not all examinations conducted by the GAD are included within the accredited scope due to the complexity and variability of forensic analyses, all laboratories function under a unified quality management system, ensuring consistency across all disciplines.

Alignment of Forensic Laboratory Practices with ISO/IEC 17025:2017 at the GAD

The GAD has established a comprehensive quality management system supported by controlled documents, including the quality manual, procedure manual, test methods, work instructions, and formats. The implementation, maintenance, and continuous improvement of the Quality Management System (QMS) are overseen by the Quality Coordinator, with the support of two Assistant Quality Coordinators. Technical operations are supervised by nine Laboratory Managers, each responsible for a respective laboratory and supported by Quality Representatives.

Impartiality, confidentiality, and professional ethics are considered fundamental requirements in forensic work. All personnel formally agree to confidentiality requirements and are expected to maintain professional neutrality while carrying out scientific examinations and reporting.

Competency of personnel is maintained through structured training programmes, competency evaluations, and continuous professional development activities. Laboratory facilities are maintained under suitable environmental conditions, while access to laboratory areas is restricted to authorized personnel to ensure sample integrity and security. Equipment used for analysis is regularly calibrated through accredited calibration laboratories to maintain measurement traceability. Certified reference materials and calibration standards are used where applicable to ensure the accuracy and reliability of analytical results.

The validity of results is ensured through several quality assurance measures, including method validation and verification, use of use of certified reference materials and control samples, replicate testing, quality control charts, intermediate equipment checks, blind samples, and intra-laboratory comparisons. Participation in proficiency testing (PT) programmes and inter-laboratory comparison programmes also provides independent verification of laboratory performance. Procedures are in place to ensure proper handling of test items, maintaining chain of custody and sample integrity. Traceability of examinations is maintained through comprehensive technical records, while reports are issued only after technical review by competent personnel. Internal audits, management reviews, corrective actions, and risk-based approaches further support continuous improvement of the quality management system.

Challenges and Special Considerations in Maintaining the Quality System in Forensic Laboratories

Maintaining nine laboratories under a single quality management system presents several challenges, particularly due to the diverse nature of forensic disciplines.

One of the main challenges is the limited availability of proficiency testing (PT) programmes for certain specialized areas, such as advanced DNA analysis and comparative examinations of questioned documents. This directly affects the ability to ensure the validity and reliability of results and limits opportunities for scope expansion.

Another significant challenge is limited access to training programmes in specialized fields such as firearms and ballistics, explosives, and questioned documents. This restricts the continuous professional development of personnel and their ability to keep up with evolving techniques and knowledge. Regional collaboration in organizing forensic training programmes and inter-laboratory comparisons, including initiatives through organizations such as the Asian Forensic Sciences Network (AFSN), would be highly beneficial in overcoming these challenges.

Obtaining certified reference materials and PT samples on time, due to licensing requirements and import regulations, is also a challenge. As several regulatory organizations are involved in these processes, delays may directly affect laboratory operations and timely completion of analyses. This is particularly critical for laboratories performing quantitative forensic analyses, where the availability of reference materials is essential for calibration and quality control.

As a government institution, the GAD is required to follow established administrative procedures, which may impact recruitment and procurement processes. This can affect the timely fulfillment of personnel and other requirements, such as equipment and chemicals, in accordance with quality requirements. Balancing confidentiality requirements with legal obligations, such as requests made under the Right to Information Act (2016) [5], also requires careful evaluation.

Increasing casework, together with limited resources, is another challenge faced by the Department. Maintaining documentation, quality control, technical reviews, and participation in proficiency testing programmes as part of routine analytical work requires strong commitment from both management and scientific staff, reflecting the importance of maintaining a strong quality culture within forensic laboratories.

Furthermore, many forensic examinations, such as firearm comparisons and questioned document analysis, are opinion-based rather than purely measurement-based. Therefore, ensuring the validity of results and the competence of personnel becomes critical. Regular competency assessments and participation in proficiency testing programmes play a key role in maintaining the reliability and consistency of such results.

Overall, maintaining quality standards in forensic laboratories requires a balanced approach that considers both technical requirements and practical limitations while maintaining the integrity and credibility of forensic results.

Conclusion

The Government Analyst's Department of Sri Lanka has established a mature quality management system aligned with ISO/IEC 17025:2017 to ensure the reliability, consistency, and credibility of forensic results across its nine laboratories. Despite operational, technical, and administrative challenges, the Department continues to maintain internationally recognized quality standards through commitment, continuous improvement, and active participation of both management and scientific staff.

Strengthening regional collaboration in training, proficiency testing, and knowledge sharing would further support forensic laboratories in the region in overcoming common challenges and enhancing the quality of forensic science services.

References

1. *Government Analyst's Department. Https://analyst.gov.lk/, 2026 (accessed 16 Apr 2026).*
2. *International Organization for Standardization. ISO/IEC 17025:2017. General requirements for the competence of testing and calibration laboratories. Geneva: ISO; 2017.*
3. *Sri Lanka Accreditation Board for Conformity Assessment (SLAB). Https://www.slab.lk/, 2026 (accessed 16 Apr 2026).*
4. *Sri Lanka Accreditation Board for Conformity Assessment (SLAB). Accredited organizations: Government Analyst's Department. Https://www.slab.lk/directory/registry/TL+069-01, 2026 (accessed 11 September 2026).*
5. *Parliament of the Democratic Socialist Republic of Sri Lanka. Right to Information Act, No. 12 of 2016. Colombo: Government of Sri Lanka; 2016.*

Advancing Public Safety Through Science: An Introduction to the Police Advanced Institute of Science and Technology (PAIST), Korean National Police University

Seongshin Gwak and Seung-jin Ryu*
Korean National Police University, South Korea
**Director: Prof Seung-jin Ryu, forensicknpu@gmail.com*

Established in 1981, the Korean National Police University (KNPU) is a prestigious four-year institution dedicated to cultivating the next generation of leadership for the Korean National Police Agency in South Korea. KNPU is renowned for its high selectivity and rigorous curriculum that integrates advanced legal studies and public administration with specialized tactical training and martial arts.

In 2021, the Police Advanced Institute of Science and Technology (PAIST) was established as a distinguished scientific research and forensic science educational institute under KNPU. PAIST provides high-level forensic analysis service to the law enforcement in South Korea driven by innovative research and specialized forensic educational programs. The PAIST Forensic Science Laboratory conducts in-depth analysis and research on diverse types of evidence in the field of forensic science. Through these activities, the institute focuses on nurturing specialized forensic scientists in public safety. In December 2025, the institute achieved a significant milestone by receiving KOLAS (Korea Laboratory Accreditation Scheme) accreditation under KS Q ISO/IEC 17025, specifically for handwriting and document examination.



Figure 1. PAIST, the Korean National Police University (KNPU).


Figure 2. Trace Evidence Analysis Laboratory.


Figure 3. Biological Evidence – DNA Analysis Laboratory.

To support the mission, PAIST operates six specialized laboratories:

- Forensic Evidence Collection Lab – Focuses on isolating and recovering target substances from forensic evidence through advanced field evidence collection and evidence pretreatment techniques.
- Trace Evidence Analysis Lab – Specializes in classifying trace evidence using microscopic techniques and performing personal identification through latent fingerprint analysis.
- Fire Debris/Explosion/Fire arm Evidence Lab - Conducts scientific analysis of debris and chemical residues from arson and explosions to determine origin and cause of incidents.
- Trace Analysis Instrumentation Lab – Utilizes state-of-the-art instrumentation to identify and quantify toxic substances, hazardous materials, and narcotics in trace amount.
- Forensic AI Big Data Lab – Leverages Big Data and Artificial Intelligence to develop advanced predictive data analysis platform for scientific crime scene investigation.
- Biological Evidence/DNA Analysis Lab - Focuses on advanced DNA profiling and biological evidence recovery to support complex criminal investigations.

PAIST is built upon a diverse human network, including KNPU undergraduates, graduate students from the Graduate School of Police Studies at the KNPU, active-duty police researchers, and forensic science practitioners. By integrating cutting-edge technologies such as AI and Big Data, PAIST is pushing the boundaries of traditional research and is committed to becoming a leading institution in the field of forensic science.

From Camp Crame to the World

Jan Paolo V. Moreno*, Aquilina P. Pia, Sheryl O. Duque and Maria Patricia C. Gregorio
Philippine National Police Forensic Group, Philippines
Email: forensicmoreno@gmail.com

A. Sharing Expertise at the Global Stage

The journey of a single bone fragment, weathered by time and elements, holds a silent genetic signature that only the right technology can unlock. In the DNA Laboratory Division of the PNP Forensic Group, science operates under pressure, moving far beyond the scripted drama of television. As DNA technology evolves through sequencing platforms and machine learning, the PNP Forensic Group actively shares its expertise on the global stage proving that Filipino forensic science is a force of international caliber.

17th Asian Forensic Sciences Network (AFSN) Annual Meeting (South Korea, September 2025)

Presented by NUP Sheryl Duque (Figure 1), co-authored with PLt.Col. Maria Theresa Bodo, PMaj. Marie Cerise-Elyn Aguilar, PMaj. Rey-Ann Valencia, and PEMS Aquilina Pia, the poster showcased the identification of fifteen fire victims in Quezon City who were charred beyond conventional



Figure 1

recognition. Utilizing STR profiling via PowerPlex® Fusion 6C and GlobalFiler™ kits, coupled with kinship comparison through CODIS, the team achieved a 100% identification rate. Twenty-eight reference samples were the key to ensuring that zero victims were left unnamed.

Different Scenes, Same Crime

The division's competence was further highlighted through the forensic reconstruction of a complex kidnap for ransom and double homicide case spanning three provinces. A poster presented by PEMS Aquilina P Pia, co-authored with PLt. Col. Edmar Dela A. Torre, PLt. Col. Jasper P. Magana, and NUP Sheryl O. Duque detailed the analysis

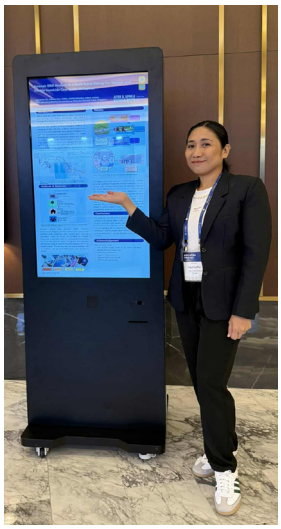


Figure 2

of 41 DNA samples collected from an abandoned vehicle, a safehouse, and remote roadsides. By utilizing DNA as a pivotal investigative tool, the team successfully placed suspects at every scene and rebuilt the criminal sequence end to end, proving that forensic science can bridge geographically dispersed crime scenes.

Bridging Between AI and Forensics at the 40th Association for the Advancement of AI (AAAI) Conference (Singapore, January 2026)

Technological advancements took center stage in Singapore at the AAAI Conference Bridge Between Law and AI with the theme Trustworthy AI for Legal and Law Enforcement Applications. PLt. Jan Paolo V. Moreno presented an innovative research project from the Asian Institute of Management titled "Generating Investigative Leads from Forensic DNA Data: Mapping Y-STR Profiles to Ancestral Haplogroups." By applying machine learning techniques to previously published DNA datasets, the study demonstrated how to predict ancestral lineage from genetic data alone. This fusion of biochemistry and data science earned a Best Presentation Honorable Mention for Poster Category, marking a significant milestone for Filipino AI applications in law enforcement.

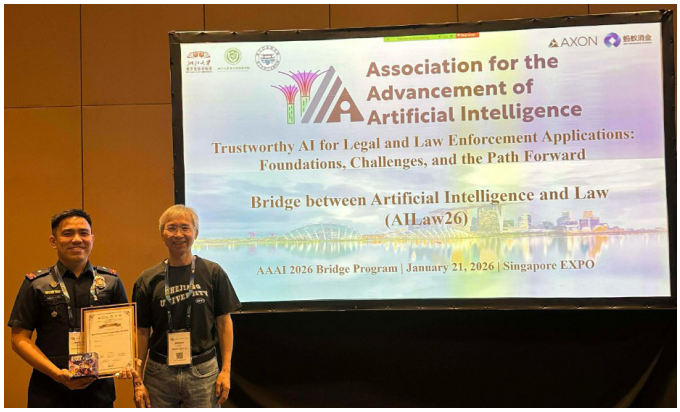


Figure 3

A Future Built on Science and Strategic Partnership

The challenges of an archipelago, including thousands of missing persons, trafficking victims, and the development of a National DNA Database, require forensic solutions that are both thoughtful and technologically advanced. When probabilistic inference and AI algorithms are trained on Filipino genetic data, they become more than just tools; they become the means to return an identity to a child or a parent. From the laboratories of Camp Crame to the high-tech forums of Singapore, the PNP Forensic Group continues to bring home the world's best practices to provide the answers that justice demands.

B. Powering International Justice Beyond Borders

From Shipwreck Victims and Trafficking to INTERPOL's Global Forensic Network

The pursuit of justice today is a collaborative, scientific endeavor that transcends geographical boundaries. A technical meeting at the PNP Forensic Group involving representatives from INTERPOL DNA, NCB Germany, NCB Norway, and the Philippine Center for Transnational Crime (PCTC) underscores this commitment. For the DNA Laboratory Division, science is the universal language used to solve complex cases: from identifying the missing in foreign seas to dismantling international criminal networks. This synergy ensures that Filipino forensic expertise remains a cornerstone of global law enforcement and human rights efforts.



Figure 4

The Shipwreck at the North Sea: A Biological Thread to Closure

Following the October 2023 sinking of the cargo ship Verity in the North Sea, the PNP Forensic Group proved that biological threads can connect families across continents. At the request of INTERPOL's National Central Bureau in Wiesbaden, Germany, the division launched a sensitive operation to locate the next of kin of a missing Filipino seafarer. By identifying and collecting DNA reference samples from the seafarer's mother, the team facilitated a definitive forensic identification for the remains recovered in 2024. While the case provided no courtroom conviction, it offered the profound justice of returning an answer to a grieving family.

Operation THUNDER: Protecting Global Biodiversity

The PNP Forensic Group's mandate extends to the protection of wildlife through INTERPOL's annual Operation Thunder series. In March 2025, the division played a critical role in a parrot smuggling case flagged by NCB Jakarta. As part of a global campaign that identified over 1,100 suspects linked to wildlife crime, Filipino analysts performed DNA profiling on apprehended individuals to map criminal networks. This contribution supports the prosecution of violators under the Wildlife Resources Conservation and Protection Act, demonstrating how forensic science safeguards both human society and the natural world across the ASEAN region.

A Trusted International Partner

Through meticulous work and international cooperation, the DNA Laboratory Division continues to serve as a pillar of integrity and accuracy. Whether assisting with INTERPOL notices, identifying international violators, or locating the next of kin for the missing, Filipino forensic analysts bridge local expertise with the global justice network. Their dedication ensures that every scientific victory, from a small laboratory in Camp Crame to a high tech forum in Singapore, provides a voice for those who can no longer speak for themselves and brings much needed closure to families waiting for answers.

Generating Investigative Leads from Forensic DNA Data: Mapping Y-STR Profiles to Ancestral Haplogroups

Jan Paolo V. Moreno[1,2]*, Kevin Ansel S. Dy[1], Francis Erdey M. Capati[1], Mia Cielo G. Oliveros[1], Kristine Ann M. Carandang[3] and Christian M. Alis[1,3]
[1] Aboitiz School of Innovation, Technology & Entrepreneurship, Asian Institute of Management
[2] DNA Laboratory Division, Philippine National Police (PNP) Forensic Group
[3] Analytics, Computing, and Complex Systems (ACCeSs) Laboratory, Asian Institute of Management
Email: forensicmoreno@gmail.com

Abstract:
Y-chromosome short tandem repeats (Y-STRs) are a cornerstone of forensic investigations, enabling differentiation of male lineages along the paternal line. However, their utility hinges on matching against reference profiles in population databases such as the Combined DNA Index System (CODIS). When no match exists, a crime scene profile yields no actionable leads. This study develops a machine learning framework for predicting Y-chromosome Single Nucleotide Polymorphism (Y-SNP) haplogroups directly from standard Y-STR profiles, providing paternal lineage ancestry information that enables investigative lead generation even in the absence of a database match. Eight supervised classifiers were evaluated on 4,064 Y-STR profiles comprising 27 markers each. The optimised XGBoost (Extreme Gradient Boosting) classifier achieved the highest accuracy (96.98%) and a Macro F1-score of 0.9810. Stratified sampling and class weighting were applied to ensure equitable performance across demographically underrepresented ancestral haplogroups. SHapley Additive exPlanations (SHAP) analysis was integrated to provide the model interpretability required for ethical and legally admissible deployment in police investigations. Key markers DYS392, DYS481, and DYS635 were identified as the strongest predictors of haplogroup membership. This framework advances trustworthy artificial intelligence (AI) in law enforcement by combining predictive accuracy, demographic fairness, and operational transparency.

Keywords: Y-STR, haplogroup prediction, forensic intelligence, XGBoost, SHAP

1. Introduction

Deoxyribonucleic acid (DNA) fingerprinting through short tandem repeat (STR) typing is the gold standard for human identification in criminal cases [1,2]. Y-STRs are short repeating segments on the Y chromosome inherited strictly along the paternal line, making them particularly valuable in sexual assault and missing-person investigations. Their forensic utility depends, however, on the existence of a reference profile in a database such as CODIS or the Y Chromosome Haplotype Reference Database (YHRD) [2,3]. When a crime scene profile produces no match, the evidence becomes static and the case risks joining the unsolved cold case backlog [4].

A complementary procedure, Y-SNP array analysis, can derive broader ancestral information by assigning a sample to a phylogenetic clade known as a haplogroup. Haplogroups correlate strongly with deep human migratory history and biogeographical ancestry, allowing law enforcers to narrow the suspect pool by likely continental or regional origin [4,5]. This process is, however, resource-intensive in cost, time, and sample quantity, and is therefore excluded from routine casework.
This study addresses that gap by training supervised machine learning classifiers to predict Y-SNP haplogroups directly from standard 27-marker Y-STR profiles, generating actionable investigative leads without additional laboratory procedures. We further apply SHAP interpretability analysis to ensure the framework meets the transparency and fairness requirements of the justice system.

Background

Early biogeographical ancestry (BGA) tools relied on autosomal SNPs [1], but Y-chromosome analysis is especially powerful due to its paternal-lineage specificity. Statistical approaches to haplogroup prediction used maximum likelihood or Bayesian methods applied to frequency databases [6,7]; however, these perform poorly on rare or novel haplotypes not well-represented in existing data.

A shift toward supervised machine learning has addressed some of these limitations, with Random Forest, Support Vector Machine (SVM), and neural network approaches demonstrating superior predictive accuracy [8,9,10]. A critical gap persists, however: most existing models prioritise raw accuracy while neglecting interpretability, fairness, and transparency — requirements that are non-negotiable when computational outputs may influence criminal proceedings [11].

2. Methods

Dataset

The Y Haplogroup Predictor (YHP) dataset [8] was used, comprising 4,064 unique samples each characterised by 27 Y-STR markers (allele scores from the Yfiler Plus kit) and confirmed Y-SNP haplogroup assignments across 13 major haplogroups. Figure 1 illustrates the allele score distributions across all 27 markers. As shown in Figure 2, the dataset is substantially imbalanced: Haplogroup O (predominant in East Asian populations) accounts for the large majority of samples, while Haplogroups G, H, and L are sparsely represented. Naive training on such data produces classifiers biased toward the majority class, which is unacceptable in a justice setting.

Model training and evaluation

Eight classifiers were trained: XGBoost, k-Nearest Neighbours (kNN), Decision Tree, SVM, Random Forest, Gaussian Naive Bayes, Linear Discriminant Analysis (LDA),

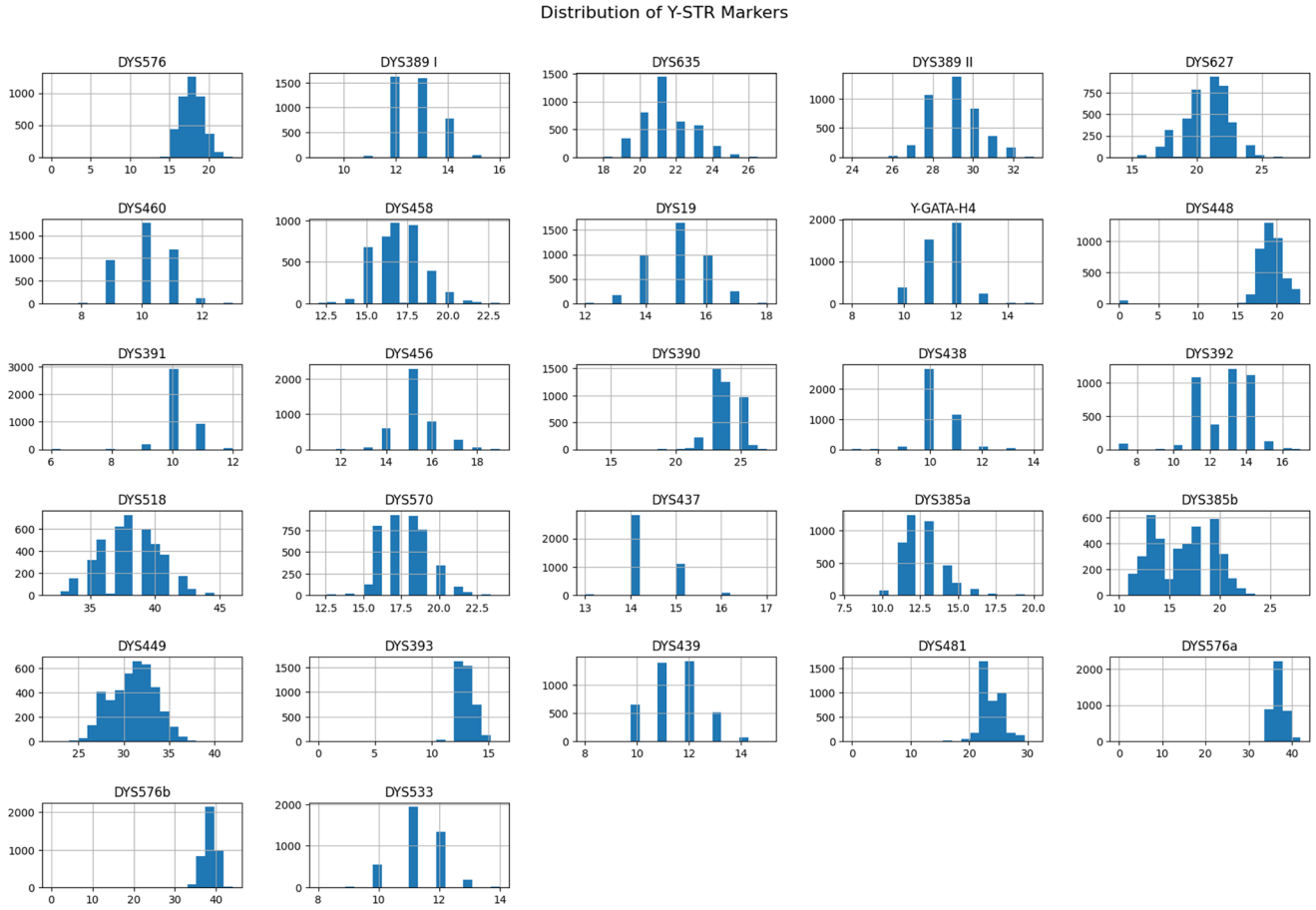


Figure 1. Distribution of Y-STR allele scores across the 27 genetic markers. Most markers show unimodal distributions with tight clustering (e.g., DYS576, DYS449), indicating population-level consistency. Markers such as DYS389II and DYS456 exhibit broader or multi-modal patterns, reflecting higher variability and greater discriminatory power.

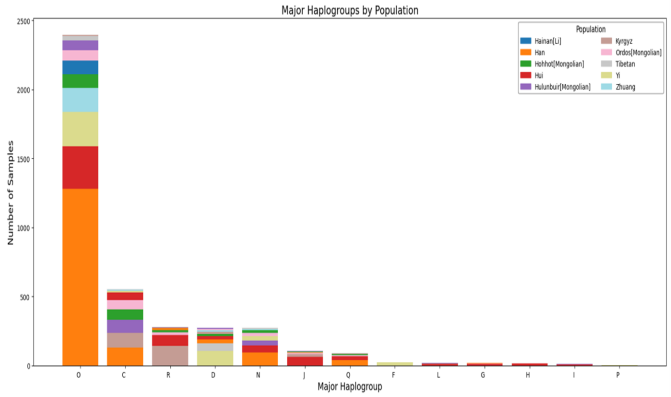


Figure 2. Distribution of major haplogroups in the YHP dataset. Haplogroup O dominates, contributing the vast majority of samples, while all other haplogroups are sparsely represented. This severe imbalance risks biassing classifiers toward the majority class and suppressing minority-haplogroup prediction. multi-modal patterns, reflecting higher variability and greater discriminatory power.

and Elastic Net. Macro-F1 score was the primary evaluation metric, treating all 13 classes equally regardless of sample size. The dataset was split into a stratified training-validation set (75%) and holdout set (25%), and hyperparameter tuning used 5-fold stratified cross-validation to maintain class proportions in every fold. Class weighting was applied during training to further protect minority haplogroups from systematic misclassification.

Interpretability analysis

SHAP was applied to the best-performing model to quantify the contribution of each Y-STR marker to individual haplogroup predictions, enabling a forensic expert to articulate the basis of any investigative lead.

3. Results and Discussion

Model performance

XGBoost achieved the highest overall accuracy (96.98%) across all eight models (Table 1). Its sequential error-correction mechanism and advanced regularisation outperformed the other classifiers on this non-linear, imbalanced dataset. The Macro F1-score of 0.9810 confirms equitable performance across all 13 haplogroup classes,, including minority groups. Elastic Net performed poorly (accuracy: 0.20), reflecting the highly non-linear relationship

Table 1. Comparison of machine learning model accuracy on the holdout set. XGBoost achieved the highest accuracy of 0.9698.

Machine Learning Model	Accuracy
XGBoost	0.9698
Random Forest	0.9679
SVM	0.9623
kNN	0.9616
LDA	0.9438
Gaussian NB	0.9351
Decision Tree	0.9342
Elastic Net	0.2029

between Y-STR markers and Y-SNP haplogroups that linear models cannot capture.

Per-haplogroup performance is summarised in Table 2. Most classes achieved F1-scores at or near 1.00. Notable exceptions are Haplogroup L (F1 = 0.33, recall = 0.20) and Haplogroup I (F1 = 0.80, recall = 0.67). Haplogroup L's low recall arises because its Y-STR profiles closely resemble those of the dominant Haplogroup O; the model defaults to the majority class when distinguishing between them, yielding high precision but poor recall. Haplogroups F, G, and H, although also minority classes, achieved perfect scores, likely because their Y-STR signatures are genetically distinct enough for clear decision boundaries to be drawn even with limited training samples.

Table 2. Per-haplogroup performance of the XGBoost model on the holdout set.

Haplogroup	Accuracy	Precision	Recall	F1-Score
O	0.97	0.97	0.99	0.98
C	0.99	0.97	0.96	0.96
R	1.00	1.00	1.00	1.00
D	0.99	0.97	0.94	0.96
N	0.99	0.97	0.94	0.96
Q	0.99	0.91	0.91	0.91
J	0.99	1.00	0.96	0.98
F	1.00	1.00	1.00	1.00
L	0.99	1.00	0.20	0.33
G	1.00	1.00	1.00	1.00
H	1.00	1.00	1.00	1.00
I	0.99	1.00	0.67	0.80

The decision to maximise Weighted F1 (0.9810) reflects the ethical stakes of forensic lead generation: a false positive—incorrectly associating a crime scene profile with a haplogroup—risks directing suspicion toward innocent individuals; a false negative may result in losing the sole investigative lead available. The framework's error profile is intentionally calibrated to align with the Blackstone Ratio ("better that ten guilty persons escape than one innocent suffer") by aggressively minimising false positives.

Interpretability and legal transparency

In the justice system, "black box" algorithms are functionally inadmissible: courts require that the basis of any computational evidence be auditable [11,12]. SHAP analysis provides both a global ranking of feature importance and a local per-prediction explanation for each crime scene profile. As shown in Figure 3, DYS392 is the most influential marker overall, with a mean absolute SHAP value nearly double that of DYS481 (the second-ranked marker). DYS635 and DYS385b also rank highly. Generating a local SHAP plot for every novel Y-STR profile enables a forensic expert to state precisely why the model assigned a particular haplogroup - e.g., that the DYS392 allele length strongly shifted the prediction away from Haplogroup O and toward Haplogroup R - thereby satisfying requirements for transparency, internal audit, and judicial scrutiny.

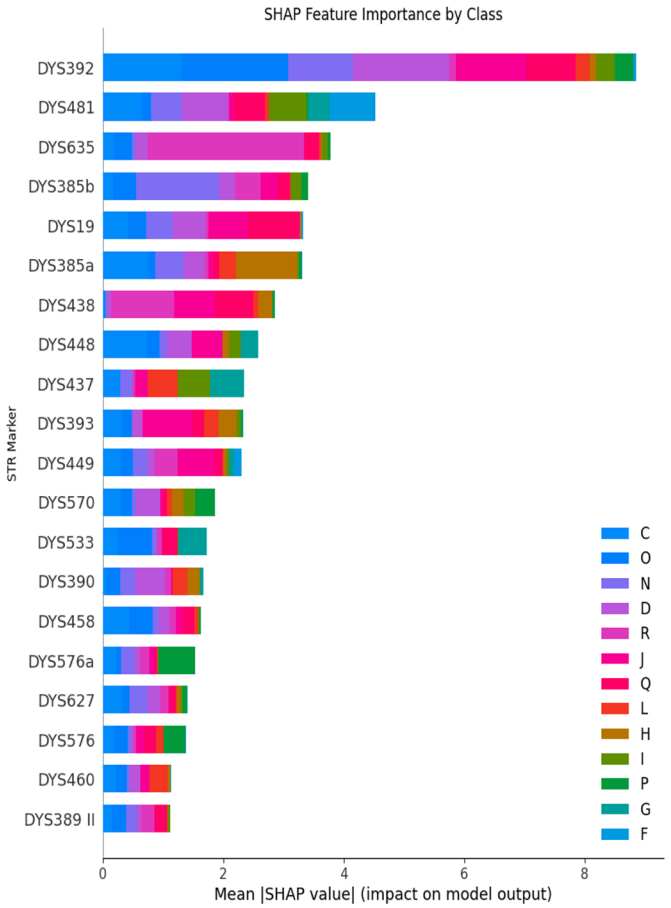


Figure 3. Mean absolute SHAP values per Y-STR marker, ranked by overall impact on haplogroup prediction. DYS392 is the dominant predictor, with an impact almost twice that of DYS481. Colour bars indicate the contribution of each marker toward specific haplogroup classes (C, O, N, D, R, J, Q, L, H, I, P, G, F), enabling class-specific interpretation of each marker's influence.

4. Conclusion

This study demonstrates that Y-SNP haplogroups can be predicted from standard 27-marker Y-STR profiles with 97% accuracy using an optimised XGBoost classifier. The framework integrates stratified sampling and class weighting for demographic fairness, and SHAP analysis for forensic transparency. By providing law enforcement with actionable ancestral leads even when no database match exists, this approach advances the paradigm of trustworthy AI in forensic investigation. Future work should re-train the model on locally representative population data (e.g., from the Philippines) to mitigate geographic bias, extend prediction to sub-clade resolution, and incorporate Bayesian or conformal prediction methods to quantify uncertainty alongside each haplogroup prediction.

Acknowledgements

The authors sincerely thank Professor Christopher Monterola, School Head of the Aboitiz School of Innovation, Technology and Entrepreneurship of Asian Institute of Management, for his leadership, guidance, and steadfast support of interdisciplinary research at the intersection of data science and public service. His encouragement and institutional support were instrumental in the completion of this work.

The authors are also grateful to Professor Kenneth T. Co and Jose Miguel G. Bautista for guiding the student authors through the formulation of the research topic and the completion of the initial project submitted for their Master of Science in Data Science course in Machine Learning I. The authors also acknowledge the Master of Science in Data Science 2026 Cohort for the shared learning journey, intellectual exchange, and mutual support that fostered growth and perseverance throughout this endeavor.

The authors respectfully recognize Police Colonel Pierre Paul F Carpio, Officer-in-Charge of the PNP Forensic Group; Police Lieutenant Colonel Edmar A Dela Torre, Chief of the DNA Laboratory Division; Police Lieutenant Colonel Jasper P Magana, Assistant Chief, DLD, Police Major Rey-Ann L Valencia; and Police Lieutenant Colonel Eleazar P Macaraeg for their valuable support, professional insights, and commitment to advancing forensic science and evidence-based policing, which significantly informed the practical contributions of this work in the field. The same commendation is extended to the men and women of the Philippine National Police Forensic Group DNA Laboratory Division.

Finally, this work is dedicated to the primary author's wife, Mrs. Mary Claire Leoncio Moreno, RPm, and daughter, Ms. Emma Haraya Celyne Leoncio Moreno whose love and patience fueled the completion of this work.

References

1. *Kayser M. Forensic use of Y-chromosome DNA: A general overview. Hum Genet. 2017;136(5):621-635.*
2. *Ndomondo S, Sharma P, Mevada V, et al. Forensic applications of rapidly mutating Y-STR markers: Current status and future perspectives. Forensic Sci Med Pathol. 2025:1-16.*
3. *Costa R, Fadoni J, Amorim A, Caine L. Y-STR databases—application in sexual crimes. Genes. 2025;16(5):484.*
4. *National Institute of Justice. Using DNA to solve cold cases: Special report. Washington DC: NIJ; 2002.*
5. *Li Y, Jiang L, Liu Q, et al. Integrated microfluidic system for rapid 89-plex Y-SNP profiling: Development and forensic validation. Electrophoresis. 2025;46(20):1534-1547.*
6. *Willuweit S, Roewer L. The new Y chromosome haplotype reference database. Forensic Sci Int Genet. 2015;15:43-48.*
7. *Babic JN, Kojovic T, Dogan S, et al. Haplogroup prediction using Y-chromosomal short tandem repeats in the general population of Bosnia and Herzegovina. Front Genet. 2021;12:671467.*
8. *Song M, Zhou Y, Zhao C, Song F, Hou Y. YHP: Y-chromosome haplogroup predictor for predicting male lineages based on Y-STRs. Forensic Sci Int. 2024;361:112113.*
9. *Yin C, He Z, Wang Y, et al. Improving the regional Y-STR haplotype resolution utilising haplogroup-determining Y-SNPs and the application of machine learning in Y-SNP haplogroup prediction in a forensic Y-STR database. Forensic Sci Int Genet. 2022;57:102659.*
10. *Fan G-Y, Jiang D-Z, Jiang Y-H, et al. Phylogenetic analyses of 41 Y-STRs and machine learning-based haplogroup prediction in the Qingdao Han population from Shandong province, Eastern China. Ann Hum Biol. 2023;50(1):35-41.*
11. *Mittelstadt B. Principles alone cannot guarantee ethical AI. Nat Mach Intell. 2019;1(11):501-507.*
12. *Lundberg SM, Lee S-I. A unified approach to interpreting model predictions. Adv Neural Inf Process Syst. 2017;30.*

Optimization of Sperm Separation Parameters in Differential Extraction Using the EZ2 DNA Investigator Sep&Prep Kit

Zulhilmi Husni*, Mahzan Md Tab, Dayang Zarifah Ataillah Awang Aemeran, Nazatul Aida Azizan, Faten Najah Mohd Kassim, Nur Fadzlina Yahaya, Siti Hajar Hussin and Nor Aidora Saedon
Department of Chemistry, Malaysia
Email: zulhilmi@kimia.gov.my

Abstract:
Efficient separation of sperm and epithelial cells is essential for recovering male DNA profiles from sexual assault evidence. This study evaluated key operational parameters in the EZ2 DNA Investigator Sep&Prep differential extraction workflow, including centrifugation speed, epithelial lysis incubation time, and sequential epithelial lysis cycles. Sperm DNA recovery was highest at 100 × g, indicating that effective sperm pelleting can be achieved at substantially lower centrifugal forces than recommended in the standard protocol. A 10-minute epithelial lysis incubation produced full STR profiles without female allele carryover, while excessive lysis cycles reduced DNA yield. Under optimized conditions, a single-source male profile was successfully recovered from a highly imbalanced 1:1000 male-to-female DNA mixture.

Keywords: *Differential extraction, sperm DNA recovery, sexual assault evidence, forensic DNA analysis*

1. Introduction

Sexual assault evidence frequently contains mixed biological material, comprising both sperm cells and non-sperm cells from multiple contributors. Accurate separation of these components is critical for forensic DNA analysis, as it enables the generation of individual DNA profiles from the perpetrator while minimizing contamination from the victim's DNA. Differential extraction (DE) has long been the gold standard for this purpose, exploiting the biochemical and structural differences between sperm cells and other cell types to selectively isolate sperm-derived DNA [1].

The EZ2 DNA Investigator Sep&Prep Kit (QIAGEN) provides a fully automated platform for differential extraction using magnetic-particle technology [2]. This system allows simultaneous separation of up to 24 samples with minimal hands-on time and reduced user-to-user variability, while producing high-quality DNA suitable for downstream STR analysis. The automated workflow also mitigates risks of contamination and processing errors associated with manual DE methods. Despite these advantages, operational parameters such as centrifugation speed, sequential epithelial lysis cycles, and incubation time may influence sperm recovery and mixture purity, particularly in challenging samples with low male-to-female DNA ratios.

Previous reports indicate that the standard Sep&Prep protocol effectively enriches sperm DNA from mixtures with moderate male-to-female ratios; however, minor female DNA carryover may still occur, limiting the ability to obtain single-source male profiles in highly imbalanced mixtures [3]. In this study, we sought to optimize key parameters of the Sep&Prep workflow to improve sperm recovery and reduce epithelial DNA contamination. Specifically, we evaluated the effects of centrifugation speed, sequential epithelial lysis cycles, and incubation time on DNA yield and STR profile completeness. Our findings provide practical insights for forensic laboratories aiming to maximize the efficiency and robustness of automated sperm separation workflows in sexual assault casework.

2. Materials and Methods

2.1 Sample Collection and Preparation

Semen samples were voluntarily donated by an adult male staff member under written informed consent for research use. Samples were used directly without further processing and stored at -20 °C until extraction.

Female epithelial DNA was obtained from saliva samples collected from an adult female staff volunteer with written informed consent. Saliva samples were centrifuged to pellet epithelial cells, thereby enriching intact cellular material while reducing free DNA in the supernatant.

Cells were extracted from each sample and subsequently quantified using real-time PCR to determine the DNA concentration per microliter suspension. This measurement provided a standardized estimate of DNA input for downstream analyses.

2.2 Male-Female Mixture Preparation

Male-to-female DNA mixtures were prepared to simulate highly unbalanced biological samples commonly encountered in sexual assault evidence. Sperm-derived male DNA was combined with epithelial cell-derived female DNA at a ratio of 1:1000, using 0.3 ng male DNA and 300 ng female DNA.

2.3 Recommended Protocol of EZ2 DNA Investigator Sep&Prep Kit

Sperm and epithelial mixtures were extracted using the EZ2 DNA Investigator Sep&Prep Kit on the EZ2 Connect Fx automated platform according to manufacturer instructions [4].

(i) Non-Sperm Fraction (NSF) Extraction

Selective lysis of non-sperm cells was achieved using lysis buffer containing proteinase K with incubation at 56 °C for 30 minutes. The resulting lysate was centrifuged at 15,000 rpm (21,130 x g), and the supernatant containing epithelial

DNA was collected. DNA from the NSF was subsequently purified using the Trace Protocol of EZ1&2 DNA Investigator Kit with elution in 50 µL of elution buffer. This DNA was used for downstream quantification and STR analysis.

(ii) Sperm Fraction Extraction

Following removal of the NSF, the remaining pellet enriched with sperm cells was processed using the Sep&Prep protocol to lyse sperm cells and purify DNA. DNA was eluted in 50 µL elution buffer for downstream quantification and STR amplification.

2.4 DNA Quantification

DNA was quantified in triplicate using the Quantifiler™ Trio DNA Quantification Kit on a QuantStudio 5 real-time PCR system.

2.5 STR Amplification and Capillary Electrophoresis

STR amplification was performed using the GlobalFiler™ PCR Amplification Kit following the manufacturer's instructions. Capillary electrophoresis was performed on an Applied Biosystems 3500xL Genetic Analyzer and analyzed using GeneMapper ID-X v1.6.

2.6 Minimum Effective Pelleting Force

To determine the minimum centrifugal force required for efficient sperm and epithelial pelleting, equal volumes (1 µL) of purified sperm or epithelial cell suspensions were prepared in TE buffer. Samples were subjected to a range of centrifugation speeds (50 × g, 100 × g, 500 × g, 1,000 × g, 5,000 × g, 10,000 × g, and 20,000 × g) for 5 minutes at room temperature. DNA was extracted from the resulting pellets and quantified to assess DNA recovery. The highest centrifugal force (20,000 × g) served as a reference for maximal pelleting efficiency.

2.7 Incubation Efficiency Test

The effect of incubation time during the epithelial lysis step was evaluated using the differential extraction workflow of the Sep & Prep kit. Sperm–epithelial mixtures at a 1:1000 ratio were incubated with lysis buffer and proteinase K at 56 °C with gentle agitation for 10, 15, and 30 minutes. These incubation periods represent the epithelial cell lysis stage of the differential extraction procedure.

Following incubation, the epithelial fraction was separated according to the Sep & Prep protocol, and the remaining sperm pellet was subjected to downstream DNA purification. Extracted DNA was quantified and STR analysis was performed to assess allele recovery and determine the presence of any female DNA carryover in the sperm fraction. This experiment was conducted to identify the shortest incubation period that allows effective epithelial cell lysis while maintaining complete STR profile recovery from the sperm fraction.

2.8 Sequential Epithelial Lysis Optimization

The effect of repeated epithelial lysis on sperm DNA recovery was evaluated within the differential extraction workflow of the Sep & Prep kit. Sperm-epithelial mixtures at a 1:1000 ratio were processed according to the Sep & Prep protocol, followed by sequential epithelial lysis cycles using lysis buffer supplemented with proteinase K.

Between one and eight lysis cycles were evaluated. For each cycle, the sperm pellet was resuspended in lysis buffer containing proteinase K and incubated according to the Sep & Prep workflow before being recentrifuged under the optimized centrifugation condition (100 × g) identified in this study. After the final lysis cycle, the sperm pellet was subjected to downstream DNA purification according to the standard workflow.

Extracted DNA was quantified and STR analysis was performed to assess allele recovery from the sperm fraction. The minimum number of epithelial lysis cycles required to maintain complete male STR profiles while minimizing potential loss of sperm DNA was determined.

2.9 Optimized Protocol of EZ2 DNA Investigator Sep&Prep Kit

Sperm and epithelial mixtures were extracted using the optimized protocol of EZ2 DNA Investigator Sep&Prep Kit on the EZ2 Connect Fx automated platform.

(i) Sample Pre-Treatment

Samples were mixed with 500 µL of TE buffer (0.1 M Tris-HCl, pH 7.5; 0.5 M EDTA, pH 8.0) and centrifuged at 100 RCF for 5 minutes to pellet large cellular material. The supernatant, which contains non-cellular proteins that represent an unnecessary substrate for proteinase K, was discarded to prevent consumption of the enzyme on irrelevant material. Notably, prostate-specific antigen (PSA) present in the supernatant can be preserved for subsequent PSA testing without affecting sperm recovery or downstream DNA extraction.

(ii) Non-Sperm Fraction (NSF) Extraction

Selective lysis of non-sperm cells was achieved using lysis buffer containing proteinase K with incubation at 56 °C for 30 minutes. The resulting lysate was centrifuged (100 RCF), and the supernatant containing epithelial DNA was collected. DNA from the NSF was subsequently purified using the Trace Protocol of EZ1&2 DNA Investigator Kit with elution in 50 µL of elution buffer. This DNA was used for downstream quantification and STR analysis.

(iii) Sperm Fraction Extraction

Following removal of the NSF, the remaining pellet enriched with sperm cells was processed using the Sep&Prep protocol to lyse sperm cells and purify DNA. DNA was eluted in 50 µL elution buffer for downstream quantification and STR amplification.

3. Results & Discussion

Optimization of key operational parameters in the Sep&Prep workflow substantially influenced sperm DNA recovery and mixture purity. The parameters evaluated - centrifugation speed, epithelial lysis incubation time, and sequential epithelial lysis cycles - are critical for efficient sperm separation in forensic sexual assault casework.

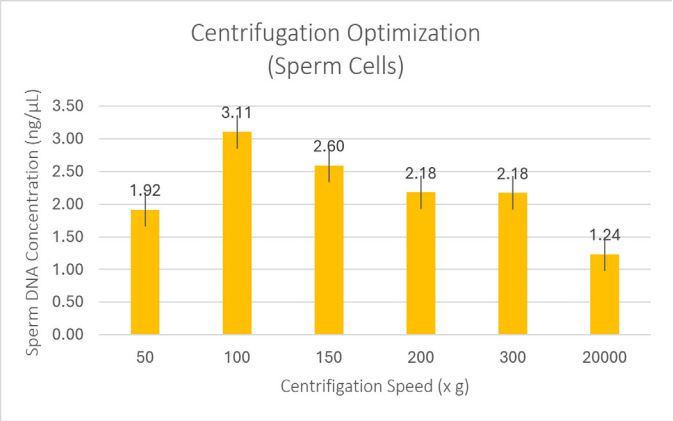


Figure 1. Effect of centrifugation speed on DNA recovery from pure sperm cell samples. DNA concentrations were measured across centrifugation conditions ranging from 50 × g to 20,000 × g.

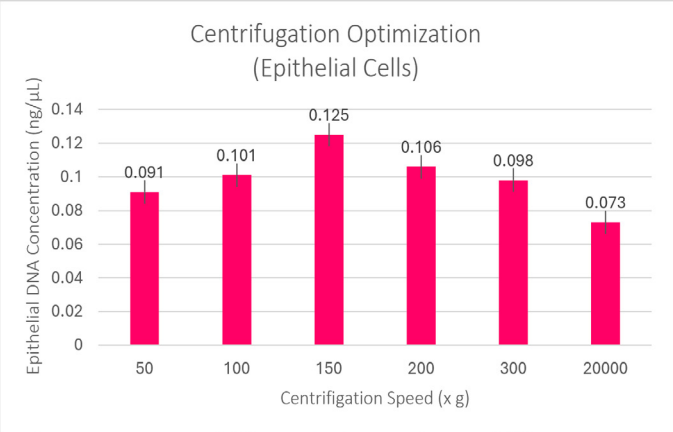


Figure 2. Effect of centrifugation speed on DNA recovery from pure epithelial cell samples. DNA concentrations were measured across centrifugation conditions ranging from 50 × g to 20,000 × g.

Centrifugation optimization - The centrifugation experiment was designed to identify the minimum centrifugal force required for effective sperm pelleting. Equal volumes of purified sperm and epithelial cell suspensions were subjected to varying centrifugal forces, with 20,000 × g included as a reference condition since such forces are expected to pellet essentially all cellular material (Figures 1& 2).

The results showed that sperm DNA recovery peaked at 100 × g, indicating that efficient sperm pelleting can be achieved at substantially lower centrifugal forces than those recommended in the default protocol. Increasing the centrifugation force beyond this level did not improve sperm DNA recovery, and the highest force tested produced comparatively lower yields.

The pre-treatment step - rehydrating samples in TE buffer and centrifuging at 100 × g - retains non-cellular proteins, including prostate-specific antigen (PSA), in the supernatant. This preserves valuable ancillary evidence and allows downstream assays, such as PSA testing, which are not feasible under the standard Qiagen protocol. This step maximizes sperm DNA recovery while maintaining other forensic evidence.

Incubation time optimization - Varying incubation between 10 and 30 minutes did not affect STR recovery, with no female alleles detected (Table 1). Low-speed centrifugation

Table 1. Evaluation of incubation time on STR profile recovery. Full STR allele recovery was observed across incubation times ranging from 10 to 30 minutes, with no detectable female allele carryover.

Incubation time (minutes)	STR recovery	Female allele present?
10	Full (21 loci)	No
15	Full (21 loci)	No
30	Full (21 loci)	No

reduces non-cellular proteins in the pellet, minimizing competition for proteinase K and allowing efficient lysis of epithelial cells. This enables a 10-minute incubation, improving workflow efficiency without compromising DNA recovery or mixture purity—particularly advantageous for routine forensic workflows.

Sequential epithelial lysis cycle optimization - The effect of repeated epithelial lysis cycles on sperm DNA recovery was also evaluated. While complete male STR profiles were obtained following up to five lysis cycles, progressive reductions in DNA yield were observed as the number of cycles increased.

Partial allele recovery was observed from the sixth cycle onward, indicating that excessive lysis processing may lead to sperm loss or reduced DNA recovery (Table 2). As a single epithelial lysis cycle already produced a complete male STR profile, additional cycles were considered unnecessary for routine forensic processing.

Table 2. Effect of sequential epithelial lysis cycles on DNA concentration in the sperm fraction and STR allele recovery. Increasing washing steps progressively reduced DNA yield, with full STR profiles observed up to five washes.

Lysis cycle	DNA concentration (ng/µL)	STR recovery
1 cycle	0.376	Full (21 loci)
2 cycles	0.144	Full (21 loci)
3 cycles	0.065	Full (21 loci)
4 cycles	0.050	Full (21 loci)
5 cycles	0.018	Full (21 loci)
6 cycles	0.016	Partial (16 loci)
7 cycles	0.005	Partial (14 loci)
8 cycles	0.004	Partial (14 loci)

These findings suggest that limiting the number of epithelial lysis cycles can preserve sperm DNA yield while maintaining effective removal of epithelial DNA.

Practical implications - These findings demonstrate that minor laboratory adjustments can significantly improve sperm separation using the Sep&Prep workflow. The optimized conditions - 100 × g centrifugation, a single epithelial lysis cycle, and a 10-minute incubation - provided consistent sperm DNA recovery and high mixture purity. In addition, low-speed pre-treatment preserves non-cellular proteins such as PSA for potential downstream screening assays. Collectively, these refinements enable recovery of single-source male DNA profiles from highly imbalanced mixtures.

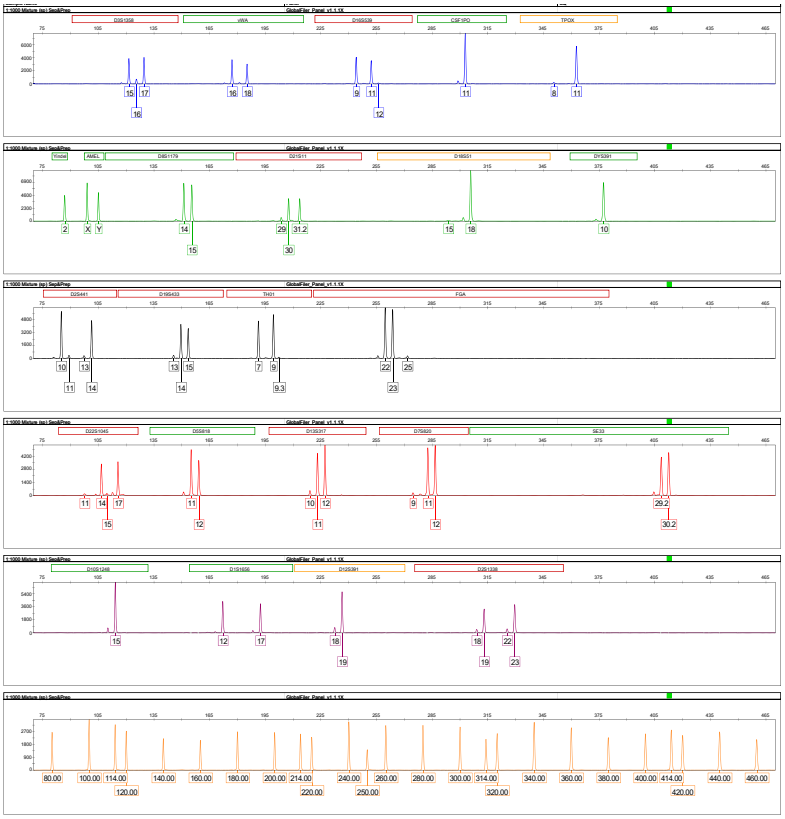


Figure 3. STR electropherogram obtained using the manufacturer-recommended Sep&Prep workflow for a 1:1000 male-to-female DNA mixture, showing a major male profile with minor female allele contributions.

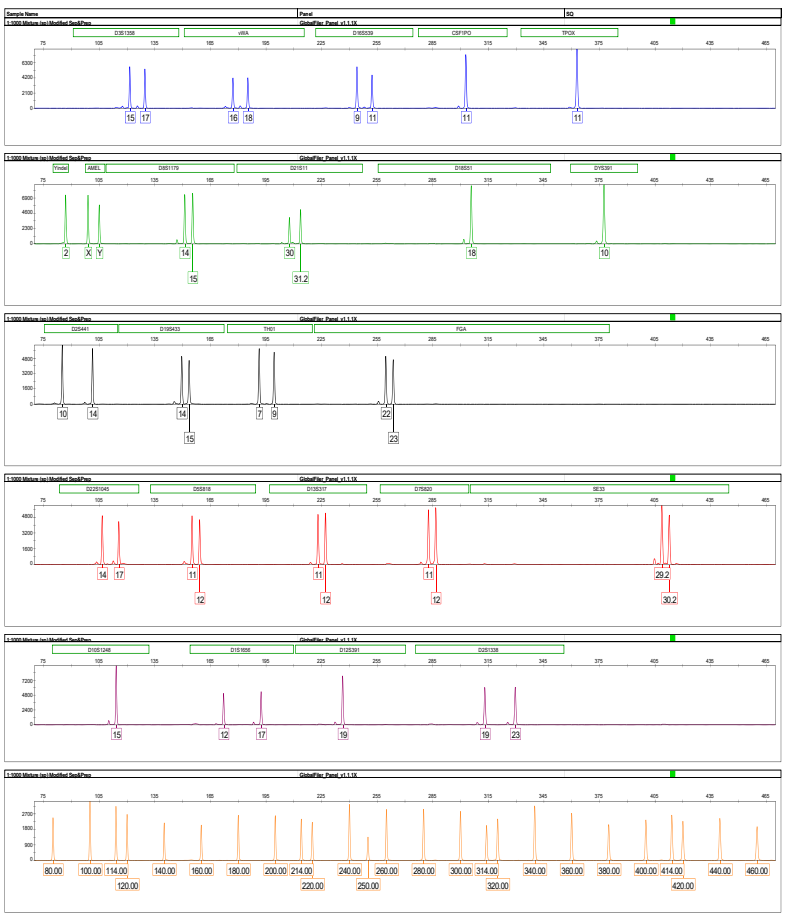


Figure 4. STR electropherogram obtained using the optimized workflow (100 × g centrifugation, 10-minute epithelial lysis incubation, and single lysis cycle) for a 1:1000 male-to-female DNA mixture, showing a single-source male profile with no detectable female alleles.

.

4. Conclusion

Optimization of key parameters in the EZ2 DNA Investigator Sep&Prep workflow significantly improved sperm DNA recovery and mixture purity. The optimized conditions - 100 × g centrifugation, a single epithelial lysis cycle, and a 10-minute incubation - enabled recovery of single-source male DNA profiles from highly imbalanced 1:1000 mixtures (Figure 3 & 4). Low-speed pre-treatment also preserves non-cellular proteins such as PSA for potential forensic screening assays. These findings demonstrate that small workflow adjustments can enhance automated sperm separation for routine forensic casework.

References

1. *Dash HR., 2024. Advancements in differentiation between sperm cells and epithelial cells for efficient forensic DNA analysis in sexual assault cases. International journal of legal medicine, 138(6), pp.2209-2227.*
2. *Qiagen EZ2 DNA Investigator Sep&Prep Kit Brochures & Guides:Automated processing of sexual assault samples using EZ2® Connect Fx.*
3. *Hess SA, Kraemer M, Terramagra D, et al. Development of a new automated EZ2® Connect Fx sexual assault sample processing kit. Poster presented at: International Symposium on Human Identification (ISHI); 2025 Nov 3–6; Palm Beach, Florida, USA.*
4. *Qiagen EZ2 DNA Investigator Sep&Prep Kit Handbook: For automated processing of sexual assault samples and sperm. cell DNA preparation using the EZ2 Connect Fx instrument, 2025, pp.1-36.*

Enhancing Forensic Sperm Detection Using Motorized Microscope and Deep Learning Improving Accuracy and Efficiency Through Automated Imaging and Neural Network Optimization

Hurin Ain Wan Abi Sabian*, Nur Fitrah Abd Ghani, Erizasyira Basri, Nor Fazelin Mat Zain, Siti Hajar Hussin, Mohd Izuan Othman and Nor Aidora Saedon
Department of Chemistry, Malaysia
Email: hurinain@kimia.gov.my

Abstract:
Rapid identification of spermatozoa is a critical component of forensic sexual assault investigations. This study evaluates the performance of the Olympus BX63–MetaSystems scanning microscope. A novel integration compared to the globally prevalent Zeiss-MetaSystem standard for automated sperm detection on Christmas Tree–stained slides. In addition, dataset-specific deep neural network (DNN) optimisation was incorporated within the Metafer system to improve classification performance and ensure reliable sperm identification during slide analysis. Notably, this research introduces a non-coverslip scanning technique, diverging from the worldwide practice of coverslip-slide pairing. Analysing 50 paired forensic samples, automated microscopy decreased average search times by 49% (from 5.99 to 3.06 minutes; $p < 0.001$). Bland–Altman analysis confirmed a consistent bias of 2.93 minutes without proportional error. Following DNN optimisation, classification accuracy improved markedly from 58.6% to 97.0%, demonstrating the effectiveness of tailored model training compared to baseline system performance. These findings demonstrate that the Olympus-based non-coverslip workflow significantly improves efficiency, consistency, and classification reliability, supporting its adoption in forensic laboratory workflows to manual microscopy.

Keywords: *Spermatozoa detection, forensic sexual assault investigations, automated microscopy, deep learning.*

1. Introduction

Microscopic sperm identification remains the cornerstone of forensic sexual assault screening. Despite advances in DNA profiling, microscopy continues to be the primary screening method in routine practice, with the Christmas Tree stain commonly used to differentiate spermatozoa from epithelial cells and background debris [1].

Traditional manual microscopy, while well established,, is labour-intensive, time-consuming, and highly dependent on the examiner's expertise. Differences in interpretation, along with fatigue during extended examinations, can affect consistency, especially in high-throughput settings.

Automated microscopy using Metafer has emerged as a promising alternative, combining motorised slide scanning with computational image analysis. This system utilises deep neural network (DNN) algorithms to classify detected objects as Spermatozoa, Unsure or Background, with recent advances in deep learning significantly enhancing object recognition in biomedical imaging [2]. Despite these advancements, there is limited evaluation of Metafer performance under real forensic casework conditions, particularly with optimised DNN models.

This study evaluates the transition from manual cover slipped microscopy to the newly integrated Olympus BX63–MetaSystems, introducing a streamlined non-coverslip scanning technique to optimize forensic workflows, focusing on search time efficiency, variability, agreement, and the effect of DNN optimisation on classification accuracy.

2. Materials and Methods

2.1. Study Design and Samples

A paired comparative study design was used to enable direct comparison between manual and automated microscopy. Fifty (n = 50) previously stained forensic slides from sexual assault casework were examined, with all samples analysed by both manual microscopy and automated microscopy (Metafer).

Additionally, a separate set of seventy-nine (n = 79) slides was assessed using automated microscopy (Metafer) to evaluate classifier performance before and after deep neural network (DNN) training.

2.2. Manual Microscopy

Slides were analysed using a Leica DM500 microscope at 100× magnification. Each slide underwent systematic scanning, with search time measured from initial placement to the end of examination. All manual assessments were conducted by a small team of trained analysts under standard laboratory conditions.

2.3. Automated Microscopy (Metafer) and DNN Classification

All slides were subsequently processed using the Metafer system under standardised conditions without coverslips. Automated scanning generated candidate objects, which were classified by a deep neural network (DNN) as Spermatozoa, Unsure or Background. All results were subsequently reviewed by an analyst for verification.

2.4. DNN Optimisation

Classifier performance was assessed both before (baseline V2 (FSPD-OD-V3.1.1)) and after (optimised V6 (FSPD-OD-V3.1.4)) dataset-specific training using annotated sperm images derived from forensic casework slides, enabling evaluation of classification improvements achieved through domain adaptation.

2.5. Statistical Analysis

Search times were analysed using paired t-tests, with statistical significance defined as $p < 0.05$. Effect sizes (Cohen's d) and 95% confidence intervals (CI) were also calculated. Agreement between the two methods was evaluated using Bland–Altman analysis.

3. Results

3.1. Search Time Comparison

Manual microscopy showed a significantly longer mean search time (5.99 minutes) compared to automated microscopy (3.06 minutes), as shown in Table 1, reflecting an average reduction of 2.93 minutes (approximately 49%). This difference was statistically significant ($p < 0.001$), with a 95% confidence interval (CI) of 2.35–3.51 minutes.A large effect size was observed (Cohen's d = 1.43, 95% CI: 1.03–1.83), indicating a substantial and consistent decrease in search time with automated microscopy. This improvement is both statistically robust and practically meaningful, supporting greater efficiency in routine forensic laboratory workflows.

Table 1. Comparison of search time performance between manual microscopy and automated microscopy (Metafer).

Parameter	Manual Microscopy	Automated Microscopy (Metafer)	Statistical Comparison
Mean search time (min)	5.99	3.06	Mean difference: 2.93 (95% CI: 2.35–3.51)
Range (min)	0.53–13.28	1.15–6.54	Greater variability in manual microscopy
Standard deviation (min)	2.35	1.35	Reduced variability with automation
Relative reduction (%)	—	—	49% reduction
Limits of agreement (min)	—	—	0 to 6
p-value	—	—	< 0.001
Effect size (Cohen's d)	—	—	1.43

As shown in Figure 1, manual microscopy showed a wider distribution of search times, with greater variability and several higher-value outliers. In contrast, automated microscopy demonstrated a more compact distribution, suggesting improved consistency across samples.

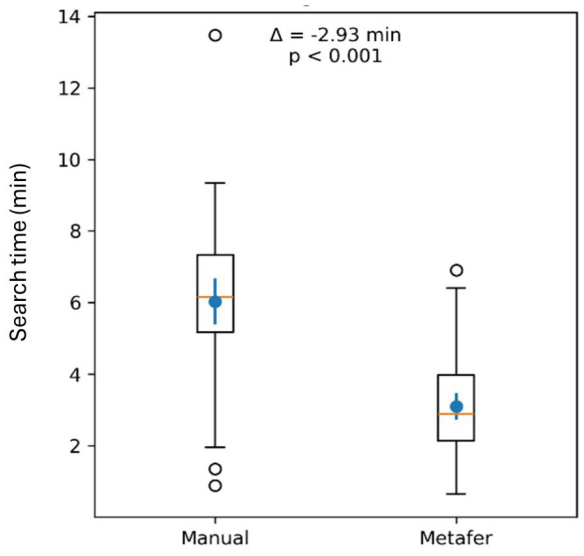


Figure 1. Distribution of search time for manual and automated microscopy (Metafer).

The paired comparison plot (Figure 2) further demonstrates this consistency. Most samples showed reduced search times when analysed using automated microscopy (Metafer), as indicated by predominantly downward-sloping lines, with only a few cases showing minimal or no improvement.

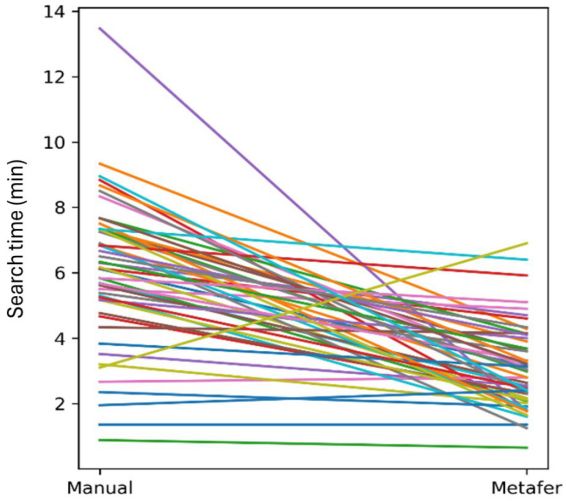


Figure 2. Paired comparison of search time between manual and automated microscopy (Metafer).

3.2. Variability and Distribution

Manual microscopy showed greater variability in search time, with values ranging from 0.53 to 13.28 minutes. Automated microscopy (Metafer) showed a narrower range of 1.15 to 6.54 minutes, with most results concentrated between 1 and 4 minutes. This pattern indicates that automated microscopy may provide more consistent performance and reduce dependence on operator-related factors.

3.3. Detection Observations

Qualitative observations showed that some spermatozoa missed during manual microscopy were subsequently identified with automated microscopy, suggesting potential improvement in detection capability, particularly in more challenging samples.

3.4. Agreement Analysis

Bland–Altman analysis showed a mean bias of 2.93 minutes, indicating that automated microscopy consistently produced shorter search times than manual microscopy. The 95% limits of agreement ranged from approximately 0 to 6 minutes, with no evidence of proportional bias, as shown in Figure 3. This supports the consistency of automated microscopy across different sample conditions.

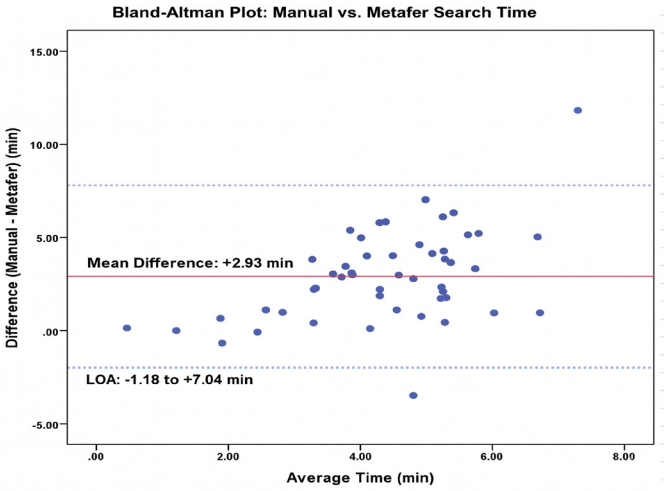


Figure 3. Bland–Altman Plot Comparing search time between manual microscopy and automated microscopy (Metafer).

3.5. DNN Classification Performance

As illustrated in Figure 4, DNN optimisation markedly improved all classification performance metrics. Classification accuracy increased from 58.6% to 97.0%, while sensitivity and specificity improved to 97.1% and 97.0%, respectively. Positive predictive value (PPV), negative predictive value (NPV), and F1-score also increased substantially following optimisation.

Overall, these findings demonstrate that DNN training significantly improved all evaluated metrics, with notable gains in specificity and PPV, indicating a reduction in false-positive detections and improved discrimination between spermatozoa and background artefacts.

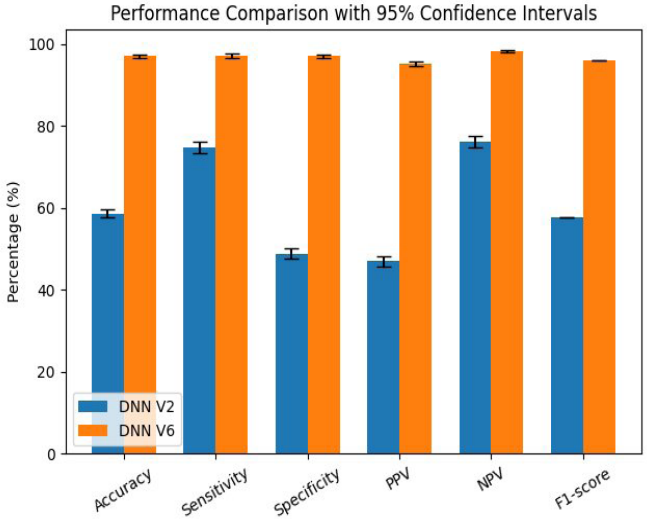


Figure 4. Performance comparison of DNN V2 and DNN V6 across classification metrics.

4. Discussion

This study indicates that automated microscopy using the Olympus BX63–MetaSystems substantially enhances both efficiency and consistency in forensic sperm detection workflows when compared with manual microscopy. The observed 49% reduction in search time reflects a meaningful improvement in laboratory throughput and has potential to reduce casework backlog and improve turnaround time in forensic sexual assault investigations. The reduced variability associated with automated microscopy and non-coverslip approach underscores its benefits in terms of standardization and reproducibility. In contrast, manual microscopic techniques with coverslip technique are inherently dependent on the operator and may be affected by fatigue-related variation, whereas automated systems maintain more consistent performance. These findings are consistent with previous studies reporting improved efficiency and reduced variability with automated or semi-automated microscopy systems [1].

The identification of spermatozoa in samples missed during manual examination suggests improved detection capability, particularly in low-concentration or high-background conditions. This supports the application of deep learning–based approaches in enhancing detection sensitivity, as reported in earlier studies [1]. Notably, DNN optimisation played a key role in overall system performance. The significant gains in specificity and PPV reflect a reduction in false-positive detections, which is critical in forensic analysis to minimise misinterpretation. The decrease in candidate objects also reduces the workload associated with manual verification, thereby further improving workflow efficiency. Bland–Altman analysis confirmed a systematic tendency toward shorter search times with automated microscopy, with no evidence of proportional bias, indicating stable performance across different sample conditions [3].

Despite these improvements, several limitations should be considered. The study was based on a relatively limited number of samples, and the performance of the DNN model may depend on the representativeness and quality of the training dataset. In addition, although false-positive rates were reduced, the potential for misclassification cannot be completely excluded, particularly in complex or degraded samples. Manual microscopy therefore remains important for confirmatory evaluation, particularly in complex or borderline cases. Accordingly, a hybrid approach combining automated screening with expert review is recommended to ensure both efficiency and reliability in forensic casework applications.

5. Conclusion

Automated microscopy with the Metafer system using non-coverslip approach, supported by DNN optimisation, enhances efficiency, consistency, and classification accuracy in forensic sperm detection. These findings support its adoption in routine forensic laboratory workflows, particularly in high-throughput settings.

References

1. *Topping DC, Egan SE., Tran T, et al, Automated microscopy in forensic biology: Validating the use of deep neural networks for the detection of human spermatozoa in Christmas Tree-stained slides. Science & Justice. 2026, 66, 1-16.*
2. *Litjens G, Kooi T, Bejnordi BE, et al, A survey on deep learning in medical image analysis. Medical Image Analysis. 2017, 42, 60-88.*
3. *Bland JM, Altman DG, Statistical methods for assessing agreement between two methods of clinical measurement. The Lancet. 1986, 1, 307–310.*

Streamlining Forensic DNA Analysis: A Strategic Approach to Laboratory Automation

Shilen Ng, An Ting Nicole Tang*, Ruizhu Patricia Ang and Suan Annabel Tay
Health Sciences Authority, Singapore
*Email: Nicole_TANG@hsa.gov.sg

Abstract:
Forensic DNA laboratories face increasing pressure to improve casework throughput and traceability without compromising analytical quality. This study validates the Hamilton STARlet automated liquid handling workstation for three critical DNA workflows: extraction using DNA IQ™ chemistry, quantification setup with Quantifiler® Trio, and PCR amplification preparation using GlobalFiler™ and YFiler™ Plus in accordance with the SWGDAM validation guidelines. Extraction efficiency was comparable to the Maxwell platform across most sample types, with sample-type dependent limitations observed for blood swabs containing high DNA volumes. The system achieved excellent precision with the coefficient variations typically below 20% for quantification and amplification workflows. No cross-contamination was detected throughout the validation studies. The Hamilton STARlet achieved a 40% reduction in hands-on time whilst providing enhanced sample tracking and complete audit trails. These results support its implementation for routine forensic casework, with significant operational advantages in throughput, traceability and sample integrity.

Keywords: *Automation, DNA extraction, DNA quantification, DNA amplification*

1. Introduction

Modern forensic laboratories face increasing caseloads whilst maintaining stringent analytical standards for DNA analysis. Traditional workflows often involve coordination between multiple platforms, presenting challenges that laboratory professionals recognise all too well. The Health Sciences Authority (HSA) DNA Profiling Laboratory's existing workflow operated across three distinct platforms: Maxwell RSC/FSC for extraction, epMotion 5070/5073 for quantification setup, and epMotion 5073 for amplification preparation. These platforms have proven reliable and well-suited to routine forensic casework. The Maxwell RSC/FSC offers a compact footprint and straightforward operation that makes it an attractive option for smaller laboratories with moderate sample volumes, whilst the epMotion series provides consistent and precise liquid handling with minimal setup complexity. However, as caseload demands grow, this multi-platform approach presents clear limitations including restricted throughput (maximum of 48 samples), single-channel pipetting constraints, limited deck space, and absence of integrated sample tracking capabilities.

The solution explored here is the implementation of the Hamilton STARlet liquid handling workstation — an open system capable of consolidating all three workflows into one seamless, automated platform with 8-channel pipetting capability, 96-sample throughput, integrated barcode scanning, and comprehensive audit trail functionality. Whilst the STARlet requires greater initial investment and setup complexity compared to the existing platforms, its consolidation of workflows and enhanced traceability features address the specific operational pressures faced by high-throughput forensic laboratories.

The work was designed according to SWGDAM validation guidelines [1], and the data presented here represent a subset of the comprehensive internal validation completed at HSA.

2. Materials and Methods

Where applicable, results from STARlet runs were compared with the laboratory's current methods. Sample swabs were pre-processed with Promega Casework Extraction Kit. The cell lysates were then loaded either into the DNA IQ™ Casework Kit sample cartridge or into 1.5 mL microfuge tubes which were subsequently placed in the microfuge carriers on the STARlet deck. Purified DNA was eluted in 56 µL elution buffer supplied in the DNA IQ™ Casework kit. DNA samples were quantified using Quantifiler® Trio DNA Quantification Kit on the QuantStudio™ 7 Real-time PCR system, and were amplified with GlobalFiler™ (GF) and YFiler™ Plus (YF) kits on the Proflex™ PCR system. Capillary electrophoresis was carried out using the 3500xL Genetic Analyzer and all data were analysed using GeneMapper™ ID-X software v1.6 or v1.7.

2.1. DNA Extraction

Extraction uniformity was evaluated using two full 96-well plates with liquid blood samples (1 µL per well), with each plate containing samples from a single donor. This design enabled identification of positional effects, including corner and edge anomalies, and assessment of both intra-plate extraction consistency and inter-plate operational reproducibility through coefficient of variation (CV) calculations. To evaluate accuracy of the extraction and purification process, the extracted NIST 2391d component E standard was amplified using GF, with the resulting STR profile checked for profile concordance. Sensitivity study was conducted using blood-stained swabs tested in triplicate across eight blood volumes ranging from 0.005 µL to 25 µL. Ten different mock casework sample types were processed in quintuplicate to evaluate DNA yield and compare performance against Maxwell extraction. Contamination studies used blanks and blood samples arranged in checkerboard and zebra formats, ensuring samples from the same donor were not positioned in adjacent wells.

2.2. DNA Quantification

Mastermix dispensing consistency was evaluated through passive reference dye analysis and Internal PCR Control (IPC) CV calculations of the THP DNA standard dilutions. Standard curve preparation performance used THP DNA standards with a modified volume (15 µL versus manufacturer's recommended 10 µL) for the first dilution whilst maintaining the dilution factor to accommodate instrument dead volume requirements. Sample dispensing precision was measured through CV analysis of the quantified values, whilst accuracy was assessed using NIST quantification standards (SRM 2372a) across different dilutions (3x, 9x and 27x) in triplicate. The STARlet's hit picking function was validated using different coloured dyes arranged in randomised sequences on the sample carrier. Contamination assessment used blanks and DNA arranged in a checkerboard pattern.

2.3. DNA Amplification

Rule-based amplification setup capabilities were tested using 14 samples run in triplicate, with automatic dilution factor calculations (2x to ≥100x) across different tube types (Eppendorf 1.5 mL, Microcon 1.5 mL, Promega 0.5 mL) using GF and YF amplification kits. Repeatability and reproducibility were assessed through CV analysis of peak heights. Contamination assessment used blanks and DNA arranged in a checkerboard pattern.

3. Results and Discussion

3.1. DNA Extraction

DNA extraction uniformity assessment across the 96-well plate demonstrated consistent performance. Figure 1 depicts the variation in DNA extraction yield across the full 96-well plate, with a similar trend observed for the second plate (data not shown). DNA concentrations ranged from 0.26-0.60 ng/µL with a mean of 0.43 ng/µL (CV 14.68%) for the first plate and 0.23-0.66 ng/µL with a mean of 0.36 ng/µL (CV 21.07%) for the second plate. The inter-plate CV was 19.60%. These results, combined with the absence of notable positional effects, confirm the instrument's suitability for routine high-throughput DNA extraction workflows.

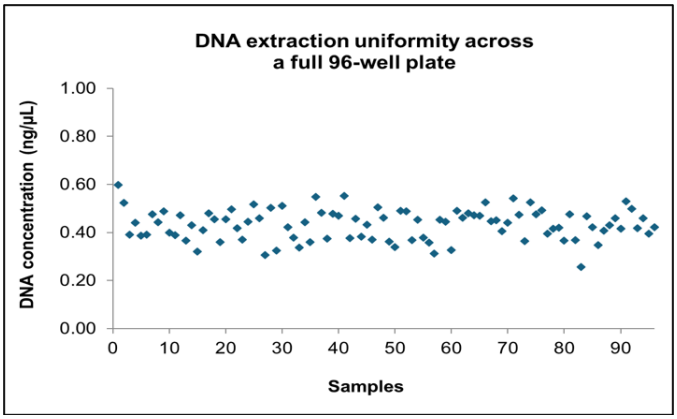


Figure 1. Dot-plot illustrating the extraction uniformity of the STARlet across a full 96-well plate, using liquid blood at 1 µL per sample from the same donor.

The NIST 2391d component E profile generated was 100% concordant to the expected genotype. The sensitivity study demonstrated effective DNA recovery from blood volumes ranging from 0.005 µL to 25 µL across two donors, with an approximately linear relationship observed up to 5-10 µL before plateauing or decreasing (Figure 2). One plausible explanation for this observation could be the presence of a large quantity of sample components competing for binding to the resin at higher blood volumes [2]. Similar decline in extraction efficiency at higher blood volumes was documented by Promega during their developmental validation of the Maxwell FSC DNA IQ™ Casework kit on the Maxwell RSC [3].

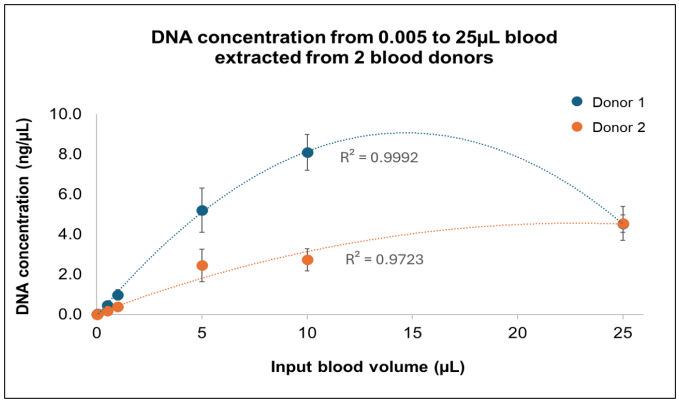


Figure 2. DNA concentrations obtained using STARlet, from swabs stained with varying blood volumes (0.005-25 µL) from two donors [mean ± SD, n = 3 per donor]. The dotted lines represent the polynomial curves of best fit for each donor, illustrating the non-linear relationship between blood volume and DNA concentrations obtained.

Full DNA profiles were obtained for blood volumes from 25 µL down to 0.05 µL, with partial profiles at 0.01 µL and 0.005 µL, showing mean allele recovery of 76-79% and 25-34% respectively. A similar trend was observed for Maxwell-extracted samples at the lower volumes tested (data not shown).

The STARlet demonstrated comparable extraction efficiency to Maxwell across most casework samples, with the notable exception of blood swabs stained with 50 µL neat blood, which consistently yielded lower DNA concentrations (Figure 3). The key distinction likely lies in their mixing mechanisms: Maxwell FSC/RSC employs plunger motion whilst STARlet uses orbital shaking, potentially affecting paramagnetic particle agitation and DNA yield. Interestingly, this reduced

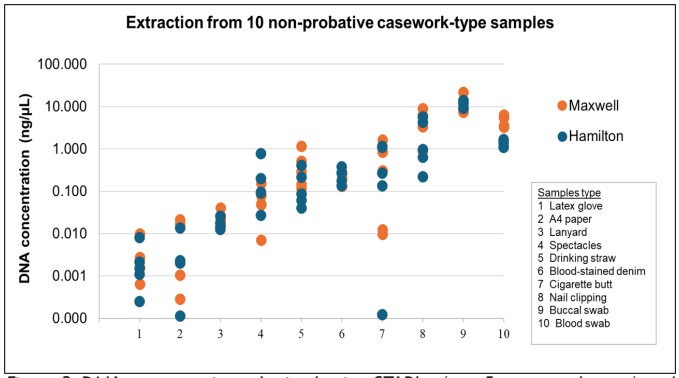


Figure 3. DNA concentrations obtained using STARlet (n = 5 per sample type) and Maxwell (n = 5 per sample type) from different casework sample types, with the Y-axis represented on a logarithmic scale.

recovery was not observed with buccal swabs despite their high DNA content, suggesting the extraction efficiency difference is sample-type dependent rather than concentration-dependent.

No contamination was detected in any of the blanks, as well as in any of the samples throughout the study, demonstrating the absence of cross-contamination between adjacent wells, and the overall reliability of the deck layout and extraction process in preventing sample-to-sample contamination.

3.2. DNA Quantification

The passive reference dye showed similar well-to-well variation between STARlet validation plates (CV ranging from 0.03-3.35%) and epMotion® 5070 casework plates (CV ranging from 0.54-3.23%) as illustrated in Figure 4, demonstrating comparable master mix dispensing consistency.

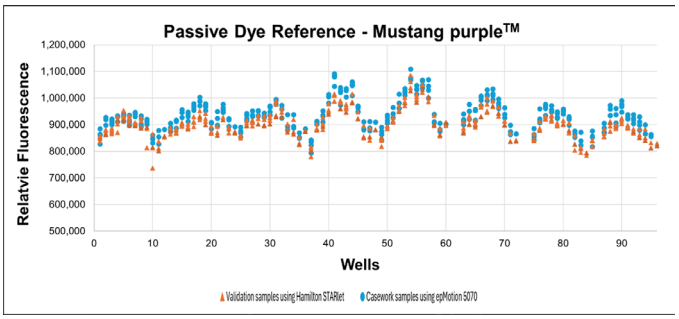


Figure 4. Fluorescence readings of Mustang™ passive reference dye from four independent runs of 96-well quantification plates prepared by STARlet (orange) versus epMotion® 5070 (blue).

The IPC CT values from the THP DNA standards further confirmed this consistency, with all validation plates achieving CV values below 1%, closely matching concurrent casework plates. This demonstrates consistent performance between STARlet and epMotion 5070 platforms (Table 1).

All validation plates achieved R^2 values ≥0.98 and slope values within manufacturer specifications (-3.0 to -3.6), confirming reliable standard curve preparation.

Intra-plate pipetting precision of samples were acceptable with CV of small autosomal target DNA ranged from 1.33% to 25.59% (majority below 15%). A similar trend

Table 1: CV for IPC CT values across four separate quantification plate runs using THP DNA standard dilutions (0.5, 0.05, and 0.005 ng/µL) in duplicate (n = 6 per run) on STARlet and epMotion 5070.

Platform	IPC C_T		
	Mean	Standard Deviation	CV (%)
STARlet (validation)	27.80	0.10	0.36
	27.04	0.16	0.60
	27.51	0.10	0.36
	27.79	0.13	0.46
epMotion 5070 (casework)	27.83	0.13	0.47
	27.34	0.12	0.45
	27.57	0.11	0.39
	27.49	0.09	0.33

was observed for the repeatability of the Y target. CV values ranged from 1.19% to 11.63%, with the majority below 10% (data not shown). Inter-plate CV was 7.00-13.89% (data not shown), demonstrating excellent run-to-run consistency.

Mean fold differences from NIST samples were within the laboratory's acceptance criteria (0.5x to 2.0x) ranging from 0.69 to 0.88 for both small autosomal and Y targets (Figure 5). concentrations from NIST quantification standard (3x, 9x and 27x dilution in triplicates).

The STARlet's hit picking function successfully dispensed samples into the correct wells despite randomised carrier sequences across the validation plates (Figure 6). No contamination was detected in the preparation of the quantification plates.

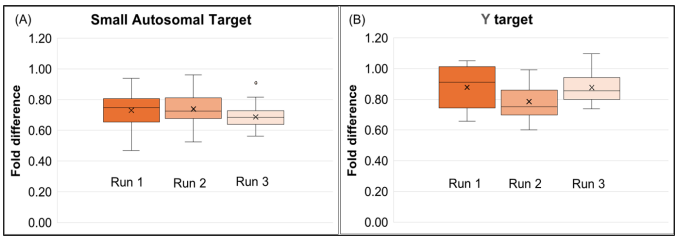


Figure 5. Fold difference of (A) small autosomal target (n = 27) and (B) Y target (n = 18, excluding NIST component B of female origin) DNA concentrations from NIST quantification standard (3x, 9x and 27x dilution in triplicates).

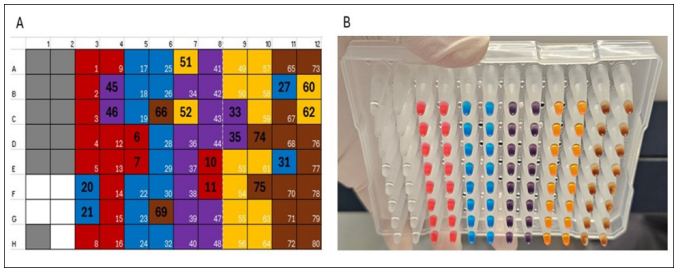


Figure 6. Diagram of a quantification plate with randomised sequence of samples that were placed onto the sample carrier (A), and diagram of quantification plate obtained after the STARlet run (B). The colours were concordant with the correct order provided by the sample worklist.

3.3. DNA Amplification

The observed average peak heights obtained from the GF and YF runs prepared by STARlet were generally consistent, regardless of the sample tube types. Average peak heights ranged from 3,394 to 14,910 RFU for GF amplifications at 1 ng input (Figure 7) and 2,847 to 12,456 RFU for YF amplifications (data not shown) at 0.5 ng input, consistently exceeding analytical thresholds. Overall, the performance of the Hamilton STARlet is comparable to that of the currently in-use Eppendorf epMotion® 5073 automated liquid handling workstation in preparing amplification setups.

The CV values of peak heights calculated for replicates within each run demonstrated acceptable repeatability across all tube types (Table 2) for GF. The average CV values were less than 20% across the different runs, indicating high precision with minimal variability between replicates. The CV values of peak heights calculated for replicates between the four GF runs ranged from 4.87% to 16.25% (Table 2), comparable to the epMotion® 5073's validated range of 8.62% to 23%.

Table 2. CV of peak heights for replicates within runs across four GF runs using three different tube types. CV was calculated across triplicates for all samples. (Note: [1]Refer to samples in Microcon tubes.)

	CV (%)				
	Within-Run				
Sample marking	Promega 0.5mL Run 1	Promega 0.5mL Run 2	Eppendorf 1.5mL	Eppendorf + Microcon 1.5mL	Between-Run
06069_1.1A	8.37	7.61	8.42	8.23[1]	15.86
06069_1.2A	5.20	5.75	11.59	10.58[1]	11.69
06069_1.3A	1.13	16.28	15.83	3.16	12.96
06069_1.4A	5.64	10.73	6.50	9.03	9.05
06069_1.9A	4.24	6.25	10.22	17.23[1]	10.99
06069_2.1A	10.51	3.72	10.99	12.17	10.26
06069_2.2A	6.80	4.59	17.04	12.98	13.44
06069_2.3A	10.39	12.94	5.62	14.74	15.39
06069_2.4A	2.95	6.88	3.40	4.82	4.87
06069_2.5A	11.48	8.04	12.47	2.76[1]	11.82
06069_2.6A	7.57	6.60	6.97	10	7.15
06069_2.7A	5.95	4.93	4.65	7.64	7.34
06069_3.5A	11.55	7.39	10.12	13.68[1]	9.95
06069_3.6A	7.51	3.79	11.71	32.13[1]	16.25
Average CV	7.09	7.53	9.68	11.37	11.22
Standard Deviation	3.18	3.58	4.02	7.34	3.42

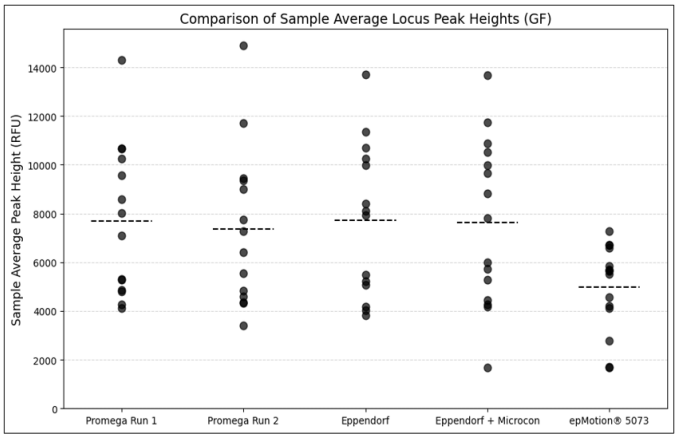


Figure 7. Comparison of sample average locus peak heights of 14 samples amplified with GlobalFiler with 1 ng DNA template across the 3 different tube types – Promega, Eppendorf, and Microcon. Each data point represents the average of 3 replicates of each of the 14 samples' average peak heights. The dashed horizontal line indicates the mean. The sample set used for the epMotion 5073 was a different set of samples amplified at 1 ng from a previous study and shown here for relative comparison.

This demonstrated acceptable reproducibility performance between different runs. The YF run demonstrated between-run CV values ranging from 6.12% to 18.94% (data not shown). Overall, these results demonstrated that the STARlet is able to perform consistently and achieve reproducible results across runs using multiple tube types and is comparable to the epMotion® 5073.

No contamination was detected in the checkerboard contamination assessments, demonstrating effective contamination control throughout the amplification workflow.

4. Conclusion

The validation revealed sample-type dependent limitations within the extraction process, with blood swabs demonstrating consistent saturation effects whilst buccal swabs containing similar high DNA content remained unaffected. The barcode-driven hit picking functionality achieved 100% accuracy, significantly improving consistency, throughput, and traceability compared to manual processes. Complete audit trails captured all sample movements, operator actions, and error events, thereby providing enhanced quality assurance capabilities that are essential for forensic applications.

Automation of the three DNA workflow processes using the Hamilton STARlet reduced manual hands-on time by approximately 40%, freeing up working hours for higher-level tasks. Despite requiring significant initial setup time and comprehensive staff training, the Hamilton STARlet successfully automates DNA processing workflows whilst maintaining analytical quality and introducing enhanced sample tracking capabilities.

The Hamilton STARlet represents a significant advancement in forensic laboratory automation, successfully consolidating three critical workflows whilst providing enhanced operational efficiency essential for modern forensic DNA laboratories.

References

1. *SWGDAM Validation Guidelines for Forensic DNA Analysis Methods; 2016.*
2. *Frégeau CJ, De Moors A. Competition for DNA binding sites using Promega DNA IQ™ paramagnetic beads. Forensic Sci Int Genet. 2012;6(5):511–22.*
3. *Developmental Validation of the Maxwell® FSC DNA IQ™ Casework Kit on the Maxwell® RSC Instrument [White Paper].*

Frequency of Y-Chromosomal Short Tandem Repeats in the Sri Lankan Population Using PowerPlex® Y23 System

Navindi Chathumini Mayakaduwa[1]*, Sujini Gamage[2] and Tharindra Weerakoon[1]
[1]University of Colombo, Sri Lanka
[2]Government Analyst's Department, Sri Lanka
Email: navindichathumini1999@gmail.com

Abstract:
This study focused on the genetic analysis of haplotype data from the Sri Lankan population, using allelic and haplotype frequencies of Y-chromosomal STRs. A sample of 185 unrelated male individuals was typed using the PowerPlex® Y23 system. A total of 182 distinct haplotypes were identified, of which 179 were unique. The gene diversity (GD) across the 23 Y-STR loci ranged from 0.352 to 0.939. The haplotype diversity was 0.9998, indicating high discrimination power (0.984) for these 23Y-STR loci in the forensic identification of Sri Lankan individuals. This discrimination power is comparable to that of neighboring Asian populations using the same markers. DYS385a/b was the most polymorphic marker (GD 0.939), while DYS391 was the least (GD 0.352). Three microvariant alleles and two null alleles were observed. The discrimination capacity of the PowerPlex® Y23 system was notably higher than that of the 12 Y-STR system, highlighting the effectiveness of the Y23 markers in differentiating male lineages. This study also aimed to establish the most common Y-DNA haplogroup for Sri Lanka.

Keywords: *Y-chromosomal STRs, Sri Lankan, Forensic analysis, Y-DNA haplogroup*

1. Introduction

Short Tandem Repeats (STRs) are highly polymorphic DNA segments consisting of 2-7 base-pair motifs repeated throughout the human genome. These markers are vital in forensic science because their extensive variability and broad distribution enable individual identification by examining differences in repeat units at various loci. The Y chromosome includes pseudoautosomal regions (PARs), which are not male-specific, and the nonrecombining region (NRY), which is male-specific owing to meiotic recombination.[1] Y-STRs are found within this nonrecombining region and serve as lineage markers, passed directly from father to son, often represented by a single haplotype. They are especially useful in forensic cases like sexual assaults, where male DNA is limited compared to female DNA, resulting in mixed profiles.

Y-STRs also play a vital role in paternity testing, missing-person identification, and disaster victim identification. Beyond forensic applications, Y-STRs aid in tracing paternal ancestry, prehistoric migrations, and understanding population structures across different ethnic and geographic groups. [2-6] Y-STR frequency data is essential in forensic casework. Allele frequency refers to how often a specific allele appears at a particular Y-STR locus within a population. It is used to calculate gene diversity, which measures the variability of alleles at that locus. The haplotype frequency of Y-STRs indicates the proportion of individuals in the population sharing a specific Y-STR profile. Haplotype diversity estimates the chance that two randomly chosen males will have different haplotypes. For forensic purposes, the match value shows the likelihood that two unrelated individuals have the same haplotype. The proportion of unique haplotypes, known as discrimination capacity, reflects the panel's ability to distinguish males within a population. Collectively, these parameters evaluate genetic variation and the effectiveness of Y-STR markers in forensic investigations.

Y-STR profiles are generated using commercial kits that target specific Y-chromosomal loci. The PowerPlex® Y23 System (Promega Corporation, USA) is a multiplex kit that co-amplifies 23 male-specific STR loci: DYS576, DYS389I/II, DYS448, DYS19, DYS391, DYS481, DYS549, DYS533, DYS438 (penta), DYS437, DYS570, DYS635, DYS390, DYS439, DYS392, DYS643 (penta), DYS393, DYS458, DYS385a/b, DYS456, and Y-GATA-H4. This offers higher resolution and better discrimination for male genetic profiling. [7]

Y-DNA haplogroups are genetic groups that share a common paternal ancestor. They are defined by unique SNP (single-nucleotide polymorphism) mutations in the Y chromosome, which is transmitted exclusively from father to son across generations. These haplogroups provide insights into evolutionary history and human migration patterns. They can help to determine the broad geographic region from which the paternal ancestors of the Sri Lankan population originated. [8]

There is a noticeable lack of detailed genetic data for the Sri Lankan population. This work focuses on establishing reference frequency values and haplotype data for the Sri Lankan population using a 23-locus panel. Frequencies help forensic practitioners evaluate Y-STR matches, especially in reporting cases, indicating how common or rare a profile is. Creating Sri Lankan Y-DNA haplogroup data provides a baseline for paternal genetic makeup. Comparing haplogroups with regional populations helps understand genetic relationships, migration, and ancestry.

2. Materials and Methods

Blood samples were collected from 185 unrelated male individuals across all nine provinces of Sri Lanka as part of a national survey. These samples reflect a diverse population, encompassing all ethnicities across Sri Lanka. Permission to use the samples was obtained from the Government Analyst's Department in Battaramulla, Sri Lanka. All survey participants provided informed written consent before inclusion in the study.

DNA extraction was performed using the QIAamp® DNA Investigator Kit (QIAGEN) following the manufacturer's recommended protocol. [9] Quantification of the DNA extracts was performed on the Applied Biosystems™ 7500 instrument using the Quantifiler™ Trio Kit.[10] DNA was amplified by PCR using the PowerPlex®Y23 (Promega) Kit [11] on the GeneAmp® PCR System 9600 thermal cycler (Applied Biosystems). Positive and negative amplification controls were used to assess amplification efficiency. The PCR amplicons were separated on the 3500/3500xL Genetic Analyzer (Applied Biosystems). [12] Allele designations were made using GeneMapper® ID-X V1.5 software (Promega). [13]

Statistical analysis

Allele and haplotype frequencies were determined through counting. Haplotype diversity was estimated using Nei's formula[4]: $HD = (1-\sum pi^2) *n/(n-1)$, where n is the sample size and pi is the frequency of the i^{th} haplotype. Gene diversity (GD) was derived as $1-\sum pi^2$, with pi indicating the allele frequency. The match probability (MP) was calculated as $\sum pi^2$, where pi is the frequency of the i^{th} haplotype. Discrimination capacity was computed as DC = h/n, with h being the number of different haplotypes.

Y-DNA Haplogroup Establishment

Genetic markers suitable for developing the Y-DNA haplogroup were identified by analyzing allele frequencies in the sampled Sri Lankan population. Alleles with a frequency greater than 0.5 were selected, based on the criterion that they are present in at least half of the population. This ensures that the constructed haplogroup represents the common genetic distribution.

3. Results and Discussion

There were 166 alleles across the 23Y-STR loci in 185 samples. The number of alleles per locus varied (Table 1). The most polymorphic marker was DYS385a/b (GD 0.939), and the least polymorphic was DYS391 (GD 0.352). Three microvariant alleles and two null alleles were identified. Two microvariant alleles appeared at the DYS481 locus, while one was found at the DYS385a/b locus. The null alleles were observed at the DYS448 and DYS389II loci, respectively.

Haplotype data were obtained from a sample of 185 unrelated Sri Lankan male individuals. A total of 182 different haplotypes were identified, of which 179 were unique, with a haplotype frequency of 0.005. Three haplotypes were observed in six individuals (two individuals each), with a haplotype frequency of 0.011. However, when the entire data set was examined, haplotype diversity was high (0.9998), indicating greater discriminatory capacity (0.984) for these 23 Y-STR loci in the forensic identification of Sri Lankan individuals. The match probability was about 0.56%, which is very low and indicates strong discriminatory power. High frequency of singleton haplotypes and comparatively low frequency of doubleton haplotypes are observed in the population (Figure 1).

Table 1. Summary statistics table listing the number of alleles, the most frequent allele and its frequency, and the genetic diversity values for each locus.

Locus	No. of alleles	Most frequent allele	Frequency	GD
DYS576	9	18	0.357	0.781
DYS389 I	5	13	0.476	0.645
DYS448	7	19	0.492	0.619
DYS389 II	7	29	0.249	0.798
DYS19	4	15	0.459	0.636
DYS391	4	10	0.789	0.352
DYS481	12	23	0.449	0.626
DYS549	6	12	0.524	0.645
DYS533	7	12	0.546	0.606
DYS438	6	11	0.449	0.672
DYS437	4	14	0.611	0.552
DYS570	11	19	0.238	0.835
DYS635	9	23	0.346	0.800
DYS390	8	22	0.297	0.768
DYS439	5	11	0.346	0.724
DYS392	6	11	0.622	0.569
DYS643	7	10	0.573	0.610
DYS393	6	13	0.416	0.743
DYS458	8	16	0.346	0.769
DYS385a/b	44	11,14	0.189	0.939
DYS456	7	15	0.584	0.589
Y-GATA-H4	5	12	0.551	0.595

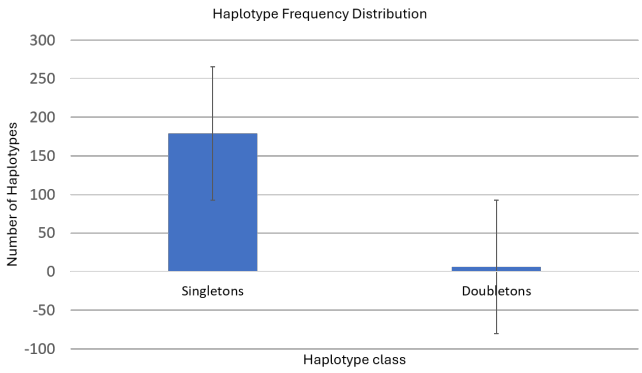


Figure 1. Haplotype frequency distribution.

Comparison of the 23-loci system and the 12-loci system

- Haplotype Diversity based on the 12-locus system using the PowerPlex® Y12 kit - 0.9948 [14]
- Haplotype Diversity based on the 23-locus system using the PowerPlex® Y23 kit- 0.9998

The 23-locus PowerPlex® Y23 system demonstrates significantly higher haplotype diversity.

Comparison of discrimination capacity among Asian Populations

This calculated discrimination ability of the Sri Lankan population is 0.984. Similar values have been reported for nearby Asian populations, including the Han population in Beijing, China (0.996), and the Chinese Yi minority (0.955). [15, 16]

Generation of the Sri Lankan Y- DNA haplogroup profile

A composite Sri Lankan haplogroup profile was generated by combining eight high-frequency alleles at individual loci (Table 2).

Table 2. Constructed Sri Lankan Y-DNA Haplogroup

Locus	Allele
DYS391	10
DYS437	14
DYS392	11
DYS643	10
DYS533	12
DYS549	12
DYS456	15
Y-GATA-H4	12

4. Conclusion

The analyzed 23 Y-STR loci demonstrated high haplotype diversity and discrimination power, and a low match probability, confirming their effectiveness for forensic identification. It demonstrates very high genetic resolution and indicates that a unique haplotype is present in almost every individual in the dataset. The high frequency of singleton haplotypes further reflects the strong discriminatory power of the panel. The multi-locus system showed greater discrimination capacity than lower-locus systems.

References

1. *Gusmão L, Angel C. Y Chromosome-specific STRs. 2003.*
2. *Kareem MA, Ameera OH, and Imad HH. Y-Chromosome short tandem repeat, typing technology, locus information and allele frequency in different population: A review. 14(27) pp. 2175-2178, July 2015.*
3. *Syndercombe Court D. The Y chromosome and its use in forensic DNA analysis. Emerging Topics in Life Sciences (2021) 5(3): 427–441.*
4. *Dogan S, Dragan P and Damir M. Genetic analysis of haplotype data for 23 Y-chromosome short tandem repeat loci in the Turkish population recently settled in Sarajevo, Bosnia and Herzegovina. Croatian Medical Journal 55, no. 5 (2014): 530–36.*
5. *Roewer, L. Y Chromosome STR typing in crime casework. Forensic Science, Medicine, and Pathology 5, no. 2 (2009): 77–84.*
6. *Jahangir I, Ajay KR and Romana R. Y-Chromosomal STR typing and case studies. In: Dash H, Shrivastava P, Mohapatra B, Das S. (eds) DNA Fingerprinting: Advancements and Future Endeavors. Springer, Singapore (2018).*
7. *PowerPlex® Y23 System. Https://worldwide.promega.com/products/forensic-dna-analysis-ce/str-amplification/powerplex-y23-system/?catNum=DC2305, 2026 (accessed 11 September 2026).*
8. *Y-DNA Tutorial - Genebase. Https://www.genebase.com/y-dna-tutorial/, 2026 (accessed 11 September 2026).*
9. *QIAamp® DNA Investigator Handbook. HB-0355-005_HB_QA_DNA_Investigator_0120_WW, 2026 (accessed 11 September 2026).*
10. *Quantifiler™ HP and Trio DNA Quantification Kits User Guide (Pub. No. 4485354 Rev. H).*
11. *PowerPlex ® Y23 System for Use on the Applied Biosystems ® Genetic Analyzers Instructions for Use of Products.*
12. *Applied Biosystems 3500/3500xL Genetic Analyzer User Guide. Https://assets.thermofisher.com/TFS-Assets/LSG/manuals/4401661.pdf, 2026 (accessed 11 September 2026).*
13. *USER BULLETIN GeneMapper ® ID-X Software Version 1.4 SUBJECT: New Features, Installation Procedures, and Software Verification Testing. Https://assets.thermofisher.com/TFS-Assets/LSG/manuals/4477684B.pdf, 2026 (accessed 11 September 2026).*
14. *Illeperuma RJ, Markalanda D, Mountain JL, Ratnasooriya WD, et al. Haplotype data for 12 Y-chromosome STR loci of Sri Lankans. Forensic Science International: Genetics. 2009 Nov 8;4(4):e119–20.*
15. *Hao S, Xuan Z, Yan L, and Di L. Genetic diversities of 23 Y-chromosome short tandem repeat loci in a Han population in the Beijing region. Journal of Forensic Science and Medicine 4, no. 2 (2018): 111.*
16. *He G, Chen P, Zou X, et al. Genetic polymorphism investigation of the Chinese Yi minority using PowerPlex® Y23 STR amplification system. International Journal of Legal Medicine. 2017 Jan 16;131(3):663–6.*

Evaluation of Carbon-13 Isotope for Mitigating Detector Saturation in Quantitation of Methamphetamine, MDMA and Ketamine in Hair

Chock Ying Soo*, Mei Ling Evelyn Goh and Hooi Yan Moy
Health Sciences Authority, Singapore
**Email: soo_chock_ying@hsa.gov.sg*

Abstract:
In routine multi-drug hair testing, laboratories often encounter samples spanning a wide concentration range, from sub-ng/mg levels to concentrations exceeding 200 ng/mg. While sensitive LC-MS/MS methods enable reliable detection at low concentrations, high-concentration samples containing methamphetamine, 3,4-methylenedioxymethamphetamine (MDMA) and ketamine may exceed the instrument's linear dynamic range, resulting in detector saturation, distorted peak shapes, inaccurate quantitation and failure to meet ion ratio criteria required for confirmatory drug testing. Conventional mitigation strategies rely on sample dilution and re-analysis, which increase turnaround time and reduce analytical efficiency. This study evaluated the use of carbon-13 (^{13}C) isotope multiple reaction monitoring (MRM) transitions as an alternative to conventional carbon-12 (^{12}C) isotope transitions for the quantitation of high-concentration analytes in hair samples. Correlation studies using 233 authentic hair samples demonstrated good agreement between concentrations obtained from diluted samples analysed using ^{12}C transitions and non-diluted samples analysed using ^{13}C transitions. Evaluation of internal standard and calibrator performance supported the continued use of D_8-methamphetamine and a 1 ng/mg calibrator for routine analysis. Overall, this study demonstrates the practical applicability of ^{13}C isotope approach for mitigating detector saturation in high-concentration hair samples, enabling reliable identification and acceptable quantitative performance without additional sample dilution or preparation in routine forensic analysis.

Keywords: *Carbon-13 isotope, multi-drug hair testing, LC-MS/MS, detector saturation*

1. Introduction

Hair testing has emerged as an alternative biological matrix in forensic toxicology and workplace drug testing because it provides a longer detection window spanning weeks to months, whereas urine typically reflects drug use over only a few days [1-3]. This extended window provides investigators with a more comprehensive history of an individual's drug exposure patterns [4, 5].

Liquid chromatography tandem mass spectrometry (LC-MS/MS) is widely employed in forensic drug testing due to its high sensitivity and selectivity, allowing reliable detection of drugs and their metabolites at low concentrations in biological matrices [6-7]. However, this high sensitivity can present analytical challenges when analysing samples with high analyte concentrations, particularly for commonly encountered drugs such as methamphetamine, 3,4-methylenedioxymethamphetamine (MDMA) and ketamine. Drug concentrations in hair may span one to three orders of magnitude, and higher levels may exceed the instrument's linear dynamic range, resulting in signal saturation and failure to meet identification criteria.

One mitigation strategy involves analysing the carbon-13 isotopes of the target analytes, which exist in lower natural abundance and thereby reduce the risk of detector saturation while maintaining analytical accuracy. This approach has previously been demonstrated for methamphetamine and MDMA in oral fluid screening, where it enabled high-throughput forensic analysis without the need for sample dilution or re-injection [8].

This study aimed to evaluate the analytical performance and practical advantages of utilising carbon-13 (^{13}C) isotopes as an alternative to conventional carbon-12 (^{12}C) isotopes for addressing instrument saturation in hair drug testing. Specifically, the study sought to assess whether this approach could streamline laboratory workflows and reduce analysis time, while maintaining analytical reliability for high concentration samples encountered in routine forensic casework.

2. Materials and Methods

Certified reference materials of methamphetamine, 3,4-methylenedioxymethamphetamine (MDMA) and ketamine (1 mg/mL) were purchased from Cerilliant (Round Rock, TX, USA). Stock standard solutions at 100 µg/mL were prepared in HPLC-grade methanol from the certified reference materials. A combined working standard solution of methamphetamine, MDMA and ketamine was prepared from the individual stock solutions at concentrations of 500 ng/mL and 80 ng/mL and stored at -20 °C until use. Calibrators and quality control samples were prepared by spiking the working standards into drug-free hair samples and were analysed alongside authentic hair specimens submitted by the drug enforcement agencies.

Approximately 20 mg of hair sample was weighed into a ball-mill tube with ceramic beads (Omni International, Kennesaw, GA, USA). Sample digestion was performed by the addition of 0.12% hydrochloric acid in LC-MS-grade methanol, followed by pulverisation. The resulting mixture was then centrifuged at 15,000 rpm for 10 min. An aliquot of 0.5 mL of the supernatant was diluted with 0.5 mL of analytical Type I grade water and filtered through a Clean Screen FASt Cartridge (200 mg/3 mL; United Chemical Technologies, Bristol, PA, USA), followed by filtration through a 0.2 µm Econofilter nylon membrane (Agilent Technologies, Santa Clara, CA, USA) using a positive pressure manifold. The eluate was collected into sample vials for instrumental analysis.

Analysis was performed using a Waters (Milford, MA, USA) liquid chromatograph–tandem mass spectrometer (LC-MS/MS) system, comprising an Acquity UPLC I-class Plus System coupled with Xevo TQ-XS tandem mass spectrometer,

operated in positive electrospray ionisation (ESI) mode. Chromatographic separation was achieved using an Acquity UPLC BEH C18 column (1.7 µm, 2.1 x 100 mm). The mobile phases consisted of 10 mM ammonium formate with 0.1% formic acid (eluent A) and acetonitrile with 0.1% formic acid (eluent B), delivered at a flow rate of 0.4 mL/min.

The elution gradient was initially held at 5% B, increased linearly to 25% B in 2.5 min, followed by an increase to 40% B in 0.3 min, then to 60% B in the subsequent 2.2 min, and finally to 95% B in 0.1 min. This was maintained at 95% B for 1.9 min, then returned to 5% B in 0.1 min and re-equilibrated at this initial condition for 2.9 min prior to the next injection. The total run time was 10 min, and the injection volume was 2 µL.

Table 1: MRM transitions and corresponding collision energies for methamphetamine, MDMA and ketamine.

Analyte	MRM transition with most abundant ^{12}C isotope (^{12}C Transition)	Additional MRM transition with one ^{13}C isotope (^{13}C Transition)	Collision energy (eV)
Methamphetamine	150.10 > 91.00 150.10 > 119.00	151.05 > 92.00 151.05 > 120.00	16 10
MDMA	194.10 > 163.00 194.10 > 105.00	195.10 > 164.00 195.10 > 106.00	12 24
Ketamine	238.10 > 125.00 238.10 > 207.00	239.10 > 126.00 239.10 > 208.00	24 14

Multiple reaction monitoring (MRM) transitions incorporating one carbon-13 isotope for methamphetamine, MDMA and ketamine were added to the mass spectrometer acquisition method. The MRM transitions and their respective collision energies are listed in Table 1.

3. Results and Discussion

Evaluation of Carbon-13 isotope MRM transitions for enhanced LC-MS/MS analysis.

Conventional LC-MS/MS methods employ MRM transitions monitoring carbon-12 isotopes to achieve optimal sensitivity for low-level detection. However, when applied to samples containing high analyte concentrations, this approach frequently leads to detector saturation, resulting in distorted peak shapes and failure to meet ion ratio identification criteria, as illustrated in Figure 1. Traditional mitigation strategies rely on sample dilution, followed by re-analysis. However, this introduces additional analytical steps, extends turnaround times, and reduces overall laboratory efficiency.

Carbon-12 (^{12}C), carbon-13 (^{13}C) and carbon-14 (^{14}C) are the three naturally occurring isotopes of carbon, with ^{12}C being the most abundant at approximately 98.89%, followed by ^{13}C at approximately 1.108% and ^{14}C at trace levels (~1 x 10-10%) [9]. Given the negligible abundance and radioactive nature of ^{14}C, only ^{12}C and ^{13}C are considered stable isotopes for analytical applications.

The relatively low natural abundance of ^{13}C results in proportionally reduced signal intensities for ^{13}C-containing analytes in mass spectrometric analysis. For analytes containing multiple carbon atoms, the probability of incorporating one or more ^{13}C atoms increases proportionally with carbon number. However, the likelihood of incorporating two ^{13}C atoms into both precursor and product ions remains substantially lower than that of singly substituted (^{13}C) isotopologues, due to their lower combined natural abundance. Consequently, MRM transitions corresponding to a two-Dalton mass increment (2 x ^{13}C transitions) exhibit significantly reduced signal intensities than transitions incorporating a one-Dalton mass increment (^{13}C transitions), as illustrated in Figure 2.

Detection of MRM transitions incorporating one ^{13}C atom, corresponding to a one-Dalton mass increment for both precursor and product ions relative to the most abundant ^{12}C isotopologue, provides an optimal balance between sensitivity and analytical reliability. This approach maintains sufficient signal intensity to support reliable detection while minimizing the risk of detector saturation, thereby enhancing quantitation accuracy across a wide concentration range, as demonstrated in the correlation study below.

The relative natural abundances of ^{13}C to ^{12}C isotopes enable estimation of the probability of ^{13}C incorporation in molecular (precursor) ions. Based on reported natural isotopic abundances, the probability of substitution of a single atom by ^{13}C atom can be calculated as follows:

$$\frac{Abundance\ of\ Carbon\ 13\ isotope}{Abundance\ of\ Carbon\ 12\ isotope} = \frac{1.108}{98.89} \approx 1.1\ \%\ per\ carbon\ atom$$

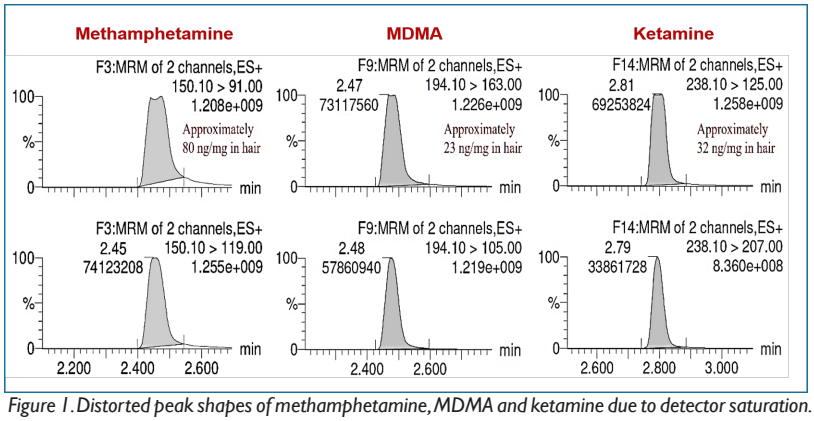


Figure 1. Distorted peak shapes of methamphetamine, MDMA and ketamine due to detector saturation.

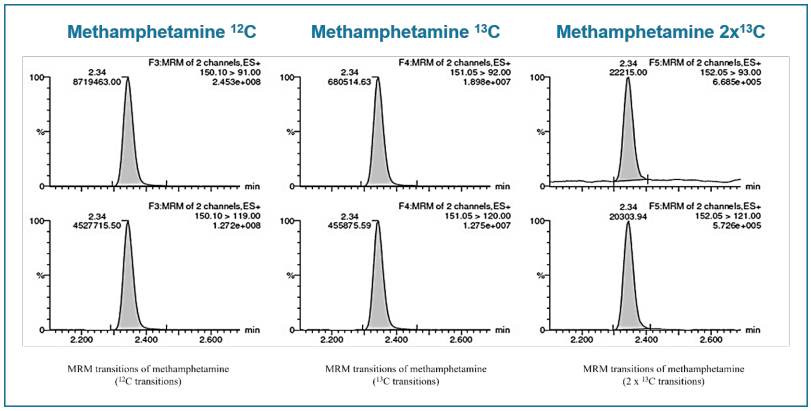


Figure 2. Signal intensities of MRM transitions of methamphetamine (^{12}C, ^{13}C and 2 x ^{13}C) of 1 ng/mg calibrator in hair.

For compounds containing multiple carbon atoms, the theoretical probability of incorporating one ^{13}C atom increases with the number of carbon atoms in the molecule. For methamphetamine ($C_{10}H_{15}N$), which contains 10 carbon atoms, the expected probability of a single substituted ^{13}C isotopologue is approximately 11.0 %. Similarly, MDMA ($C_{11}H_{15}NO_2$) and ketamine ($C_{13}H_{16}ClNO$) exhibit theoretical probabilities of approximately 12.1 % and 14.3 %, respectively.

However, the experimental observations did not fully align with these theoretical estimates. As summarised in Table 2, the observed signal intensities of the ^{13}C MRM transitions were lower than predicted based on the total carbon content of the precursor ions. This discrepancy is likely attributable to the loss of the ^{13}C atom during collision-induced dissociation, resulting in product ions that do not retain the isotopic substitution. These findings suggested that the observed isotopic abundance ratios are more strongly influenced by the number of carbon atoms retained within the monitored product ions than by the total carbon content in the precursor ions. Consequently, larger fragment ions are more likely to retain a ^{13}C atom and exhibit proportionally higher signal intensities than smaller fragments, consistent with the experimental data.

Table 2. Theoretical and experimental ratios of ^{13}C MRM transitions relative to ^{12}C MRM transitions for methamphetamine, MDMA and ketamine.

Analytes	Theoretical ratio of ^{13}C transition to ^{12}C transition	MRM Transitions (^{13}C)	Average experimental ratio of ^{13}C transition to ^{12}C transition[a] (n=10)
Methamphetamine	11.0 %	151.05 > 92.00	7.61 ± 0.17%
		151.05 > 120.00	9.81 ± 0.25 %
MDMA	12.1 %	195.10 > 164.00	11.08 ± 0.11 %
		195.10 > 106.00	8.94 ± 0.12 %
Ketamine	14.3 %	239.10 > 126.00	7.69 ± 0.08 %
		239.10 > 208.00	13.20 ± 0.13 %

[a]Experimental ratio of ^{13}C transition to ^{12}C transition = $\frac{\text{Abundance of 13C Transition}}{\text{Abundance of 12C Transition}}$

Correlation Study

A correlation study was conducted using 233 authentic hair samples to compare the concentrations of methamphetamine, MDMA and ketamine obtained from diluted samples analysed using ^{12}C MRM transitions with those from non-diluted samples analysed using ^{13}C MRM transitions. As illustrated in Figure 3, the degree of variance observed was found to be analyte- and concentration range-dependent.

Based on experimental observations, the differing correlation patterns among the three analytes could be attributed to differences in their ionisation efficiencies. MDMA, which exhibited the highest ionisation efficiency among the three analytes, demonstrated the most rapid onset of saturation, even when monitored using ^{13}C transitions. Consequently, greater deviations were observed for samples with MDMA concentrations exceeding 50 ng/mg, as these concentrations likely exceeded the instrument's linear dynamic range. Methamphetamine, with intermediate ionisation efficiency, showed good correlation ($R^2 > 0.98$) between the two approaches for concentrations up to 100 ng/mg. However, at higher concentrations, increasing deviations and non-linear behaviour were observed in the correlation plot, likely due to detector saturation. In contrast, ketamine, being the least sensitive among the three analytes, demonstrated the strongest correlation ($R^2 > 0.99$) across the entire evaluated concentration range, up to 138.0 ng/mg. Agreement between the two analytical approaches was further assessed by calculating the percentage differences from mean concentrations of methamphetamine, MDMA and ketamine determined using ^{12}C transitions in diluted samples and ^{13}C transitions in non-diluted samples, as summarised in Table 3.

Table 3. Percentage differences from mean concentrations of methamphetamine, MDMA and ketamine determined using ^{12}C transitions in diluted samples and ^{13}C transitions in non-diluted samples.

Analyte	Concentration Range (ng/mg)	Percentage Difference from Mean
Methamphetamine	5.8 - 98.3	0.02 % - 16.8 %
	101.3 - 165.3	10.1 % - 25.5 %
MDMA	7.7 - 37.7	0.7 % - 15.5 %
	55.3 - 130.4	16.4 % - 28.4 %
Ketamine	11.4 - 138.0	1.0 % - 9.0 %

As shown in Table 3, the percentage differences across all concentration ranges were within ±30 % and fulfilled the identification criteria. As this method is primarily intended for qualitative identification using pre-defined cut-off concentrations, the level of agreement observed between the two approaches is considered acceptable and fit for purpose.

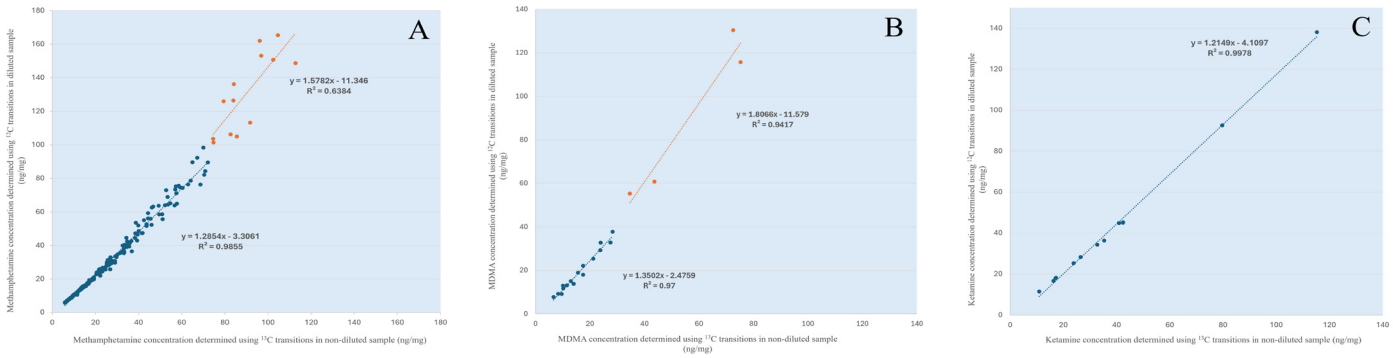


Figure 3. Correlation plots of concentrations of methamphetamine (A), MDMA (B), and ketamine (C) determined using ^{12}C MRM transitions in diluted hair samples versus ^{13}C MRM transitions in non-diluted hair samples.

Internal Standard and Calibrator Study

To further assess the quantitative performance in samples containing higher drug concentrations, 41 authentic hair samples from the correlation study were selected to evaluate the internal standard and calibrator used in the analysis. The ^{13}C MRM transition of the internal standard, D_8-methamphetamine (as listed in Table 4), was incorporated into the acquisition method to enable direct comparison of methamphetamine quantitation using both ^{12}C and ^{13}C MRM transitions.

Table 4. MRM transitions and corresponding collision energies for D_8-methamphetamine in the MS acquisition method.

Analyte	MRM transition	Collision energy (eV)
D_8-Methamphetamine	158.10 > 93.00	16
D_8-Methamphetamine with one ^{13}C isotope	159.10 > 94.00	16

The results indicated no significant improvement in analytical performance when employing the ^{13}C transition for the internal standard. Quantitation using the ^{12}C transition showed percentage differences from the mean ranging from 0.06 to 11.28%, with a coefficient of variation (CV) of 0.81%, while ^{13}C transition demonstrated differences of 0.01 to 10.15%, with a CV of 0.92%. Given the comparable performance between the two approaches and to maintain analytical simplicity, D_8-Methamphetamine using ^{12}C transition was retained as the internal standard for routine analysis.

In addition, the impact of calibrator concentration on methamphetamine quantitation using ^{13}C transitions was evaluated. A higher calibrator concentration of 10 ng/mg was applied for comparison against the 1 ng/mg calibrator used in routine quantitation of methamphetamine in hair samples. Comparison of these two calibrator concentrations showed minimal impact on analytical performance. Quantitation using the 1 ng/mg calibrator yielded percentage differences ranging from 0.06% to 11.28%, with a CV of 0.81%, while the 10 ng/mg calibrator resulted in percentage differences of 0.08% to 9.25% with a CV of 0.89%. Given the similar performance observed, the 1 ng/mg calibrator was retained for both ^{12}C- and ^{13}C-based quantitation, ensuring methodological consistency while maintaining good quantitative precision.

4. Conclusion

This study demonstrates that the use of ^{13}C isotope in LC-MS/MS analysis provides an effective approach for mitigating instrument detector saturation, a common challenge in forensic toxicology analysis. The proposed approach enables reliable quantitation of methamphetamine, MDMA and ketamine in high concentration hair samples that would otherwise exhibit signal saturation and failure to meet ion ratio identification criteria when analysed using the conventional ^{12}C transitions.

By eliminating the need for sample dilution, the method reduces analytical processing steps and turnaround time while maintaining acceptable quantitative accuracy across an extended concentration range. Correlation studies showed good agreement between results obtained using diluted samples analysed with ^{12}C transitions and non diluted samples analysed with ^{13}C transitions, supporting the robustness and applicability of the approach for multi-drug analysis. Overall, this approach represents a practical advancement in forensic hair analysis workflow, particularly for the assessment of high-level exposure to multiple drugs encountered in routine casework.

References

1. *Palamar JJ, Le A, Guarino H, et al. A comparison of the utility of urine- and hair testing in detecting self-reported drug use among young adult opioid users. Drug and Alcohol Dependence. 2019;200:161-167.*
2. *Rygaard K, Linnet K, Johansen SS. A systematic review of metabolite-to-drug ratios of pharmaceuticals in hair for forensic investigations. Metabolites. 2021;11(10):686.*
3. *Simão AY, Tokuyama PY, Zampieri G, et al. Analysis of drugs of abuse and contaminants in individuals under drug surveillance programs: A study in hair samples. Forensic Science International. 2025;371:112493.*
4. *Cooper GAA. Hair analysis in clinical and forensic toxicology (Chapter 1: Anatomy and physiology of hair, and principles for its collection). United States of America: Academic Press; 2015.*
5. *Skopp G, Strohbeck-Kuehner P, Mann K, et al. Deposition of cannabinoids in hair after long-term use of cannabis. Forensic Science International. 2007;170:46-50.*
6. *Orfanidis A, Mastrogianni O, Koukou A, et al. A GC–MS method for the detection and quantitation of ten major drugs of abuse in human hair samples. Journal of Chromatography B. 2017;1047:141-150.*
7. *Baciu T, Borrull F, Aguilar C, et al. Recent trends in analytical methods and separation techniques for drugs of abuse in hair. Analytica Chimica Acta. 2015;856:1-26.*
8. *Di Rago M, Chu M, Rodda LN, et al. Ultra-rapid targeted analysis of 40 drugs of abuse in oral fluid by LC-MS/MS using carbon-13 isotopes of methamphetamine and MDMA to reduce detector saturation. Anal. Bioanal. Chem. 2016;408(14):3737-3749.*
9. *Kim SH, Chuang JC, Kelly PB, et al. Carbon isotopes profiles of human whole blood, plasma, red blood cells, urine and feces for biological/biomedical 14C-accelerator mass spectrometry applications. Anal Chem. 2011;83(9):3312-3318.*

Application of Fortified Hair as Quality Control Sample in Multi-drug Analysis

Si Jia Chan* and Hooi Yan Moy
Health Sciences Authority, Singapore
**Email: chan_si_jia@hsa.gov.sg*

Abstract:
Authentic drug users' hair, although useful, is often unavailable for use as quality control sample in hair analysis. In-house prepared soaked hair can serve as practical alternative. In this study, drug-free hair (A) was immersed in aqueous solution containing 6-monoacetylmorphine (MAM), morphine, methamphetamine, methylenedioxymethamphetamine (MDMA), ketamine and flunitrazepam for five hours. Following washing and drying, the soaked hair (A1) was analysed using six replicates by liquid chromatography-tandem mass spectrometry (LC-MS/MS) to determine mean concentrations, standard deviation (SD) and coefficient of variation (CV). Additional data were collected over five months using LC-MS/MS (n=39) and gas chromatography-tandem mass spectrometry (GC-MS/MS) (n=17) to assess analytical variability and stability. A1 exhibited good stability over time, with reproducible results across both methods. Concentration ranges were evaluated against three acceptance ranges: mean ± 2SD, mean ± 20 % and mean ± 30 %. The ± 30 % range was most appropriate, accommodating day-to-day analytical variation with acceptable precision. To assess within-source and between-source variability, another soaked hair (A2) was prepared from the same hair source as A1 at a different time, while two additional preparations (B1 and B2) were made from a separate hair source (B). Differences in mean concentrations and acceptance ranges were observed between preparations and hair sources, indicating that each soaked hair preparation requires establishment of its own mean concentration and acceptance range for each individual drug analyte. In conclusion, in-house prepared soaked hair is a suitable quality control sample for routine hair analysis when specific ranges are established for each preparation.

Keywords: *multi-drug analysis, soaked hair, quality control, toxicology*

1. Introduction

Quality control (QC) is essential in toxicology testing as it ensures that results generated by the laboratory are valid and reliable. QC for hair analysis constitutes two parts: external and internal. External QC involves participation in a proficiency testing program, in which the laboratory analyses hair specimens provided by an external proficiency testing provider [1-3].

For internal QC, it is common practice to spike drug standards onto a drug-free hair matrix (hair blank) to mimic drug-containing hair. However, as hair is a heterogeneous matrix, spiked standards tend to remain on the outer surface of the hair and do not fully replicate the distribution of drugs in drug users' hair. This approach therefore cannot fully be used to replace authentic hair samples.

To address this problem, authentic hair from drug users should ideally be incorporated as part of QC, but supply is limited. Proficiency testing samples or commercially supplied controls offer a convenient alternative, but it is not cost effective for laboratories that analyse multiple hair batches per day.

Another approach is to prepare in-house QC by soaking drug-free hair in solution containing drug(s) of interest. This allows the drug(s) to be incorporated into hair matrix rather than residing on the surface [4]. A key advantage of this approach is the flexibility to customise drug content according to laboratory's specific requirements, such as the choice of drugs and their target concentrations [4]. Preparation of these drug-soaked hairs has been described in literature, with soaking duration ranging from 1 hour to several days, depending on the solvent used and drug(s) of interest [4-9].

In this study, soaked hair samples containing 6-monoacetylmorphine (MAM), morphine, ketamine, flunitrazepam, methamphetamine and methylenedioxymethamphetamine (MDMA) were prepared in-house. Using liquid chromatography-tandem mass spectrometry (LC-MS/MS) and gas chromatography-tandem mass spectrometry (GC-MS/MS), its suitability as routine QC was evaluated by assessing precision, stability and establishing appropriate concentration ranges. Variability across preparations using the same and different hair sources were also investigated.

2. Materials and Methods

Chemicals and reagents

Reference standards and internal standards (IS) were purchased from LGC, UK or Cerilliant, USA: codeine, morphine, MAM, amphetamine, methamphetamine, MDA, MDMA, norketamine, ketamine, flunitrazepam, benzoylecgonine, cocaine, D_3-codeine, D_3-morphine, D_6-MAM, D_5-amphetamine, D_8-methamphetamine, D_5-MDA, D_5-MDMA, D_4-norketamine, D_4-ketamine, D_5-nitrazepam, D_3-benzoylecgonine and D_3-cocaine.

Methanol, acetonitrile, dichloromethane, formic acid, ammonium formate, hydrochloric acid and ethyl acetate were of analytical grade. Heptafluorobutyric anhydride and 1,1,1,3,3,3-hexafluoro-2-propanol were purchased from Sigma-Aldrich, USA. SLE columns. ISOLUTE SLE+ 1 mL cartridges were purchased from Biotage AB, Sweden. 2 mL pre-filled tubes with ceramic beads were purchased from Revvity, USA. Clean Screen FASt cartridges (200 mg/3 mL) were purchased from United Chem Technologies (UCT), USA and 0.2 mm nylon Econofilters were purchased from Agilent Technologies, USA.

Drug-free hair

Two drug-free hair (sources A and B), collected from distal end, were obtained from friends and family members of laboratory staff. Prior to use, both hairs were decontaminated sequentially with dichloromethane, water and methanol. They were dried separately in an oven at 60 °C for a few hours and cut into approximately 5 mm segments to facilitate homogenization and enhance absorption of drugs into the matrix during soaking.

Preparation of drug-soaked hair

This preparation method was adapted from procedure previously described by Edder et al [9]. Approximately 3 g of drug-free hair was immersed in 100 mL aqueous solution containing 0.5 µg/mL of MAM, morphine, ketamine and flunitrazepam, and 0.15 µg/mL of methamphetamine and MDMA. The mixture was stirred using a magnetic stirrer for about 5 hours to facilitate drug incorporation into hair matrix. The aqueous solution was discarded and the hair was washed with 100 mL of water, followed by 100 mL of methanol. The washed hair was dried in an oven at 60 °C, transferred to a 30 mL amber bottle and stored at room temperature (about 25 °C). No additional washing was performed prior to analysis. To assess variability in the preparation process using same and different sources of hair, two independent preparations were performed for each hair: A1 and A2 from source A, and B1 and B2 from source B.

LC-MS/MS method

Sample preparation and instrumental analysis

About 20 mg of hair was processed in a 2 mL tube pre-filled with ceramic beads. 1 mL of acidified methanol [0.12% HCl (w/v)] and 40 µL IS consisting of 500 ng/mL of D_3-morphine, D_6-MAM, D_8-methamphetamine, D_4-ketamine and 250 ng/mL of D_5-nitrazepam were added and mixture was pulverised using the Omni Bead Ruptor 24 System. Pulverisation occurred at 5 m/s for 45 s with dwell time of 30 s for 10 cycles. Subsequently, centrifugation was carried out at 15000 rpm for 10 min. 500 µL of supernatant and 500 µL of Analytical Type 1 water were filtered using Clean Screen FASt cartridge attached to 0.2 µm nylon Econofilter under positive pressure. The filtrate was collected in an LC-MS/MS vial and analysed using instrumental conditions published by Chan et al [10]. Table 1 shows the drug, corresponding IS and MRM transitions for the method.

Table 1. Drug, corresponding IS and MRM transitions for the LC-MS/MS method.

Drug	MRM[a]	Corresponding IS	MRM[a]
Morphine	286.2 > 201.1 286.2 > 165.0	D_3-morphine	289.2 > 201.1
MAM	328.2 > 165.0 328.2 > 211.1	D_6-MAM	334.2 > 165.1
Methamphetamine	150.1 > 91.0 150.1 > 119.0	D_8-methamphetamine	158.1 > 93.0
MDMA	194.1 > 163.0 194.1 > 105.0		
Ketamine	238.1 > 125.0 238.1 > 207.0	D_4-ketamine	242.1 > 129.0
Flunitrazepam	314.1 > 267.9 314.1 > 238.9	D_5-nitrazepam	287.0 > 241.0

GC-MS/MS method

Sample preparation and instrumental analysis

The sample preparation and instrumental analysis have been discussed by Zhang et al [11].

3. Results and Discussion

Determination of soaked hair concentration

Target drug concentrations in the soaked hair were set at approximately 1 to 2 ng/mg, as this falls within the linearity range of both GC-MS/MS and LC-MS/MS methods. To achieve this, soaking solution containing MAM, morphine, ketamine and flunitrazepam were prepared at 0.5 µg/mL, while methamphetamine and MDMA were prepared at a lower concentration of 0.15 µg/mL.

This adjustment was necessary because an initial preparation at 0.5 µg/mL for all six drugs yielded methamphetamine and MDMA concentrations at approximately 3 to 4 ng/mg (data not shown). Such variability is consistent with differences in drug incorporation into hair, attributable to the inherent heterogeneity of the hair matrix and the physicochemical properties of individual drugs [12,13]. Accordingly, concentrations of methamphetamine and MDMA were reduced to 0.15 µg/mL to achieve the desired concentration range.

Evaluation of a preparation from a single hair matrix source

The laboratory employed a two-tier approach for detection of controlled drugs in hair. The first method utilised rapid sample preparation procedure in which pulverised hair was filtered via Clean Screen FASt cartridges prior to LC-MS/MS analysis. The second method incorporated sample clean up via supported-liquid extraction (SLE) followed by derivatisation prior to GC-MS/MS analysis. Analysis of authentic hair samples and proficiency test samples using both methods demonstrated good agreement [11], indicating either method can be used for establishing the mean concentration of individual drugs in soaked hair batches. However, due to its simpler and rapid sample preparation, the LC-MS/MS method was selected for determining mean concentrations in this study.

Soaked hair A1, prepared from hair source (A), was used to demonstrate statistical calculations and establish appropriate concentration range for routine monitoring. Six replicates of A1 were analysed using LC-MS/MS to determine mean drug concentrations, with each replicate analysed in separate run to maximise analytical variability. Statistically, a sampling size of n=6 provides 95 % confidence interval of approximately ±1 standard deviation (SD) around the mean concentration [14]. The coefficient of variation (CV) for A1 ranged from 4.2 % to 8.3 % (Table 2), indicating good analytical precision.

Table 2. Precision of 6 drugs in A1 using LC-MS/MS (n=6).

Drug	Mean (ng/mg)	SD	CV (%)	Concentration range (ng/mg)		
				mean ± 2SD	mean ± 20 %	mean ± 30 %
MAM	1.56	0.074	4.7	1.42 - 1.71	1.25 - 1.88	1.09 - 2.03
Morphine	1.51	0.063	4.2	1.38 - 1.63	1.20 - 1.81	1.05 - 1.96
Methamphetamine	1.11	0.084	7.6	0.941 - 1.28	0.887 - 1.33	0.776 - 1.44
MDMA	1.39	0.115	8.3	1.15 - 1.62	1.11 - 1.66	0.970 - 1.80
Ketamine	2.23	0.097	4.3	2.03 - 2.42	1.78 - 2.67	1.56 - 2.90
Flunitrazepam	1.48	0.121	8.2	1.24 - 1.72	1.18 - 1.78	1.04 -1.92

To further evaluate the performance of A1 and define the acceptable concentration ranges for routine analysis (mean ± 2SD, mean ± 20 %, or mean ± 30 %), additional data were collected over a five-month period using LC-MS/MS (n=39) and GC-MS/MS (n=17). The concentration ranges and precision for individual drugs obtained from both methods are summarised in Table 3.

The CV for LC-MS/MS method ranged from 3.6 % to 7.4 %, while GC-MS/MS ranged from 3.7 % to 10.4 % (Table 3), further demonstrating good precision of A1 across both methods. However, most drugs did not fall within the concentration range of ± 2SD from the mean for either method (Table 4), likely reflecting relatively narrower acceptable limits defined by SD-based approach.

For repeated analyses of biological specimens, acceptance range of ± 20 % from the mean is commonly applied [15]. Most drugs fit well to this range, except flunitrazepam, which could be due to its non-deuterated analogue as IS in the LC-MS/MS method. In addition, MDMA analysis by GC-MS/MS method slightly exceeded the upper concentration limit (Tables 3 & 4) and did not fall within the "mean ± 20 %" range. Although both methods employed the same pulverisation parameters for drug extraction from hair matrices, differences in subsequent sample preparation procedures likely contributed to greater variability observed between the two methods over the five-month period. Considering day-to-day variations, setting an acceptance concentration range of ± 30 % from the mean is appropriate for soaked hair in monitoring routine analysis [16]. This is supported by the observation that all drug concentrations obtained from both methods fitted well within the "mean ± 30 %" range, as shown in Table 4.

Table 3. Concentration ranges and precision for LC-MS/MS (n=39) and GC-MS/MS (n=17) of A1 over a five-month period. (Note: NA - Not analysed)

Drug / Method	LC-MS/MS			GC-MS/MS		
	mean ± 2SD	mean ± 20 %	mean ± 30 %	mean ± 2SD	mean ± 20 %	mean ± 30 %
MAM	X	Y	Y	X	Y	Y
Morphine	X	Y	Y	X	Y	Y
Methamphetamine	Y	Y	Y	X	Y	Y
MDMA	Y	Y	Y	X	X	Y
Ketamine	X	Y	Y	Y	Y	Y
Flunitrazepam	X	X	Y	NA	NA	NA

Table 4. Evaluation of drug concentration ranges in A1 over 5 months using LC-MS/MS and GC-MS/MS. (Note: Y - Range fits; X - Range does not fit; NA - Not analysed)

Drug	LC-MS/MS Concentration (ng/mg)	CV (%)	GC-MS/MS Concentration (ng/mg)	CV (%)
MAM	1.40 - 1.71	4.5	1.26 - 1.79	10.4
Morphine	1.33 - 1.60	3.9	1.23- 1.79	8.9
Methamphetamine	1.01 - 1.19	3.7	0.968 - 1.32	6.6
MDMA	1.24 - 1.60	4.9	1.21 - 1.69	7.5
Ketamine	1.97 - 2.17	3.6	2.06 - 2.34	3.7
Flunitrazepam	1.13 - 1.55	7.4	NA	NA

Stability of A1

A1 was stored at room temperature throughout the study. The good precision observed in Table 3 demonstrates the soaked hair is stable and reproducible across different analysis days for both methods.

Stability studies of soaked hair samples have also been reported by Nielsen et al and Lee et al [4,17]. In the study by Nielsen et al, soaked hair containing 29 commonly encountered pharmaceuticals and drugs of abuse was evaluated over a one-year period. Their findings, which included MAM, morphine, methamphetamine, MDMA, ketamine and flunitrazepam, demonstrated good stability and reproducibility. Similarly, Lee et al reported amphetamine- and methamphetamine-soaked hair samples remained stable for three months in both room temperature and 4 °C storage conditions. Although the present study experimentally demonstrated soaked hair stability over a five-month period, the findings are consistent with literatures, suggesting soaked hair samples may remain stable for up to one year when stored under appropriate conditions.

Comparison of soaked hair preparations from different hair sources

Figure 1 presents the mean concentrations and corresponding acceptance ranges (mean ± 30 %) for soaked hair preparations A1, A2, B1 and B2. Preparations A1 and A2 were derived from the same source of hair (A) but prepared at different times. Despite the same hair source, differences in mean concentrations and corresponding ranges for individual drugs were observed between the two preparations. Consequently, the acceptance range established for A1 cannot be directly applied to A2, and vice versa. A similar pattern was observed for preparations B1 and B2, which were derived from a different source of hair (B).

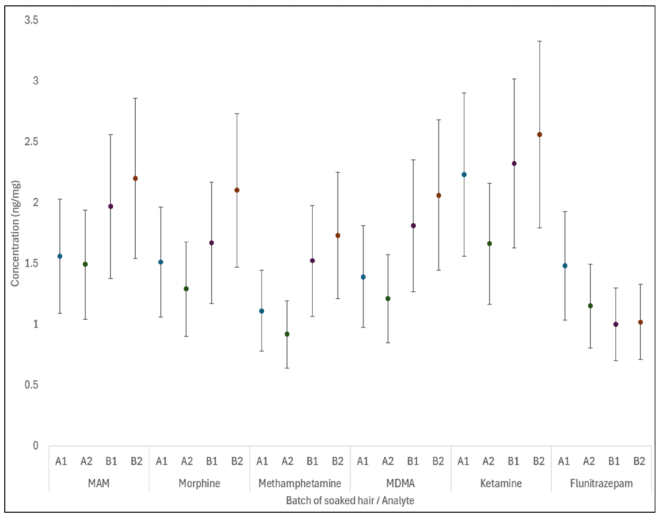


Figure 1. Mean and ± 30 % range of drug analytes of four different preparations determined by the LC-MS/MS method.

Overall, mean drug concentrations in hair source (A) were generally lower than hair source (B), except for flunitrazepam. This observation reinforces the inherent heterogeneity of hair matrices and drug incorporations may vary depending on specific characteristics of the hair source and physicochemical properties of the individual drugs. Hence, it is important to establish the mean concentrations and acceptance ranges for each soaked hair preparation, regardless of the hair source.

Future work

Thus far, this soaked hair preparation has only been evaluated in-house. Although it is fit for the laboratory's purpose, more work can be done to assess the robustness of this preparation through inter-laboratory collaborative exercise.

4. Conclusion

Soaked hair preparations containing MAM, morphine, methamphetamine, MDMA, ketamine and flunitrazepam were evaluated and demonstrated to be suitable QC samples for monitoring the performance of routine hair analysis methods. The soaked hair remained stable for at least five months when stored at room temperature. However, regardless of the hair source, each batch of soaked hair requires the establishment of its own acceptance concentration ranges for individual drugs. This can be achieved by analysing six replicates to determine the mean concentration and defining an acceptance range of ± 30 % for each drug.

Acknowledgement

The authors would like to acknowledge Ms Soo Chock Ying, Ms Lim Cheng Min and Ms Evelyn Goh, who validated the LC-MS/MS method, Ms Tan Joo Chin and the QC team who revised the soaked hair preparation.

References

1. *Society of Hair Testing. Consensus on Hair Testing (Revision 2022). Available at: https://www.soht.org/consensus.*
2. *Salomone A, Tsanaclis L, Agius R, et al. European guidelines for workplace drug and alcohol testing in hair. Drug Test Anal. 2016; 8(10): 996-1004.*
3. *Forensic & Clinical Toxicology Association Inc. FACTA recommended practice guidelines for drug testing in hair. Available at: https://www.facta.org.au/guidelines-policies/.*
4. *Nielsen MKK, Johansen SS. Internal quality control samples for hair testing. J. Pharm Biomed Anal. 2020; 188: 113459.*
5. *Turfus SC, Beyer J, Gerostamoulos D, et al. A comparison of the performance of quality controls prepared from spiked, fortified and authentic hair for ethyl glucuronide analysis. Forensic Sci.Int. 2013; 232: 60-66.*
6. *Lee S, Park Y, Han E, et al. Preparation and application of a fortified hair reference material for the determination of methamphetamine and amphetamine. Forensic Sci.Int. 2008; 178: 207-212.*
7. *Welch MJ, Sniegoski LT, Tai S. Two new standard reference materials for the determination of drugs of abuse in hair. Anal. Bioanal. Chem. 2003; 376: 1205-1211.*
8. *Roveri FL, Pego AMF, Eller S, et al. Evaluation of artificial drug incorporation into hair for production of quality control samples. Drug Anal. Res. 2021; 5(2): 30-35.*
9. *Edder P, Staub C, Veuthey JL, et al. Subcritical fluid extraction of opiates in hair of drug addicts. J. Chromatogr B 1994; 658: 75-86.*
10. *Chan SJ, Tan-Lee NL, Lui CP, et al. Romancing the three states of methamphetamine. Drug Test. Anal. 2025; 17(10): 1848-1856.*
11. *Zhang HH, Loh JYH, Moy HY, et al. An improved GC-MS/MS method for a fast multidrug analysis in hair. Drug Test. Anal. 2025; 17(8): 1344-1356.*
12. *Davies C, Gautam L, Grela A, et al. Variability associated with interpreting drug within forensic hair analysis: A three-stage interpretation. J. Appl Toxicol. 2020; 40:868-888.*
13. *Hubbard JA. Review on toxicology testing in hair. J. Appl Lab Med. 2025; 1(10):983-1000.*
14. *Burgess C. Is a sample size of n=6 a 'magic' number? Pharm Tech 2014; 38(6). Available at: Is a Sample Size of n=6 a 'Magic' Number? | Pharmaceutical Technology*
15. Society of Forensic Toxicologists and American Academy of Forensic Sciences, "SOFT/AAFS Forensic Toxicology Laboratory *Guidelines" (USA: SOFT/AAFS Publication, 2006).*
16. *CAP Accreditation Program Forensic Drug Testing Checklist ©2020, page 11.*
17. *Lee S, Miyaguchi H, Han E, et al. Homogenity and stability of a candidate certified reference material for the determination of methamphetamine and amphetamine in hair. J. Pharm Biomed Anal. 2010; 53: 1037-1041.*

Optimization and Stability Assessment of SEM-EDS Parameters for High-Throughput Automated iGSR Analysis

Chalampoo Wongworavivat*, Nattapon Likittananan, Tassamon Kongyou and Napaporn Chuetragoon
Central Institute of Forensic Science, Thailand
*Email: aomchalampoo@gmail.com

Abstract:
Automated detection of inorganic gunshot residue (iGSR) using scanning electron microscopy coupled with energy-dispersive X-ray spectroscopy (SEM–EDS) is an established technique in the forensic examination of suspected firearm discharge events. To balance analytical performance with operational efficiency in high-throughput forensic laboratories, key SEM–EDS parameters – working distance, accelerating voltage, and scan speed – were systematically optimised using a high-purity copper standard. At a fixed probe current of 1.2 nA, optimal conditions were determined to be a working distance of 13 mm to maximise Cu Kα X-ray signal intensity, accelerating voltage of 20 keV to ensure adequate excitation of the characteristic X-ray lines of lead, barium, and antimony, and an EDS detector dead time within 5–10%. Scan speed 4 (3.2 µs dwell time) provided a practical balance between backscattered electron detector response time and analysis time. Probe current stability, monitored over short-term (5 min), medium-term (4 h), and long-term (24 h) intervals, confirmed minimal drift over all monitoring intervals, with standard deviations of 0.0004 nA, 0.0007 nA, and 0.0009 nA, respectively. Although specific to the instrument configuration evaluated in this study, the optimisation approach can be applied to other SEM–EDS configurations for establishing instrument-specific operating conditions for iGSR examinations.

Keywords: *iGSR, SEM–EDS, optimisation, forensic science*

1. Introduction

Gunshot residue (GSR) is commonly encountered as trace evidence in firearm-related investigations and may provide valuable information regarding firearm discharge events. During firearm discharge, microscopic particles may be deposited on the shooter, clothing, and surrounding surfaces. In particular, inorganic GSR (iGSR) has traditionally been characterised by elemental compositions associated with primer mixtures, most notably lead (Pb), barium (Ba), and antimony (Sb) [1,2]. According to ASTM E1588–20, particles containing Pb, Ba, and Sb are classified as characteristic of GSR. In addition, modern ammunition formulations may be heavy-metal-free, producing particles with alternative compositions such as gadolinium (Gd), titanium (Ti), and zinc (Zn), or gallium (Ga), copper (Cu), and tin (Sn) [3]. The identification of iGSR particles using scanning electron microscopy coupled with energy-dispersive X-ray spectroscopy (SEM–EDS) relies primarily on elemental composition, supported by particle morphology and contextual interpretation in accordance with ASTM E1588–20 [2–4].

Automated SEM–EDS analysis is widely recognised as the standard method for iGSR examination because of its capability for automated particle detection and elemental characterisation [1–3]. However, analytical performance can vary substantially depending on instrument configuration, detector geometry, and operating conditions. Instrumental parameters such as working distance, accelerating voltage, and scan speed influence X-ray generation efficiency, EDS detector dead time, backscattered electron detector response time, and analytical throughput [5,6]. These factors highlight the need for laboratory-specific optimisation and validation under practical high-throughput operating conditions [5–7].

This study systematically evaluated key SEM–EDS operating parameters, namely working distance, accelerating voltage, and scan speed, using a TESCAN VEGA 4 GMU SEM equipped with an Oxford Instruments Ultim Max 100 EDS detector. The optimised conditions are intended to support reliable and efficient automated SEM–EDS workflows for routine high-throughput iGSR examinations conducted in the laboratory.

2. Materials and Methods

2.1 Instrumentation

Analyses were conducted using a TESCAN VEGA 4 GMU SEM under high-vacuum conditions and equipped with a tungsten thermionic electron source and an integrated Faraday cup for probe current monitoring. Elemental analysis was performed using an Oxford Instruments Ultim Max 100 EDS detector with a 100-mm2 active area. Automated particle search and elemental characterisation were managed via Oxford Instruments AZtec software.

2.2 Analytical Standard Preparation

A flat, polished high-purity copper standard (99.999%, Micro-Analysis Consultants Limited, UK) was mounted on conductive carbon adhesive tape attached to an aluminium SEM stub and analysed without conductive coating. The copper standard was used exclusively for instrumental parameter optimisation and evaluation throughout this study.

2.3 Fixed Instrumental Parameters

A fixed probe current of 1.2 nA was maintained throughout the optimisation study. EDS acquisition parameters were kept constant, with a process time setting of 3, an energy calibration of 10 eV/channel, and 2048 spectral channels, and the EDS detector dead time was maintained within 5–10%. The aperture configuration used for routine high-vacuum conditions on TESCAN VEGA 4 GMU SEM, consisting of 500 µm and 50 µm apertures, was used throughout the study.

2.4 Working Distance Optimisation and Accelerating Voltage Evaluation

Working distance was optimised by varying the distance between 10 mm and 16 mm using the flat, polished

high-purity copper standard at an accelerating voltage of 20 keV, and the working distance giving the maximum Cu Kα X-ray signal intensity at the EDS detector was selected. Accelerating voltage was then evaluated over a range of 18–25 keV at the optimised working distance by examining the EDS continuum spectra to verify the effective beam energy and to ensure adequate excitation of the characteristic X-ray lines of Pb, Ba, and Sb relevant to iGSR analysis.

2.5 Scan Speed Evaluation

Scan speed was evaluated across ten levels by measuring the interface width (10–90% rise interval) across a Cu/C (carbon) interface as a measure of backscattered electron detector (BSED) response time, with a lower interface width associated with a faster BSED response. Measurements were repeated three times at each scan speed, and the mean interface width and standard deviation were used to assess repeatability. A suitable scan speed was selected by considering the interface width measurements and analysis time.

2.6 Probe Current Stability Monitoring

Probe current stability was monitored over short-term (every 10 s for 5 min), medium-term (every 10 min for 4 h), and long-term (every 1 h for 24 h) intervals.

3. Results and Discussion

3.1 Working Distance Optimisation

Cu Kα X-ray signal intensity was evaluated across working distances of 10–16 mm at an accelerating voltage of 20 keV, with the highest intensity observed at a working distance of 13 mm (Figure 1). Therefore, a working distance of 13 mm was selected as the optimal working distance for the TESCAN VEGA 4 GMU SEM equipped with the Oxford Instruments Ultim Max 100 EDS detector.

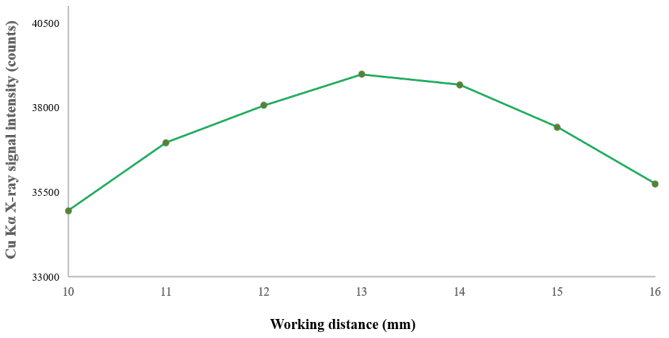


Figure 1. CuK$_\alpha$ X-ray signal intensities across varying working distances (10–16 mm) at a constant probe current of 1.2 nA and accelerating voltage of 20 keV, with the maximum intensity observed at 13 mm.

3.2. Accelerating Voltage Evaluation

Accelerating voltage was evaluated over the range of 18–25 keV at the optimal working distance of 13 mm by examining the EDS continuum spectra to identify operating conditions capable of adequately exciting characteristic X-ray lines associated with iGSR elements. As shown in Figure 2, the EDS continuum spectra confirmed that the effective beam energy closely corresponded to the nominal accelerating voltage across the tested range (18–25 keV). An accelerating voltage of 20 keV was selected because it provides sufficient excitation of the characteristic X-ray lines of Pb, Ba, and Sb associated with iGSR; higher accelerating voltages provide no additional analytical benefit and may reduce the ability to resolve closely-spaced iGSR particles due to an increased electron beam interaction volume. The selected operating voltage is also consistent with the minimum accelerating voltage stated in ASTM E1588–20 [3].

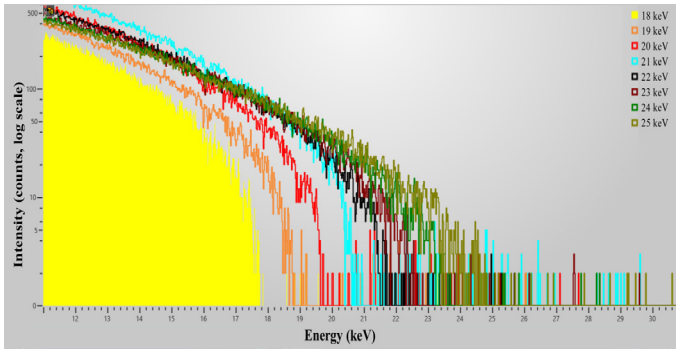


Figure 2. EDS continuum spectra obtained at different accelerating voltages (18–25 keV). The high-energy cut-off for each spectrum demonstrates the effective beam energy arriving at the sample surface.

3.3. Scan Speed Evaluation

The influence of scan speed was systematically evaluated based on the mean and standard deviation (SD) of interface width (10 - 90% rise interval) measured across a Cu/C interface at ten scan speed levels. As illustrated in Figure 3, a non-linear relationship between scan speed and interface width was observed. While scan speed 10 (3.2 ms dwell time) produced the smallest mean interface width with the lowest variability, it is impractical for high-throughput automated searches due to the excessive dwell time.

Scan speed 4 (3.2 µs dwell time) provided a practical balance between BSED response time, assessed based on the interface width measurements, and analysis time. As indicated by the error bars in Figure 3, scan speed 4 exhibited lower variability compared to both faster (levels 1–3) and slightly slower (levels 5–6) settings. Consequently, scan speed 4 was selected as the optimal scan speed, providing a favourable balance between BSED response time and analysis time at a microsecond-scale dwell time, substantially reducing analysis time compared to the millisecond-scale required for scan speed 10.

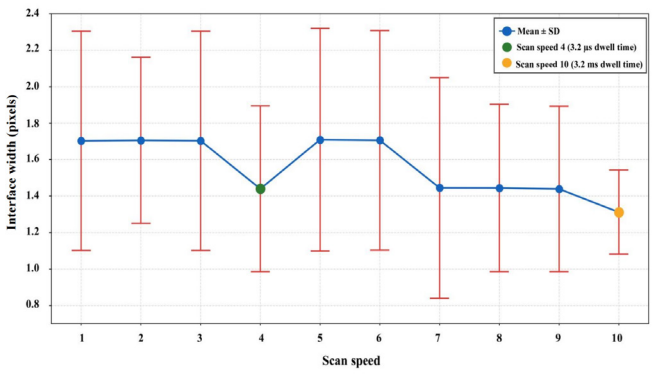


Figure 3. Influence of scan speed on the mean interface width (10 - 90% rise interval) measured across a Cu/C interface, with the error bars representing ± SD (n = 3). The green marker highlights scan speed 4 (3.2 µs dwell time), selected as the optimal scan speed for automated iGSR analysis, and the yellow marker highlights scan speed 10 (3.2 ms dwell time), which produced the smallest interface width and the lowest variability.

3.4. Probe Current Stability Monitoring

Probe current was monitored over short-term (5 min), medium-term (4 h), and long-term (24 h) intervals to assess its stability during extended unattended analytical sessions typical of automated iGSR analysis (Figure 4). The use of an integrated Faraday cup confirmed minimal probe current drift throughout all monitoring periods, with standard deviations of 0.0004 nA, 0.0007 nA, and 0.0009 nA for short-term, medium-term, and long-term intervals, respectively. A stable probe current across extended analytical sessions ensures reproducible backscattered electron and X-ray signals, which are critical for reliable automated particle detection and classification using SEM–EDS in iGSR analysis.

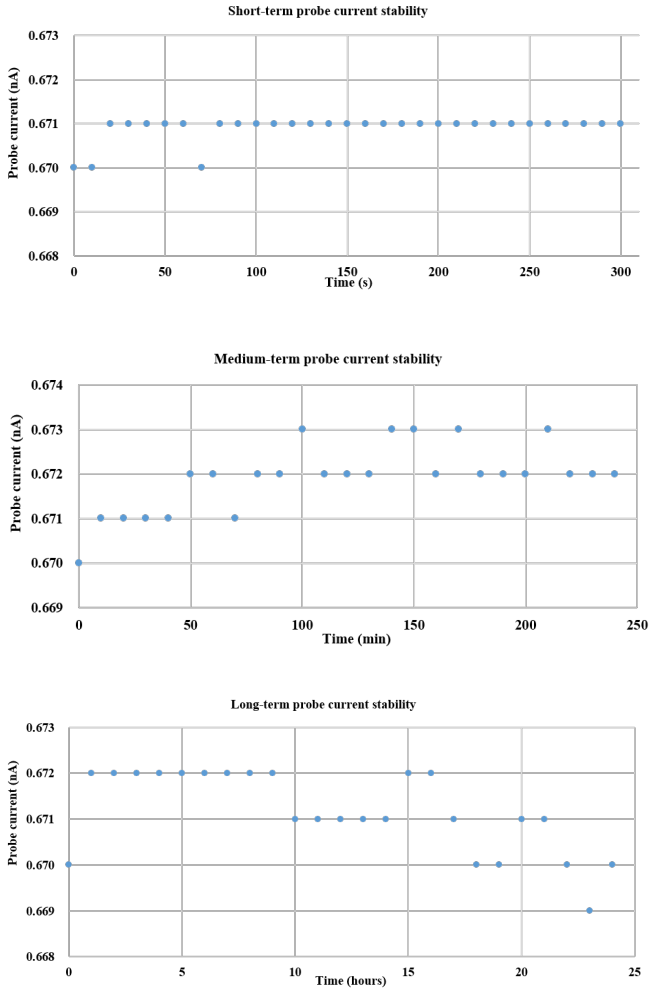


Figure 4. Time-series measurements of probe current stability monitored using the integrated Faraday cup during (A) short-term (5 min), (B) medium-term (4 h), and (C) long-term (24 h) operating periods. The probe current values represent the actual beam current measured using the integrated Faraday cup, and therefore differ from the nominal operating setting of 1.2 nA.

4. Conclusion

This study established optimised SEM–EDS operating conditions intended for high-throughput automated iGSR analysis. At a probe current of 1.2 nA, a working distance of 13 mm maximised Cu Kα X-ray signal intensity, and an accelerating voltage of 20 keV ensured adequate excitation of characteristic X-ray lines associated with iGSR, including Pb, Ba, and Sb, as classified under ASTM E1588–20. Scan speed 4 provided a practical balance between BSED response time, as assessed by interface width measurements at a Cu/C interface, and analysis time. Probe current stability monitoring using the integrated Faraday cup confirmed minimal probe current drift during extended analytical sessions, with standard deviations of 0.0004 nA, 0.0007 nA, and 0.0009 nA for short-term, medium-term, and long-term intervals, respectively. Although the optimised parameters are specific to the instrumentation used, the systematic optimisation approach can be applied to other SEM–EDS platforms to support laboratory-specific optimisation and implementation of automated iGSR analytical workflows.

References

1. *Dalby O, Butler D, Birkett JW. Analysis of gunshot residue and associated materials—a review. J Forensic Sci. 2010;55(4):924-43.*
2. *Romolo FS, Margot P. Identification of gunshot residue: a critical review. Forensic Sci Int. 2001;119(2):195-211.*
3. *ASTM International. ASTM E1588-20: Standard practice for gunshot residue analysis by scanning electron microscopy/energy dispersive X-ray spectroscopy. West Conshohocken, PA: ASTM International; 2020.*
4. *Schwoeble AJ, Spears DL. Current methods in forensic gunshot residue analysis. Boca Raton: CRC Press; 2000.*
5. *Goldstein JI, Newbury DE, Echlin P, et al. Scanning Electron Microscopy and X-ray Microanalysis. 4th ed. New York: Springer; 2018.*
6. *International Organization for Standardization. ISO 15632:2012 Microbeam analysis — Selected instrumental performance parameters for the specification and checking of energy-dispersive X-ray spectrometers for use in electron probe microanalysis. Geneva: ISO; 2012.*
7. *Ritchie NW, DeGaetano D, Edwards D, et al. Proposed practices for validating the performance of instruments used for automated inorganic gunshot residue analysis. Forensic Chem. 2020;20:100252.*

Simplified Urine Detection Workflow for Stained Fabrics

Sher Lin Charlynn Koh*, Kang Hua Lee and Thiam Bon Lim
Health Sciences Authority, Singapore
*Email: Charlynn_KOH@hsa.gov.sg

Abstract:
Urine stain detection combined with drug analysis on fabric can provide evidence of illicit drug use by individuals who have urinated in their underpants. Our study explored the use of the RSID™-Urine test, which detects Tamm-Horsfall glycoprotein (THP), as a primary detection method, leveraging on its rapid procedure and low cross-reactivity with other biological fluids. We assessed the effect of citric acid on fabric to evaluate possible false positives and investigated potential false negatives caused by diffusion of urine constituents across fabric layers and between stained underpants using a simulation study. Results showed that citric acid did not produce false positives when current extraction protocols using buffer solutions were followed. However, THP was found to be unevenly distributed within dried urine stains and to diminish in intensity when spreading across layers of fabric, potentially yielding false negatives when testing near the peripheral areas or adjacent layers. Overall, the findings support a simplified urine detection workflow on visibly stained fabric using RSID™-Urine test. Additional instrumental analyses, such as GC-MS, could confirm urea presence in samples with invisible stains that test negative for THP.

Keywords: *Urine detection, RSIDTM-Urine test, Tamm-Horsfall glycoprotein (THP), false positives, false negatives*

1. Introduction

Detection of urine stains on fabric, together with subsequent drug analysis, can provide evidence of activities such as illicit drug consumption by an individual who urinated in their underpants. Current detection protocol in our laboratory typically involves several analyses [1], mainly to analyse urine components such as creatinine, urea, and the Tamm-Horsfall glycoprotein (THP). The presence of THP, a protein abundant in urine, can be detected with the Rapid Stain Identification urine test (RSIDTM-Urine test), a fast and sensitive immunochromatographic assay specific to THP with low cross-reactivity with other biological fluids. Considering its advantages, this study evaluated whether the RSIDTM-Urine test could serve as the primary method to streamline urine detection protocols.

To achieve this, the reliability of the RSIDTM-Urine test results was verified by investigating potential causes of false positives and false negatives. Literature research [2] highlighted that direct addition of citric acid (0.0093 M - 0.3 M) to the test kits across a pH range of 3 – 12 produced false positives. False positives also occurred when a 1:1 ratio of kit buffer to 0.3 M citric acid was used. These studies did not include extraction of citric acid from stains on fabric although such scenarios are typical in local forensic cases. Given that citric acid is a common ingredient in various commercial products such as citrus juices and cleaning agents [3] [4], it is of interest to verify whether citric acid stains on fabric can cause false positives.

In laboratory analysis, false negatives may occur when screening clothing for suspected but invisible urine stains. This is often due to sample selection. A study involving four fabric types (cotton, silk, polyester, nylon) [5] found that all fabric types except nylon had lower THP content at the peripheral areas compared to the centre. THP levels were 10 times lower at the peripheral than the centre for stains on cotton and silk, indicating that THP does not spread uniformly across fabric. Therefore, sampling a dried stain with inhomogeneous THP distribution may yield false negative findings depending on the sample selection.

The project investigated false positives and false negatives associated with the RSIDTM-Urine test: (i) to verify the effect of citric acid and citric acid-containing products on false positives when using the RSIDTM-Urine kit on fabric swatches, and (ii) to investigate false negatives due to diffusion of urine constituents across fabric. To achieve this, we designed a simulated experiment to model a person urinating in the underpants, followed by the analysis of various cuttings at the underwear and pants. This study aimed to strengthen the interpretation of RSIDTM-Urine test results in casework, with the goal of streamlining the laboratory's urine detection procedures.

2. Materials and Methods

2.1. Testing of THP using RSIDTM-Urine kit

The RSIDTM-Urine kit (Independent Forensics) was used to test the presence of THP following manufacturer's recommendations [6]. In brief, about 150 µL - 300 µL of buffer solution was added to a cotton swab or a cut fabric sample, followed by vortex and sonication for approximately 15 minutes. After incubation at room temperature for about 1 hour, 100 µL of extract was then loaded onto the RSIDTM test strip, and observations were made after 15 minutes. For direct testing of neat liquid samples, the sample was mixed with buffer in a 1:1 ratio before adding 100 µL onto the RSIDTM test strip. The expected results on the test strip are:

i. Positive: blue lines at Control (C) and Test (T) positions.
ii. Weak positive: blue line at (C) and a faint blue line at (T).
iii. Negative: Only a blue line at (C).
iv. Invalid (Fail): No blue line at (C).
v. Inconclusive: All other observations that deviate from above.

2.2. Preparation of citric acid solutions, commercial and stained samples

0.3 M citric acid (pH 4) solution was prepared by adding 1.19 g of anhydrous citric acid (Sigma Aldrich) to 20.6 mL of ultrapure water. The pH was adjusted using universal pH indicator (Supelco) to pH 4 by adding sodium hydroxide (Sigma Aldrich). Non-pH adjusted 2.6 M (0.5 g/mL) citric acid was separately prepared (2 mL of water to 1 g of citric acid), followed by serial dilutions to prepare lower concentrations [1 M (0.2 g/mL), 0.26 M (0.05 g/mL) and 0.005 M (0.001 g/mL)]. Minute Maid orange juice drink and Coca-Cola were purchased commercially. For cuttings and swab samples, 20 µL and 100 µL of citric acid solutions were added to white flannelette cloth cuttings (1x0.5 cm) and cotton swabs respectively and incubated for 10 minutes. The cuttings and swabs were then extracted with buffer and tested for THP using the RSIDTM-Urine kit.

2.3. Testing of THP across fabric layers

To investigate whether THP can diffuse across multiple clothing layers (e.g. from underwear to outer garments), we first examined THP transfer across two fabric cuttings. A 4 x 4 cm cutting from cotton underwear was placed directly on top of a similar cutting size of polyester pants. The underwear and pants were hand-washed with detergent and rinsed before use. Urine from a volunteer was used as positive control. Approximately 600 µL of urine was added dropwise from corner A and visually observed to spread to corner B and then left to air-dry for approximately 30 minutes. Cuttings (1 x 0.5 cm) were obtained and tested for the presence of THP using the RSIDTM-Urine kit (Figure 1).

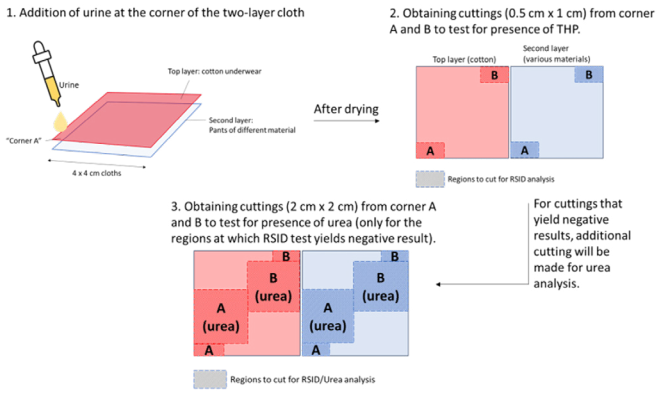


Figure 1. Schematic of the workflow for spiking urine onto two-layered cloth cuttings.

2.4. Extraction and analysis of urea from fabric cuttings

The 2 x 2 cm cuttings in Figure 1 were extracted using 2 mL of methanol (J.T. Baker), vortexed, and then concentrated down to 500 µL by blowing with nitrogen gas. The resultant extract was filtered through a 0.45 µm filter and concentrated down to 200 µL for GC-MS analysis if deemed necessary. Shimadzu GC-MS/MS TQ8030 installed with DB-1MS (30 m x 0.25 mm x 0.25 µm) column was used. The injector temperature was set at 250°C and ion source temperature at 230°C while helium carrier gas flow rate was 1.52 mL/min. GC oven temperature program started at 40°C (hold 1 min) and was ramped to 110°C at 8°C/min followed by 10°C/min until final temperature of 300°C (hold 5 min). All samples (1 µL) were injected using a 1:10 split ratio. Urea (Sigma Aldrich) was used as a reference material.

2.5. Testing of THP on underwear and pants in a simulation study

To simulate a person urinating in the underwear, a snap-lock bag filled with nitrogen gas was placed inside the underwear (100% cotton) and pants (100% polyester) to inflate the setup (Figure 2). Composite urine was prepared by combining approximately 50 mL of urine from each of four individuals. Approximately 200 mL (typical urination volume) [7] of the composite urine was dispensed into the crotch of the inner side of the underwear using a plastic squeeze bottle. The setup was air-dried for about 20 minutes before the underwear and pants were crumpled together and stored overnight at room temperature to mimic the condition of submitted exhibits. The next day, several 2 x 2.5 cm cuttings were taken from both garments for analysis.



Figure 2. Photographs of the setup for the simulation study.

3. Results and Discussion

3.1. Effects of citric acid and its concentrations on the occurrence of false positive results.

pH-adjusted citric acid was added directly to the test kits to replicate the results described in the literature [2] (Table 1). An invalid result was obtained instead of the expected false positive, while a weak false positive was observed at the lower concentration of 0.03 M (Test 1 and 2). In contrast to the literature, the addition of buffer solution

Table 1. Results of the RSIDTM-Urine test when citric acid (pH 4) was added.

Test no.	Sample	Concentration	Buffer added?	Result
1	Neat	0.3 M	No	Invalid
2	Neat	0.03 M	No	Weak false positive
3	Neat	0.3 M	Yes	Negative
4	Neat	0.03 M	Yes	Negative
5	Swab	0.3 M	Yes	Negative
6	Cutting	0.3 M	Yes	Negative

appeared to mitigate the effect of citric acid, yielding negative results at both concentrations (Figure 3). Similarly, spiking a fabric cutting or swab with citric acid followed by extraction with buffer produced negative results. Therefore, these findings highlighted the importance of adding buffer to enable the kit to perform as intended. The discrepancy with the literature may be due to a different batch or version of the test kit.

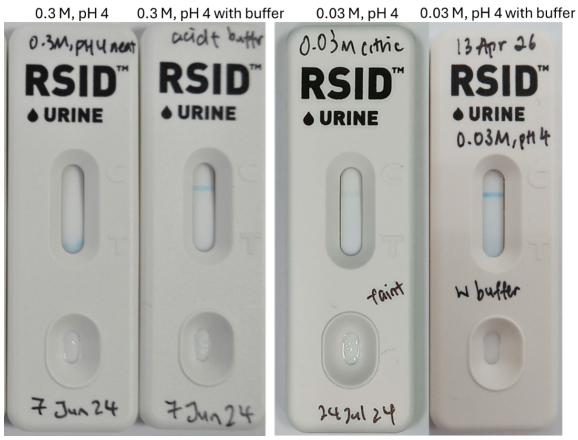


Figure 3. Photographs of the RSIDTM Urine kits when citric acid (0.3 M and 0.03 M) were directly added with and without buffer.

Solutions of citric acid at concentrations from 0.005 M – 2.6 M were tested (Table 2, Figure 4). These concentrations were chosen to encompass levels below, above and similar to those in citrus juice and citric acid-based cleaning agents [3], [4]. The pH was not adjusted. Overall, negative results were obtained, indicating a low likelihood of false positives. Initially, tests at high concentrations (2.6 M and 1 M) produced invalid results, while tests at 0.005 M were inconclusive, with a partial blue line observed (Figure 4). Therefore, we recommend performing replicate experiments if results are invalid or inconclusive. Acidic orange juice and cola drinks were also tested. Cola was included because, although its major acidic component is phosphoric acid, soft drinks have been reported to produce false positives in similar test kits [8]. The addition of orange juice gave negative results. Adding cola directly to the test strip yielded a possible false positive (Figure 5); however, the test line (T) faded after subsequent addition of buffer. Cola spiked onto a swab produced negative results. Therefore, with samples extracted with the provided buffer according to the standard protocol, citric acid and soft drinks do not appear to produce false positives.

Table 2. Results of the RSIDTM-urine test when varying concentrations of citric acid and acidic drink samples were added (Note: a - Replicates were done to confirm results; b - Refer to figure 4; c - Refer to figure 5).

Test no.	Sample description	Substrate	Concentration	Buffer added?	Results
1	Citric acid solution	Cutting	2.6 M	Yes	Invalid[b]
2	Citric acid solution	Cutting	1 M	Yes	Invalid[b]
3[a]	Citric acid solution	Cutting	1 M	Yes	Negative
3	Citric acid solution	Cutting	0.26 M	Yes	Negative
4[a]	Citric acid solution	Cutting	0.26 M	Yes	Negative
5	Citric acid solution	Cutting	0.005 M	Yes	Inconclusive[b]
6[a]	Citric acid solution	Cutting	0.005 M	Yes	Negative
7	Orange juice drink	Neat	NA	No	Negative
8	Cola drink	Neat	NA	No	False Positive[c]
9	Cola drink	Swab	NA	Yes	Negative

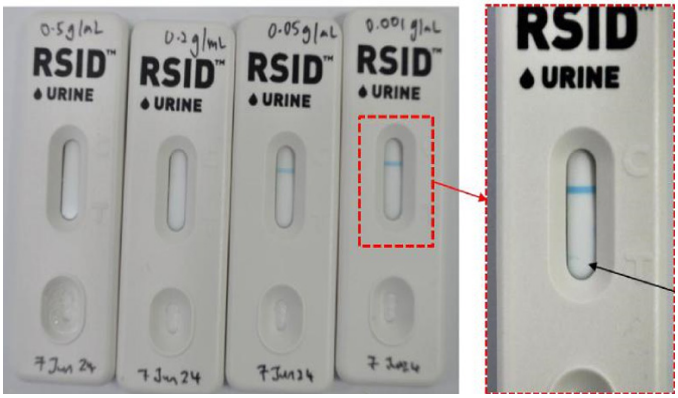


Figure 4. Photograph of the RSIDTM-Urine kits when different concentrations of citric acid were used. Left to right: 2.6 M (0.5 g/mL), 1 M (0.2 g/mL), 0.26 M (0.05 g/mL), and 0.005 M (0.001 g/mL).



Figure 5. Photograph of the RSIDTM Urine kits after orange (left) and cola drink (right) were added.

3.2. Detection of THP and urea on two-layered cloth cuttings

Table 3 presents findings from fabric cuttings after urine was added to corner A of a two-layered cloth with cotton positioned directly above a polyester layer. All cuttings from both layers at corner A yielded positive results, indicating successful THP transfer from the cotton layer to the polyester cloth below. These outcomes indicated potential transfer of THP across the two layers, suggesting that THP can be detected on outer layers, such as pants, when urine was present on underwear. In contrast, varied results were observed for cuttings at corner B. In three replicates, two cotton cuttings were weakly positive, and one was negative. Both polyester cuttings at corner B displayed weak positive results. This experiment demonstrated that THP flow is non-uniform, with cuttings further from the centre of urine flow potentially yielding false negatives.

Table 3. Results of the RSIDTM-Urine test (NT denotes "not tested", Test 3 was only performed if the duplicate tests gave opposing results).

	Corner A			Corner B		
Material	Test 1	Test 2	Test 3	Test 1	Test 2	Test 3
Cotton	Positive	Positive	NT	Negative	Weak positive	Weak positive
Polyester	Positive	Positive	NT	Weak positive	Weak positive	NT

The study further investigated whether urea detection by GC-MS can verify the presence or absence of urine when THP tested negative in fabric samples. Urea was detected in all three cuttings, including cotton 1B, where THP

was not detected by the RSIDTM-urine test (Table 4). This may be due to higher water solubility of urea, which enables its wider distribution in the fabric. The findings demonstrate that GC-MS detection of urea can support urine identification and should be used when THP is not detected.

3.3. Detection of THP on cuttings made at different regions of underwear and pants

The simulation showed urine flowing through the underwear and dripping from the inner thigh regions of the pants. Stains were visible at the crotch of the underwear and were not significantly altered by crumpling and storage. Stains on the pants were difficult to see because of their colour but were noticeably wet. All cuttings tested positive with RSIDTM-urine test, although intensity varied (Table 5). For underwear cuttings, C1, taken near the peripheral of the stain, showed moderate intensity, while other cuttings were strongly positive (Figure 6). For the pants, all cuttings were positive, indicating detectable THP in outerwear. However, cuttings from underwear produced stronger positive results, highlighting the importance of analysing underwear over outerwear. Cuttings from near the inner thigh were strongly positive, while those further away were weakly positive (Figure 7). The findings suggest that THP is not evenly distributed; therefore, cuttings close to the inner thigh are recommended, especially when stains are not obvious. It is important to note that the results from the simulation study are dependent on the position/angle of the squeeze bottle and where the urine was directed. Furthermore, results may also differ depending on the type of fabric of underwear and pants, the posture of the person (e.g. whether sitting or lying down etc.), amount of urine, and any movement after urination. Nonetheless, our study affirms that THP can be transferred across to the outerwear, and our results underscore the importance of sample selection.

4. Conclusion

The RSIDTM-Urine kit is a common immunochromatographic assay used to test for the presumptive presence of urine. This project investigated potential false positives caused by citric acid at various concentrations and false negatives resulting from urine diffusion across fabrics when using the RSIDTM-Urine kit. Our study showed that citric acid does not cause false positives when the kit extraction buffer is used according to the RSIDTM-Urine test protocol. For urine-stained fabrics, THP is detectable in cuttings near the centre of deposition, while false negatives may occur in cuttings further away. In a simulated scenario of a person urinating in underwear and pants worn together, THP spreads across layers but decreases in detectable intensity with distance from the initial deposition layer. Therefore, for samples with indiscernible stains, negative RSIDTM-Urine test results should be supported by other analyses (for example, analysis of urea using GC-MS). Our findings support the use of RSIDTM-Urine kit as the primary method for urine detection.

*Table 4. Comparison of the RSIDTM-Urine test results with the GC-MS . results to detect presence of urea on cotton cutting (Note: *The label is based on the test number and the corner at which the cotton cutting was obtained).*

Sample label*	RSID™-Urine test	GC-MS
Cotton 1B	Negative	Urea detected
Cotton 2B	Weak positive	Urea detected
Cotton 3B	Weak positive	Urea detected

Table 5. Results of the RSIDTM-Urine test for the simulation study.

Material/Fabric	Cutting	Result
Cotton underwear	C1	Weak positive
	C3	Positive
	C6	Positive
Polyester pants	C1	Weak positive
	C3	Positive
	C5	Weak positive
	C6	Weak positive

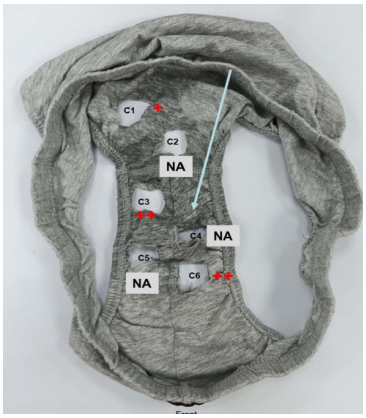


Figure 6. Position of cuttings and the RSIDTM urine test results for underwear. The urine flow was directed towards the front of the underwear as indicated by the blue arrow. "NA" denotes cuttings that were not analysed ('++' denotes a positive result, while '+' denotes a weak positive result).

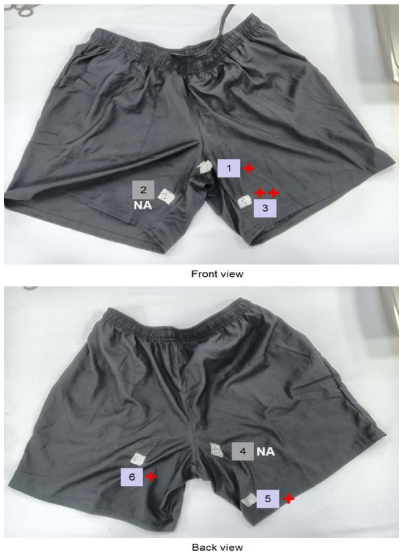


Figure 7. Position of cuttings and the RSIDTM urine test results for pants ('++' denotes a positive result, while '+' denotes a weak positive result).

References

1. *Virkler K, Lednev IK. Analysis of body fluids for forensic purposes: From laboratory testing to non-destructive rapid confirmatory identification at a crime scene. Forensic Sci Int. 2009, 188(1-3): 1 - 17.*
2. *Foleya MM, Browna CO, Westring CG, et al. Effects of organic acids and common household products on the occurrence of false positive test results using immunochromatographic assays. Forensic Sci. Int. 2020, 308: 110165.*
3. *Penniston KL, Nakada SY, Holmes RP, et al. Quantitative assessment of citric acid in lemon juice, lime juice, and commercially available fruit juice products. J. Endourol. 2008, 22(3): 567 - 570.*
4. *Taraborelli JA, Upton RP. Enzymatic Determination of Citrate in Detergent Products. J. Am. Oil. Chem. Soc. 1975, 52: 248 - 251.*
5. *Tsutsumi H, Sato K, Tamaki K, et al. Identification of human urine stains on cloth. Int. J. Legal Med. 1991, 104: 105 - 108.*
6. *Independent Forensics, "Rapid Stain Identification of Urine (RSID™-Urine) Technical Information and Protocol Sheet"*
7. *Blanker MH, Groeneveld FPMJ, Bohnen AM, et al. Voided volumes: normal values and relation to lower urinary tract symptoms in elderly men, a community-based study. Urology, 2001, 57, 6: 1093 – 1098.*
8. *Velavan T, Pallerla S, Kremsner P. How to (ab)use a COVID-19 antigen rapid test with soft drinks? Int. J. Infect. Dis. 2021, 111: 28 - 30.*

A Rare Case of Heteropaternal Superfecundation: A Case Study from Sri Lanka

Udumalagala Gamage Sujini Tharanga Gamage*, Piyanka Ganhewage de Silva, Eshani Marasinghe and Liyanage Rasika Tharangani Perera
Government Analysts' Department, Sri Lanka
**Email: sujinigamage@gmail.com*

1. Introduction

Heteropaternal superfecundation refers to the fertilization of two or more ova released during the same ovulatory cycle by sperms from separate acts of sexual intercourse involving two different males. The first case of heteropaternal superfecundation was reported in 1810 by Archer using phenotypic differences between female twins [1]. In another study it was revealed that the percentage of occurrence of heteropaternal superfecundation is 2.4% among dizygotic twin births [2]. However, by 2020 there were only about 19 documented cases of heteropaternal superfecundation officially reported in scientific literature worldwide [3].With the 2025 case report from the Dominican Republic [4] this number had risen to 21. That figure reflects a reporting problem more than a biological one: as this condition goes undetected until a paternity dispute occurs and even then both twins are required to be tested separately. Therefore, this case paper intends to present a case of heteropaternal superfecundation detected in Sri Lanka as evidenced by autosomal short tandem repeats (STR) markers and lineage short tandem repeat markers.

2. Materials and Methods

The DNA Laboratory of the Government Analysts' Department received a court order to conduct DNA paternity test pertaining to case of disputed paternity. Accordingly, blood samples from the alleged father, mother and the twins were separately obtained onto FTA cards at the DNA Laboratory of the Government Analysts' Department. The four blood samples were subjected to DNA extraction using QIAamp® DNA Investigator Extraction kit (QIAGEN). The extracted DNA was quantified using QuantifilerTM DNA Quantification kit (Applied Biosystems) on an ABI® 7500 Real-time PCR system followed by polymerase chain reaction (PCR) to amplify 15 autosomal Short Tandem Repeats (STRs) i.e. D8S1179, D21S11, D7S820, CSF1PO, D3S1358, TH01, D13S317, D16S539, D2S1338, D19S433, vWA, TPOX, D18S51, D5S818, FGA. PCR amplification was performed using AmpFLSTRTM IdentifilerTM Plus kit (Applied Biosystems) on a 9600® Thermal CyclerTM (Applied Biosystems).

For samples indicating negative paternal relationship based on the autosomal STR analysis, investigation was repeated to confirm the results. To strengthen the autosomal STR results, lineage marker tests are also conducted. Accordingly, Y-chromosomal STR (Y-STR) markers were analysed using the PowerPlex® Y23 Kit for samples from the alleged father and the twins. Simultaneously, X-chromosomal STR (X-STR) analysis was performed for samples from the mother and the twins using the Investigator Argus X-12 QS kit (QIAGEN) to affirm the maternal relationship.

The amplified products were subjected to capillary electrophoresis and detection on ABI 3500 Genetic Analyser (Applied Biosystems) and the results were analysed with GeneMapper ID-XTM software, version 1.5 (Applied Biosystems). Statistical calculations were conducted using eDNA software version 3.0.7 with Sri Lankan population allele frequencies.

3. Results and Discussion

The results of the possible genotypes of each individual are given in Table 1. Statistical calculation of the Combined Relatedness Index (CRI) for autosomal STR profiles obtained for the Twin 2, the mother and the alleged father, revealed that Twin 2 is biologically related to both the mother and the alleged father with a CRI of 4.79×10^6 (Paternity Probability - 99.9999%).

In contrast, Twin 1 showed no biological relationship with the alleged father (Paternity Probability - 0%). The results excluded the alleged father as the biological father of Twin 1 based on 10 genetic inconsistencies (D7S820, D3S1358, D16S539, D2S1338, D19S433, vWA, TPOX, D18S51, D5S818 and FGA) observed among the 15 autosomal loci analysed.

Table 1. Genotypes of the mother, the alleged father and the twins for 15 autosomal loci.

Locus	Mother	Twin 1	Twin 2	Alleged father
D8S1179	11, 12	11, 13	11, 13	13, 13
D21S11	30.2, 33.2	31.2, 33.2	30, 33.2	30, 31.2
D7S820	10, 10	10, 16	8, 10	8, 12
CSF1PO	11, 13	11, 11	11, 11	11, 12
D3S1358	15, 16	15, 15	16, 17	16, 17
TH01	6, 8	8, 9	8, 9.3	9, 9.3
D13S317	8, 11	8, 16	8, 10	10, 12
D16S539	11, 12	12, 12	9, 11	9, 9
D2S1338	19, 22	20, 22	19, 23	18, 23
D19S433	13, 13	13, 14	13, 13	13, 15
vWA	17, 19	14, 19	17, 18	16, 18
TPOX	9, 11	8, 11	11, 11	9, 11
D18S51	15, 19	14, 15	12, 19	12, 16
D5S818	12, 12	12, 13	11, 12	11, 12
FGA	20, 25	20, 23	21, 25	21, 22

Table 2. Genotypes of the alleged father and the twins for 23 Y-chromosome loci.

Locus	Twin 1	Twin 2	Alleged father
DYS576	17	17	17
DYS389I	12	13	13
DYS448	19	20	20
DYS389II	28	31	31
DYS19	14	13	13
DYS391	10	11	11
DYS481	23	26	26
DYS549	13	15	15
DYS533	12	12	12
DYS438	10	10	10
DYS437	15	14	14
DYS570	14	17	17
DYS635	24	21	21
DYS390	22	24	24
DYS439	12	12	12
DYS392	14	11	11
DYS643	10	12	12
DYS393	11	14	14
DYS458	16	15	15
DYS385a/ DYS385b	13,17	16	16
DYS456	16	16	16
YGATAH4	11	12	12

Table 3. Genotypes of the mother and the twins for 12 X-chromosome loci.

Locus	Mother	Twin 1	Twin 2
DXS10103	16, 16	16	16
DXS8378	11, 12	12	12
DXS10101	29, 33	33	33
DXS10134	36, 40.3	36	40.3
DXS10074	17, 17	17	17
DXS7132	14, 14	14	14
DXS10135	27, 30	30	30
DXS7423	14, 15	14	15
DXS10146	28, 41.2	28	41.2
DXS10079	20, 21	21	20
HPRTB	12, 12	12	12
DXS10148	18, 25.1	18	18

Results obtained for Y-STR analysis further supported the above findings (Table 2 & 3). The alleged father and Twin 2 shared identical Y-STR profiles, whereas different Y-STR profiles were obtained for the alleged father and Twin 1, indicating distinct paternal lineages.

Since Twin 1 showed no biological relationship with the alleged father, a Combined Maternity Index (CMI) with the mother was also calculated and the value was 4.22×10^{6}. This value corresponds to a probability of maternity equal of 99.9999%. Additionally, the X-STR results further supported the maternal relationship between the mother and both twins. The combined use of autosomal STR, Y-STR and X-STR markers provided robust confirmation of this case. The autosomal STR results first identified the paternal discrepancy, while Y-STR results provided evidence of two distinct paternal lineages. The X-STR results affirmed the maternal relationship between the mother and the twins.

4. Conclusion

These findings confirm that the dizygotic twins represent a rare case of heteropaternal superfecundation, in which twins from same pregnancy have different biological fathers.

References

1. *Archer J. Facts illustrating a disease peculiar to the female children of Negro slaves, Med Repos. 1810;1:319-23.*
2. *Wenk RE, Houtz T, Brooks M, Chifari FA. How frequent is heteropaternal superfecundation? Acta Genet. Med Gemellol (Roma). 1992;41:43-47.*
3. *Mogollan F, Casas-Vargas A, Rodriguez F, Usaquen W. Twins from different fathers: A heteropaternal superfecundation case report in Colombia. Biomedica 2020;40:604-8.*
4. *Reyes T, Rivero R, Jiminez S, Figueroa K, Riego E. First documented cases of heteropaternal superfecundation in dizygotic twins from the Dominican Republic: A case report. Forensic Science International: Reports. 2025:12 100433.*

The Protection of Children from Sexual Offences (POCSO) Act and the Case Scenario in Forensic Science Laboratory, Delhi, India

Monika Chakravarty
Forensic Science Laboratory, India
Email: monika42@gmail.com

1. Introduction

According to the World Health Organization, there exist four dominant kinds of child abuse and maltreatment, namely physical, sexual, emotional, and neglect [1]. Acts of physical, emotional and sexual abuse are of great concern. According to an estimate around 3 million children become victims of abuse yearly [2]. Out of the several issues faced by India today, the issue of child sexual abuse is one of the major issues, but the problem is often underreported because of the social stigmas associated. Child sexual abuse is very often committed by a person known to the victim or a person in a position of trust or authority including neighbours, relative or family friends [3].

To address child sexual abuse India has enacted laws. The Protection of Children from Sexual Offences (POCSO Act) came into force in 2012 in India to cater to the heinous crimes of sexual abuse and exploitation of children through a well-defined and strict legal mechanism which provides severe punishments for sexual offenders [4]. The legislature denotes the type of punishment for sexual assault along with the guidelines for the legal authorities and police personnel to deal with the crimes and makes it mandatory for them to report the cases. Failing to report the child sexual assault cases on the part of health care professionals has provisions to draw punishment. Sexual assault on a child is to be considered a medical emergency and emergency medical care has to be provided by a medical facility whether private or public [4]. Special fast track courts were constituted to deal with such cases in a child-friendly manner.

2. POCSO Amendments

On 5th August 2019, the POCSO (Amendment) Act, 2019 received the President's assent with the aim to strengthen the act. It addresses the need for stringent measures to deter the increasing trends of child sexual abuse in the country. An amendment was made to it wherein punishment for aggravated and penetrative sexual assault on children below the age of 16 was increased from 10 to 20 years extending up to life imprisonment or death. It has provisions for death penalty for rape of a child below twelve years of age. The act also included punishment for people in positions of trust such as custodians, public servants, police etc.

POCSO Act involves punishments stringent than that under Indian Penal Code. Accordingly, whoever commits penetrative sexual assault on a child below sixteen years of age shall be punished with imprisonment for a term which shall not be less than twenty years but which may extend to imprisonment for life, which shall mean imprisonment for the remainder of natural life of that person, and shall also be liable to fine. Further amendment was made in 2020, which proposes that child offenders between the age group of fifteen to eighteen years should be covered under the ambit of the POCSO Act, 2012 and be given the same punishment as is given to adults.

3. Case Scenario

Sexual assault cases are classified as a dominant crime in Delhi, India. Rising awareness via campaigns on TV and social media has resulted in an increase in reporting of cases. Still many incidents were not reported owing to social stigmas attached or fear of the perpetrator. Around 60-120 cases are deposited under the POCSO act per month in the laboratory, including attempted sexual assault, vaginal fingering, anal fingering, vaginal or/and anal penetration. Despite the occurrence of large number of such crimes, most of the incidents go unreported either because of negligence, poor economic status or lack of awareness and trust in the legal system associated with the fear of social humiliation mixed with feelings of shame while reporting such crimes [5]. Another reason for the crime not being reported is that the offender is an acquaintance, a known or a family member. The family of the survivor prefers non-disclosure.

4. Analysis of POCSO Cases by Age of Victim and Circumstantial Factors

Most of the child victims belong to the age group of around 2 months to 10 years having very low socio-economic status as well as lack of education. Juvenile offenders or close relatives are often involved in most of these crimes. In cases involving age group 14-18 years it is observed that the victim had consensual sexual intercourse and later the relationship is disapproved by the girl's family and a criminal case is registered by them. In some instances, the victim was abused in the pretext of marriage, forcing her to file a police complaint. There have been few cases where laws were misused by women for monetary gains or enmities. Such kind of false cases not only burden the legal system but also hamper the real POCSO cases.

5. Nature of Biological Samples Received in POCSO Cases

Before the advent of DNA technology, case of the prosecution was largely dependent on the victim's testimony. Since 1985, DNA has proven a boon to the criminal justice system. DNA can be extracted from a wide variety of samples such as blood, semen, saliva, teeth, bone, hair and fetal tissues. In cases of sexual assaults culminating in pregnancy, paternity can be established by fetal tissues from the aborted fetus as a source of DNA [6].

Primarily the cases/samples received in can be separated in the following three broad categories – types of samples collected through SAFE Kits (Sexual assault evidence collection kit) comprising of the swabs from the vulval, cervical, vaginal, anal, oral regions (biological samples) as well as debris collection samples (trace evidence samples) including clothes

of the victim (clothing and fabric evidence) as shown in the Figure 1 and 2. The other type of samples are the product of conception (POC) i.e. fetal tissues, placental tissue or fetus etc. when there is a need to establish pregnancy resulting from sexual assault [Figure 3 (a), (b) & (c)] and the third category include the blood samples in EDTA or on dry gauzes in disputed paternity cases (Figure 3 (d) & (e)].

6. Challenges and considerations in analyzing POCSO cases

Frequently, penetrated sexual assault is not committed in child sexual abuse. Thus, it becomes problematic to prove such offences. Delayed disclosure also results in negative DNA results. Some of the technical challenges faced by the laboratory include the masking of the male profile, often a minor contributor, due to the presence of excessive female DNA. Detection of male DNA becomes difficult when female DNA is in excess [7]. This occurs either due to low semen deposition in the sample or a delay in sample collection, which may lead to male DNA degradation. Y-STRs help detect male DNA even when mixed with female DNA to an extent [8].

7. Failure to Obtain DNA Profile Due to Improper Sample Preservation

In few cases it is observed that the body swabs of the victim collected by the doctor, who conducts the medical examination of the victim, were preserved in a medium tube such as Amies medium containing charcoal, which results in failure to generate DNA profile either due to microbial growth, sample degradation or inhibition [Figure 4 (a)]. It contains moist conditions, which can fragment DNA [9].

This results in loss of important evidence as also described by Collin-Vezina and others [10]. Dry swabs are preferred for DNA analysis. Improper preservation of the evidence such as preserving fetal tissues in formalin often leads to sample degradation and failure to generate DNA profile [Figure 4 (b) & (c)]. In a forensic context, formalin preservation is not ideal for DNA analysis as formalin fragments DNA and cross links DNA with proteins and yields partial or no profiles [11].

Sometimes reference blood samples of the victim or suspect were improperly preserved in plain vials (without EDTA)/gel medium tubes or in wet gauzes kept in tubes or in plastic containers which fail to generate DNA profile [Figure 5 (a), (b), (c) & (d)]. Damp conditions in wet gauze can promote microbial growth and enzymatic activity, leading to DNA degradation [9]. Similarly, blood stored in plain vials without anticoagulants or preservatives may undergo clotting and breakdown, which can hamper DNA profiling [12]. Proper collection and preservation of these samples are of utmost importance, as degraded or contaminated samples leads to failure in obtaining a DNA profile.

8. Case Statistics

Distribution of POCSO Cases with DNA Profiling Failure Attributable to Improper Sample Preservation

Blood samples in 56 out of 272 cases studied did not yield DNA

Step No.	Name of the Steps	Content of Step
1	Consent	
2	History	
3(a)	Clothing outer	
3(b)	Clothing inner	
4(a)	Body fluid collection	One cotton swab with tube
4(b)	In between fingers	Cotton swab + one A4 size paper
4(c)	Nail scrapping	Nail cutter + one A4 size paper, cotton swab + one A4 size paper
4(d)	Debris collection	One pair of forceps + one A4 size paper + distilled water + one cotton swab with tube
5	Breast swab	One cotton swab + distilled water
6	Combing of pubic hair	One comb + one A4 size paper
7	Clipping of pubic Hair	Pair of Scissors + one A4 size paper
8	Matted pubic hair	One A4 size paper
9A	Cervical mucus collection	One cotton swab with tube
9B	Vaginal secretion	Slide + cotton swab
9C	Urethral swab	One cotton swab with tube
10	Culture	One HI-media tube MS684
11	Washing from vagina	5 ml syringe + one rubber tube + one distilled water vial 5ml
12	Rectal examination	One slide + one cotton swab
13	Oral swab	One slide + one cotton swab
14	Blood collection of victim	One 5 ml syringe + Vacutainer clot activator + Vacutainer EDTA K2
15	Urine and oxalate blood vial	Urine container + 5 ml syringe + sterile surgical gloves size 7.0

Figure 1. List of SAFE kit samples.

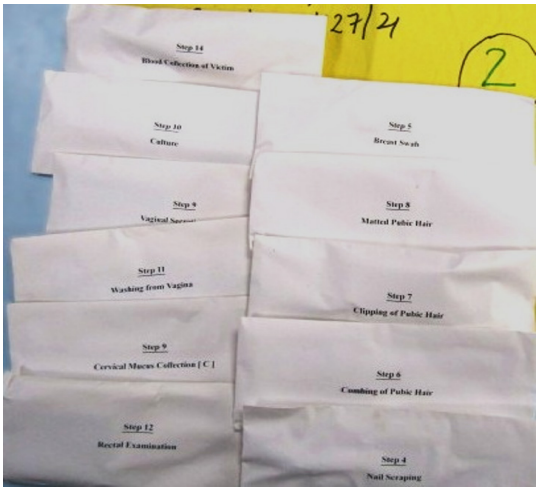


Figure 2. Examples of SAFE kit samples.



Figure 3. (a) and (b) Products of conception (POC); (c) Fetus/ placenta; (d) Blood sample in EDTA tube; (e) Blood sample on gauze.

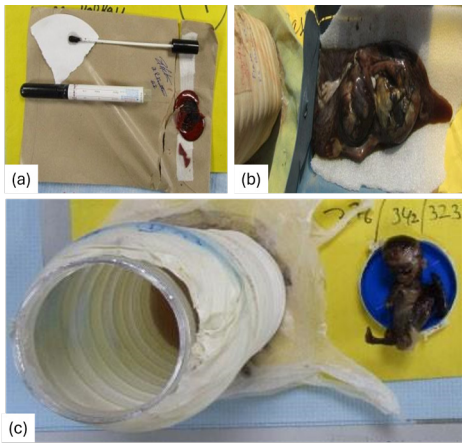


Figure 4. (a) Vaginal swab preserved in Amies medium product: (b) and (c) Formalin preserved fetus.

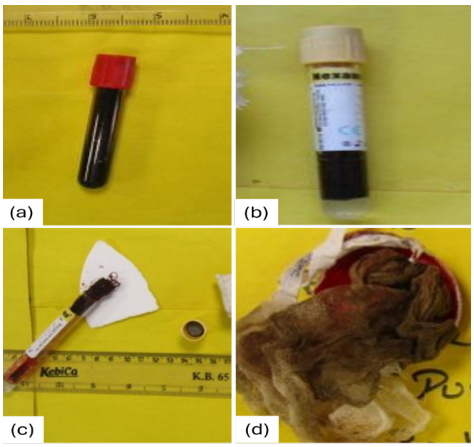


Figure 5. (a) Plain vial; (b) Gel medium tube; (c) Wet gauze kept in a tube; (d) Gauze in plastic container.

profile due to improper preservation (Figure 6). Similarly, 26 (62%) out of 42 fetal tissues fail to generate DNA profiles due to improper preservation.

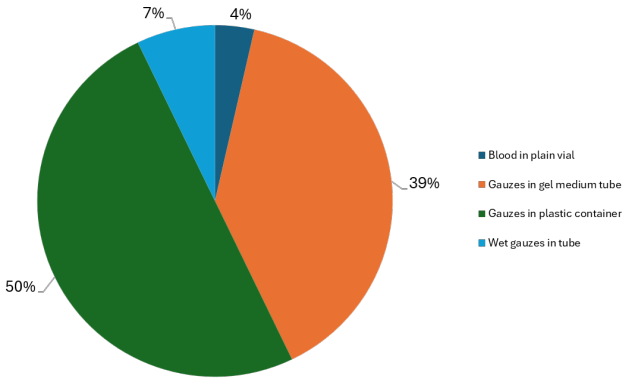


Figure 6: No DNA profile due to improper preservation of reference blood samples.

Distribution of POCSO Cases by Relationship and Circumstances

Out of the 256 POCSO cases examined, 56 cases are of eloping under romantic relationship, 40 cases are of eloping and marriage, 56 cases are on the pretext of marriage, 24 cases are of forceful sexual assault by a friend or acquaintances, 4 cases are of assault by the employer, 24 cases are of sexual assault by father/stepfather/nearest relative, 28 cases are of assault by a neighbor, 12 cases are of assault by an unknown person/ stranger and 12 cases are of gang rape as also shown in Figure 7.

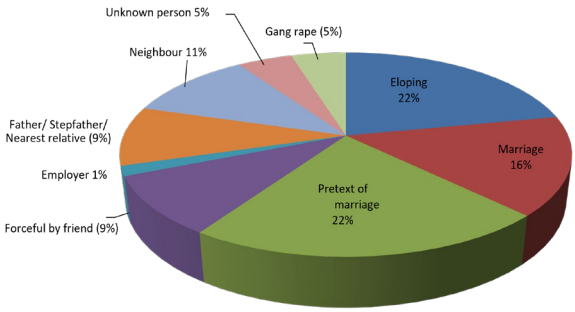


Figure 7: Distribution of POCSO cases by relationship and circumstances.

9. Conclusion

Forensic science is the backbone of the criminal justice system. While, it is our duty as forensic experts to committedly examine all the samples and do the analysis, irrespective of whatever be the back story; it needs however, to be mentioned that false cases, consensual relationships between adolescents including elopement and love marriages being registered as POCSO cases, result in wastage of material resources, a concern that must be addressed by the legislature.

The stigma surrounding the crime leads to delay of the medico legal examination and eventually sample collection that is the sole means to link the crime and the culprit. Victim's unwillingness often leads to underreporting of cases. Improper preservation of evidence also causes contamination or degradation of the evidence resulting in negative DNA results or failure to generate DNA profile. Proper collection, preservation and transportation of DNA evidence are important for accurate analysis. There needs to be adequate training of medical and forensic professionals to ensure quality examination of the case. Medical examination without delay so as to preserve the evidence, proper training and capacity building of the medical and forensic staff, and standardization of the protocols so that the evidence can be collected and preserved properly would certainly augment the positive DNA results.

Acknowledgements

The author is grateful to the Principal Director, Director (T), and Division Head, Biology, Forensic Science Laboratory, Delhi and Delhi Govt. for providing support and facilities to carry out this work.

References

1. *Slep AMS, Heyman RE, Foran HM. Child maltreatment in DSM-5 and ICD-11. Fam Process. 2015.*
2. *Krug EG, Mercy JA, Dahlberg LL, Zwi AB. The world report on violence and health. Lancet. 2002.*
3. *Ganesha JS. Issues and challenges in the implementation of POCSO Act: A review. Int J Soc Econ Res. 2019.*
4. *Seth R, Srivastava RN. Child sexual abuse: Management and prevention, and Protection of Children from Sexual Offences (POCSO) Act. Indian Pediatr. 2017.*
5. *Kaur S, Kaur S, Varshney K. Recent trends in child rape crisis in Delhi (India): A forensic overview. Forensic Sci Int Rep. 2019.*
6. *Briody M. The effects of DNA evidence on sexual offence cases in court. Curr Issues Crim Justice. 2002.*
7. *Prinz M, et al. Male/female DNA mixtures: A challenge for Y-STR analysis. Int Congr Ser. 2003.*
8. *Kayser M. Forensic use of Y-chromosome DNA: A general overview. Hum Genet. 2017.*
9. *van Oorschot RAH, et al. DNA transfer and persistence: Environmental effects on DNA evidence. Forensic Sci Int Genet. 2010.*
10. *Collin-Vézina D, De La Sablonnière-Griffin M, Palmer AM, Milne L. A preliminary mapping of individual, relational, and social factors that impede disclosure of childhood sexual abuse. Child Abuse Negl. 2015.*
11. *Gilbert MTP, et al. The isolation of nucleic acids from fixed, paraffin-embedded tissues. Mol Ecol Notes. 2007;7(6):1013–1019.*
12. *Lee SB, et al. The effect of storage conditions on DNA yield and quality from blood samples. Forensic Sci Int. 2010.*

Uncovering MDMB-4en-PINACA in "Tuklaw" Cigarette Sticks: Evidence of Synthetic Cannabinoid Adulteration

Aleah Marie P. Oseña*, Marie Angeline L. Lee, Jocel Carlo M. Borja, Anna Loe R. Montilla, Shane T. Mendez, Richard Angelo M. Solis, Ronald Jefferson A. Narceda, Jasmyne Lora M. Jaranilla, Severino P. Jr. Uy and Angela D. Salvador
Philippine Drug Enforcement Agency, Philippines
**Email: yanyosena@gmail.com*

1. Introduction

In July 2025, Philippine law enforcement agencies were alerted to reports of youth experiencing seizures after allegedly smoking so-called "black cigarettes" [1,2]. These black cigarettes, locally referred to as "tuklaw", were allegedly made from leaves sourced from Vietnam [2]. The alleged leaves source, thuốc lào (*Nicotiana rustica*), are said to have higher levels of nicotine [3] as compared to the commercially-used tobacco, *Nicotiana tabacum*. In response, the Philippine Drug Enforcement Agency (PDEA) has taken the initiative to identify the psychoactive substances present in these so-called black cigarettes. Preliminary laboratory analysis of the cigarettes confirmed the presence of MDMB-4en-PINACA, a type of synthetic cannabinoid.

According to the European Monitoring Centre for Drugs and Drug Addiction (EMCDDA), exposure to this synthetic cannabinoid has led to non-fatal poisoning with symptoms such as loss of consciousness, seizures, changes in behavior, and cardiovascular effects [4,5]. It was further reported that MDMB-4en-PINACA was in powder form as first identified in Europe, which is consistent with the observed market trend of synthetic cannabinoids [4].



Figure 1.
(a) The concealment box and black cigarette sticks as submitted by operatives of PDEA.
(b) The concealment box and the black cigarette stick as submitted by operative of PDEA. This set of pieces of evidence is observed to have the same as the photograph depicted in Figure (a).
(c) A brown cigarette stick as submitted by PDEA operatives on a separate occasion as featured in Figure 1 (a) and (b).
(d) A heat-sealed transparent plastic sachet, and
(e) cylindrical tube both containing dried leaves.

The Case

PDEA operatives submitted the "tuklaw" samples to the laboratory for examination. Photographs of the specimens submitted at different instances are shown in Figure 1. The cigarette samples were contained in black boxes with a brand label "RICHMOND" with no defined variety. Figure 1(c) to (e) featured a single brown cigarette stick, and photographs of dried leaves contained in a plastic sachet and a glass vial, respectively.

Upon verification of the cigarette brand, a legitimate product package was found, but the same was released for a limited time in 2010 [6]. Photos of the authentic variant are shown in Figure 2 for comparison. Figure 3 shows the current packaging of the same cigarette brand [7]. As observed, the legitimate packaging in Figures 2(a) and 2(b) have holographic embossed brand name, logo and variant, while those in Figures 1(a) and 1(b) were noticeably only printed in white. No other labels were observed in Figures 1(a) and 1(b) as opposed to those in Figures 2(a) and 2(b). The cigarette samples contained dried plant material resembling that of conventional tobacco as shown in Figure 4. It was noted that a white circular sticker with the label "Open" is present on all the cigarette stick samples. This paper discusses the identification of the psychoactive compound in the plant material contained in the packaging as shown in Figure 1.



Figure 2. Photos of the legitimate packaging as archived by an avid collector and posted on the internet (6).



Figure 3. Current packaging of the cigarette brand as advertised in an online shopping platform (7).

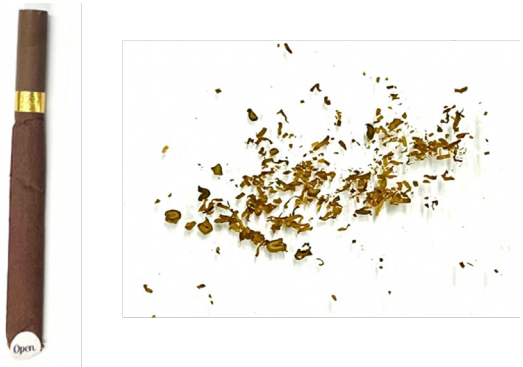


Figure 4. The plant material contained in cigarette sticks.

2. Materials and Methods

The laboratory analysis conducted by the PDEA focused on the qualitative identification of the psychoactive compounds present in the cigarette samples. Further studies such as definitive identification of the plant material, quantitative nicotine analysis, and screening for presence of other alkaloids are outside the scope of this case report, but efforts are being made to bring this information to light.

Materials and Instruments

The solvents used were methanol (99.9% purity, RCI Labscan), n-hexane (97.8% purity, RCI Labscan), and chloroform (99.8% purity, Merck). The certified reference material (CRM) was a neat solid MDMB-4en-PINACA (99.33% purity, Cayman Chemical Company, Batch no. 0597712-80). The GC-MS and GC-MS/MS analyses were performed on a Shimadzu TQ 8040 triple quadrupole MS system equipped with a Shimadzu capillary column (SH-Rxi-5Sil MS: 30m x 0.25mm I.D., df=0.25µm (320/350°C), and an autoinjector AOC-20i. The GC-MS method was adopted from the UNODC recommended methods of analysis with the following parameters (Table 1). The parameters for the triple quadrupole analysis were adopted from a previous study conducted by Wang and colleagues [13] with the conditions listed below (Table 2). The SEM system was JEOL Model JSM1500 ITHR/LA Field Emission Scanning Electron Microscope. Microscopic examination was performed using a Nikon SMZ18 stereomicroscope coupled with NIS-Element Software.

Sample Preparation

Light Microscopy

The samples were placed onto clean petri dish prior to microscopic analysis. Some portion of the samples were finely crushed for comparison of the microscopic images.

Scanning Electron Microscopy

Prior to analysis, surface dust was lightly removed with a squeeze blower to minimize interferences. The bulk plant materials were mounted on aluminum stubs with a double-sided conductive carbon tape. Then the mounted samples were coated with platinum using the Auto Fine Coater for 70 seconds. The samples were loaded onto the SEM for imaging.

Chromatographic and Spectroscopic Analyses

To ensure sample homogeneity, the plant material was finely crushed. Ten milligrams of the homogenized plant material were placed in three separate vessels and extracted in 5 mL each of the following solvents: methanol, chloroform, and n-hexane. This was followed by sonication for 30 minutes with no heat applied to enhance extraction efficiency. The resulting solids of the extracts were allowed to settle. Afterwards, the extracts were filtered using PES syringe filter with pore size of 0.2 µm and were subjected to chromatographic and spectroscopic analysis. One milligram of the MDMB-4en-PINACA standard was dissolved in 5 mL of methanol and separately injected into the GC-MS.



Figure 5. (a) and (b) Bulk plant material observed under stereomicroscope. (c) The observed white powdery adulterant in crushed plant material in stereomicroscope.

Table 1. Parameters for the GC-MS analysis.

GC Conditions	
Carrier Gas	Helium
Flow Rate	0.8 mL/min
Oven Temperature	Gradient program: Total running time 40 mins Initial temperature: 100°C for 1 min Ramp to 290°C at a rate of 10°C/min final hold for 20 mins
Solvent Delay Time	3.0 mins
Forward Inlet Temperature	260°C
Injection Mode	Splitless
Injection volume	1µL
MS Conditions	
Ion Source Temperature	230°C
Data Acquisition Method	Q3 Scan

Table 2. Parameters for the GC-MS/MS analysis

GC Conditions	
Carrier Gas	Helium
Flow Rate	1.65 mL/min
Collision Gas	Nitrogen
Flow Rate	1.5 mL/min
Oven Temperature	Gradient program: Total running time 25 mins Initial temperature: 80°C for 1.0 min Ramp to 220°C at a rate of 15°C/min Ramp to 300°C at a rate of 30°C/min final hold for 12 mins
Solvent Delay Time	3.0 min
Forward Inlet Temperature	250°C
Injection Mode	Splitless
Injection Volume	1 µL
MS Conditions	
Ion Source Temperature	230°C
Quadrupole Temperature	125°C
Positive Electron Ionization (IE) voltage	70eV
Data Acquisition Method	Multiple Reaction Monitoring (MRM) mode

3. Results and Discussion

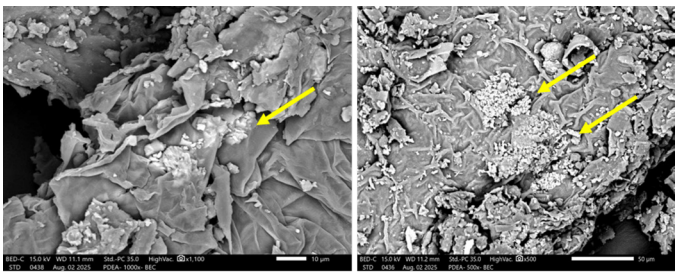
Light Microscopy

Homogenized and bulk portions of the plant materials were examined under a light stereomicroscope. The bulk sample exhibited fragmented leaf-like structures of varying sizes, while a homogenized sample consisted of finely crushed particles with reduced morphological structure Figure 5 (a) and (b). Microscopic examination revealed the possible presence of a white powdery substance distributed across the leafy plant material as highlighted in (c). This observation suggests adulteration of the tobacco product.

Scanning Electron Microscopy (SEM)

SEM analysis was carried out to confirm findings of light microscopy. Figure 6 (a) and (b) are SEM images showing textured surfaces characteristic of plant epidermal tissue [8–10]. In both images, backscattered electron imaging (BSE) highlights the white particles (indicated by arrows)

with increased contrast, suggesting that the white particles are made of heavier elements. Measurements of the particles at the magnification of 1000X were also taken with average particle sizes of 3.223 to 3.858 µm. Furthermore, the measurements of the maximum and minimum size, and their standard deviations were comparable for both images, implying a relatively uniform particle size distribution. This observation supports the possibility that the cigarette leaves were coated or laced with another substance.



(a) (b)

Figure 6. SEM image of plant material at (a) 1000X and (b) 500X respectively.

GC-MS

Each solvent extract was filtered and diluted prior to injection into the GC-MS. The method parameters used for the GC-MS analysis was based on the laboratory's routine analysis of unknown substances. Since the methanol extracts were found to have the best separation and resolution, the chromatogram of the methanol extracts was reported in this paper. Figure 7 (a) and (b) shows the chromatogram of sample extracted with methanol which has three distinct peaks at Rt = retention times 7.395, 19.760, 20.620 minutes. The peak at 7.395 min was identified as nicotine while that at 20.620 min was determined to be MDMB-4en-PINACA, based on mass spectral matches with the SWGDRUG library.

Furthermore, the top ten spectral peaks Figure 7 (c) and (d) of the chromatographic peak at 20.620 min were 213, 301, 145, 298, 171, 214, 357, 269, 185, and 131 m/z which are consistent with those reported in a previous elucidation study [11]. The chromatographic peak at 7.395 min has spectral base peaks of 84 and 133 m/z which are the known base peaks of nicotine [12]. The chromatographic peak at 19.760 min showed no consistent MS library match and could not be elucidated at the time writing.

MDMB-4en-PINACA standard was also analyzed under the same GC-MS method as the extracted samples. The retention time of the standard was 20.550 min. The difference (0.341%) was within the window (± 2%) as per the UNODC Guidance for the Validation of Analytical Methodology and Calibration of Equipment used for Testing of Illicit Drugs in Seized Materials and Biological Specimens [14]. Analysis by GC-MS confirmed the presence of the MDMB-4en-PINACA through comparison with a reference standard and library matching using SWGDRUG version 3.13.

GC-MS/MS

Following the preliminary identification of the substance, relevant literature concerning its possible identity was reviewed, and further examination by GC-MS/MS was carried out for a targeted analysis. The chromatograms and mass spectra of the sample and standard are presented in Figure 8. The GC-MS/MS retention time of the methanol extracts from the sample and MDMB-4en-PINACA standard were found at 14.356 and 14.367 minutes, respectively. The percent error was determined to be 0.077%, which is within the window (± 2%) as stated in the UNODC guidelines [14]. The difference in retention time between the GC-MS analysis and GC-MS/MS analysis was due to changes in method parameters such as the carrier gas flow rate and oven temperature gradient. Such changes to the method parameters were chosen to focus on the isolation of the MDMB-4en-PINACA content of the samples.

The parent-daughter ion transitions 213 > 145 and 301 > 213 as reported by Wang et al [13] were all detected. The same fragmentation was observed for both the sample and the standard. The mass spectra show the fragmented ions in the first quadrupole then the specific product ions detected in the third quadrupole. The ions detected in the third quadrupole are 145 m/z as fragmented from 213 m/z, and 213 m/z as fragmented from 301 m/z.

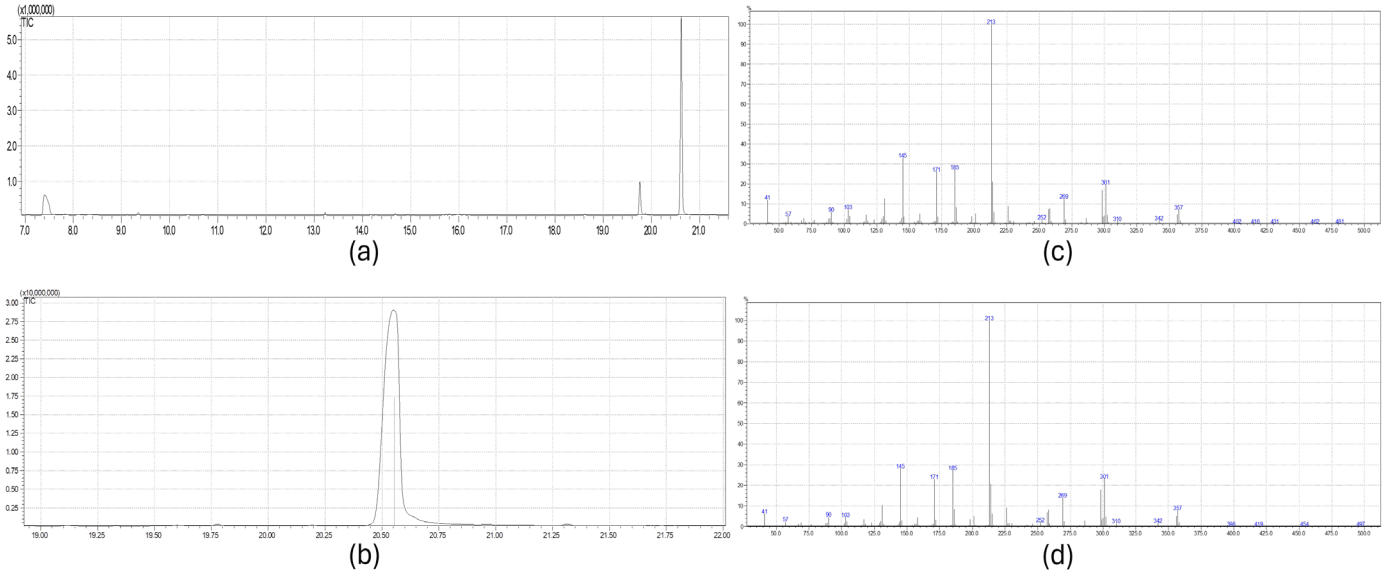


Figure 7. Chromatograms of (a) the methanol extract showing three peaks at 7.395, 19.760, 20.620 minutes and (b) MDMB-4en-PINACA standard at the retention time at 20.550 mins. Mass spectra of (c) the sample and (d) MDMB-4en-PINACA standard showing the base peaks (213, 145, 301 m/z).

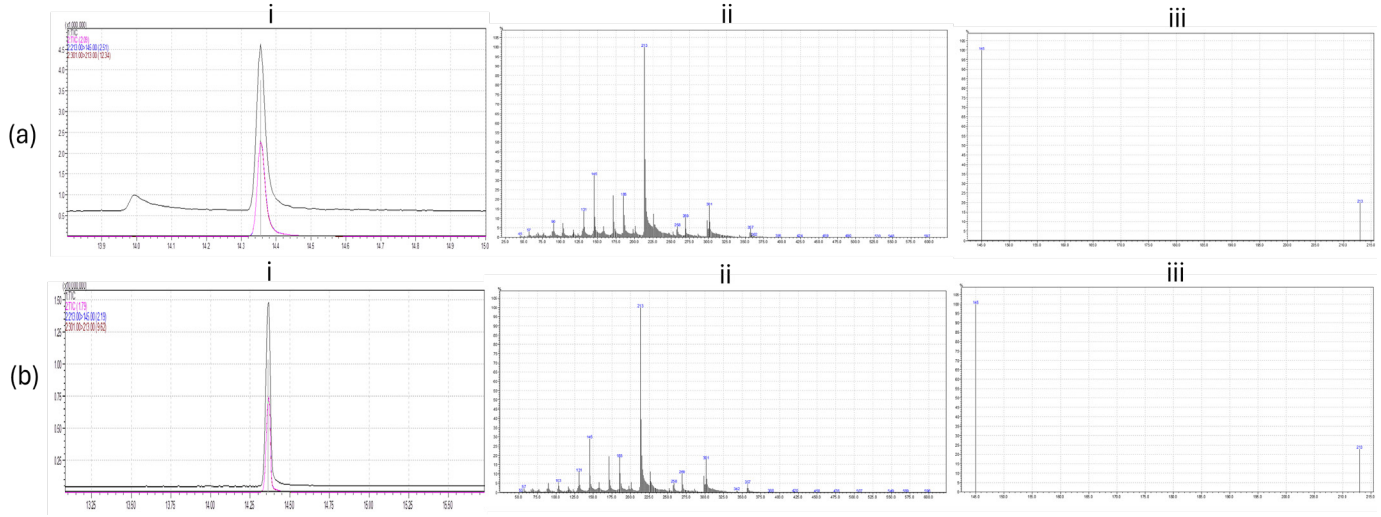


Figure 8. (i) Chromatograms of GC-MS/MS analysis, (ii) mass spectra of the detected fragmented ions in the first quadrupole and (iii) the third quadrupole of (a) the methanol extract and (b) MDMB-4en-PINACA standard at the retention times of 14.356 min and 14.367 min respectively.

Table 3 summarizes the ion ratio comparison between the MDMB-4en-PINACA standard and methanol extract sample. The 213>145 transition was observed to have relative intensity of 20.00 for the sample and 22.46 for the standard. This yielded a difference of 10.96% which falls between the tolerance window. The accepted criteria were adopted from the UNODC Guidance [14]. The fragmentation pattern was observed to be the same between the sample and the standard. Hence, it could be concluded that the identity of the peak was MDMB-4en-PINACA.

Table 3. Comparison of ion ratios between the MDMB-4en-PINACA standard and methanol extract sample.

Parameter	Relative Intensity (%)		% Error	Accepted Criteria (UNODC Guidance)
Transition Ion	MDMB-4en-PINACA standard	Methanol Extract Sample		
301 > 213	100.00	100.00	-	±20%
213 > 145	22.46	20.00	10.96%	

4. Conclusions

Reports of a black cigarette locally referred to as "tuklaw", allegedly causing seizures and other adverse health effects to youth have alerted the Philippine law enforcement agencies, prompting the initiative to uncover the psychoactive components present in these cigarettes. The packaging of such cigarettes was black and labeled with RICHMOND which resembled authentic variant of the same brand. The cigarette sticks contained dried plant material resembling conventional tobacco. Physical characterization by microscopy and SEM imaging revealed that the surface of the plant material was adulterated with white powder. Qualitative analysis of the plant material by GC-MS and GC-MS/MS confirmed the presence MDMB-4en-PINACA in the powder.

Acknowledgements

The authors would like to acknowledge the De La Salle University – Central Instrumentation Facility, especially Mr. Joem A. Viyar and Dr. Jose M. Esmeria Jr for their contributions to the SEM analysis.

References

1. *Sigales J. INQUIRER.net. PNP eyes crackdown on 'tuklaw' cigarettes. Https://newsinfo.inquirer.net/2164264/pnp-eyes-crackdown-on-tuklaw-cigarettes, 2026 (accessed 27 Apr 2026).*
2. *News GI. GMA News Online: Why smokers suffered seizures after puffing on "tuklaw" or black cigarette. Https://www.gmanetwork.com/news/topstories/nation/954890/pdea-black-cigarette-tuklaw-seizures/story/, 2026 (accessed 25 Apr 2026).*
3. *Kaminski KP, Bovet L, Laparra H, et al. Alkaloid chemophenetics and transcriptomics of the Nicotiana genus. Phytochemistry. 2020 Sep;177:112424.*
4. *Oomen PE, Schori D, Tögel-Lins K, et al. Cannabis adulterated with the synthetic cannabinoid receptor agonist MDMB-4en-PINACA and the role of European drug checking services. Int J Drug Policy. 2022 Feb;100:103493.*
5. *EMCDDA initial report on the new psychoactive substance MDMB-4en-PINACA | The European Union Drugs Agency (EUDA). Https://www.euda.europa.eu/publications/initial-reports/mdmb-4en-pinaca_en, 2026 (accessed 27 Apr 2026).*
6. *ZIGSAM - THE AUSTRIAN CIGARETTE COLLECTION. Https://www.zigsam.at/F_AddMenuB.htm?https://www.zigsam.at/B_Richmond.htm, 2026 (accessed 27 April 2026).*
7. *Richmond Original Cigarettes 20 Pack | Buy Online | Bull Brand. Https://www.bullbrand.co.uk/products/richmond-king-size-real-blue-20s-cigarettes, 2026 (accessed 27 April 2026).*
8. *Pathan AK, Bond J, Gaskin RE. Sample preparation for SEM of plant surfaces. Mater Today. 2010;12:32–43.*
9. *Talbot MJ, White RG. Cell surface and cell outline imaging in plant tissues using the backscattered electron detector in a variable pressure scanning electron microscope. Plant Methods. 2013;9(1):40.*
10. *Scanning Electron Microscope A To Z [lab manual]. Tokyo, Japan: JEOL Ltd.*
11. *Abbott MJ, Dunnett J, Wheeler J, Davidson A. The identification of synthetic cannabinoids in English prisons. Forensic Sci Int. 2023 Jul;348:111613.*
12. *Patel PH, Conrad KL, Pathiranage AL, Hiatt LA. Practical Applications of Organic Chemistry: Improving Student Knowledge of GC–MS through Qualitative Analysis of Nicotine in Electronic Cigarette Vapors. J Chem Educ. 2020 Nov 10;97(11):4117–22.*
13. *Wang Y, Pan Y, Yang H, et al. Quantification of MDMB-4en-PINACA and ADB-BUTINACA in human hair by gas chromatography–tandem mass spectrometry. Forensic Toxicol. 2022 Jul;40(2):340–8.*
14. *Vereinte N. Guidance for the validation of analytical methodology and calibration of equipment used for testing of illicit drugs in seized materials and biological specimens: a commitment to quality and continuous improvement. New York: United Nations; 2009.*

Persistence of MDMB-4en-PINACA in Indonesia's Illicit Drug Market: Evidence of Continued Supply and Local Synthesis from MDMB-INACA

Tanti*, Supiyanto, Carolina Tonggo Marisi Tambunan, Maimunah, Christien Andriyani Lalangi, Dwi Handayani, Rina Siska, Erlana Nindya Maulida, Utari Pramudita, Verawati Rahman, Martin Luther Silubun, Widianti Ningtias and Windi Septiarini
Center of Drugs Testing Laboratory of National Narcotics Board, Indonesia
**Email: risetpuslabbnn@gmail.com*

1. Introduction

Synthetic cannabinoids continue to evolve and diversify. Since their first emergence in the year of 2013, various new types of synthetic cannabinoids have been discovered every year in Indonesia. By the end of April 2026, 100 New Psychoactive Substances (NPS) had been identified in the country, 40 among these were synthetic cannabinoids. Most of them were found blended with tobacco leaves with or without packaging, less commonly found in powder and tablets form, and recently detected in e-liquid vape. To restrict market expansion, Indonesia has legal procedures to classify new types of identified NPS, including synthetic cannabinoids, into narcotics or psychotropics regulation. Once NPS are regulated, new synthetic cannabinoids emerged to evade legal control, resulting in a recurring cycle.

We took interest in MDMB-4en-PINACA. Despite being regulated in 2020 as a Schedule I narcotic list in Indonesia, it has continued to exist and detected in the market until recently. It is widely circulating in various forms, whether as a single compound or in mixtures with other substances. As reported by several publications, MDMB-4en-PINACA can be synthesized by using the tail-less indazole carboxamide synthetic cannabinoid, MDMB-INACA, as a precursor via one-step reaction [1-3]. MDMB-INACA has also been regulated as Schedule I narcotic list in Indonesia. This article highlights the various cases of MDMB-4en-PINACA identified, including its illicit production site dismantled in Indonesia, which may affect the long existence of this drug in illicit drug market.

2. MDMB-4en-PINACA Scene in Indonesia

2.1. Structure-activity Relationship

MDMB-4en-PINACA (Methyl (S)-3,3-dimethyl-2-(1-(pent-4-en-1-yl)-1H-indazole-3-carboxamido)butanoate), belongs to subclass of synthetic cannabinoids with an indazole core (1) substituted by a tert-leucine methyl ester (3), both linked by a carboxamide group (2). MDMB-4en-PINACA bears structure similarity to 5F-ADB (5F-MDMB-PINACA), except that it replaces fluoropentyl tail with an alkene terminal (4) on the side chain of its structure [4-6] (Figure 1).

MDMB-4en-PINACA is a full and potent CB1 and CB2 receptor agonist, produces cannabinoid-like behavioral effects with 107-fold greater potency than Δ9-THC [7], and poses severe health consequences, which in some cases can be fatal (Table 1). Based on its structure-activity relationship by radioligand binding studies, indazole core showed greater affinities for CB1 and CB2 than indole group, resulting in its greater potency [4]. The presence of an alkene group on the

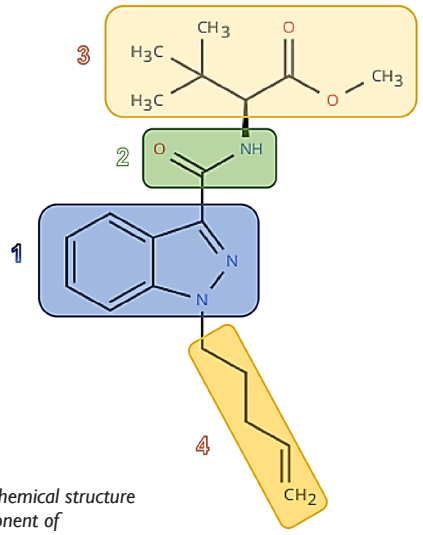


Figure 1. Chemical structure and component of MDMB-4en-PINACA

side chain of MDMB-4en-PINACA structure may relate to the previous research involving indole synthetic cannabinoid where the alkene terminal like 4-pentenyl showed less affinity than the single bond n-pentyl tail [8], while fluoro-substituted tail might enhance blood–brain barrier penetration and CB1 binding affinity, resulting in higher potency [7] than n-pentyl tail. In a preclinical study carried out by observing the effect on locomotor activity, body temperature, pain sensitivity, and catalepsy of indazole-carboxamide groups in mice, MDMB-4en-PINACA has lower potency than 5F-ADB yet greater potency than ADB-4en-PINACA. Moreover, MDMB-4en-PINACA showed much greater potency when compared to its precursor, MDMB-INACA [1].

Table 1. Adverse effects from overdosing MDMB-4en-PINACA [6].

Gastrointestinal	Nausea, vomiting
Neurological	Hallucination, seizures, convulsions, agitation, anxiety, paranoia, confusion, delusions, catatonia, lethargy, psychosis, loss of consciousness/coma
Cardiovascular	Tachycardia, hypertension, acute myocardial infarction, sudden cardiac death
Renal	Acute kidney failure
Respiratory	Respiratory depression

2.2. Case Reports

Trends of MDMB-4en-PINACA

MDMB-4en-PINACA was first identified in 2019 by our laboratory, with a total of three samples reported. A year later, the substance was officially regulated and classified as a Schedule I Narcotic list in Indonesia. However, there has been a huge increase in the number of MDMB-4en-PINACA cases in the following years, reaching its peak in 2023 with a total of 2,471 samples, of these 1,259 samples were found to contain MDMB-4en-PINACA as a single compound, while 1,212 samples were multi-compound products containing MDMB-4en-PINACA (Figure 2).

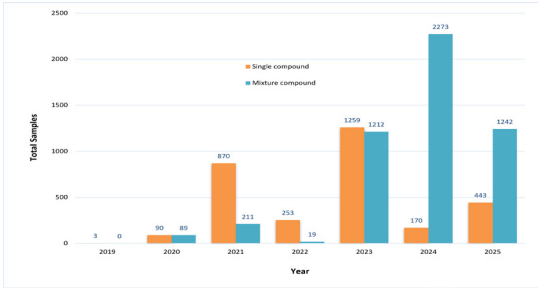


Figure 2. MDMB-4en-PINACA cases analyzed by BNN Laboratory.

In the last six years, MDMB-4en-PINACA quickly became one of the most popular synthetic cannabinoids in Indonesia. It has dominated the synthetic cannabinoids class detected in our laboratory since 2021 (Figure 3), and most frequently found in adulterated plant materials and vaping products. Figure 4 depicts various forms of MDMB-4en-PINACA concealment in Indonesia analyzed by BNN Laboratory.

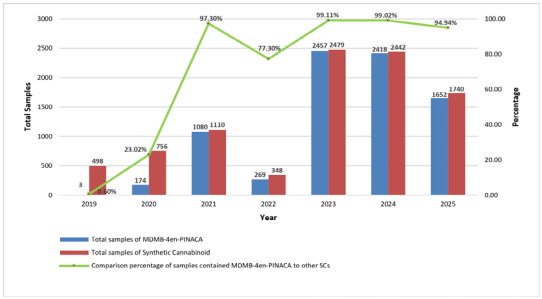


Figure 3. Data comparison of MDMB-4en-PINACA among other synthetic cannabinoids.

Illicit production site of MDMB-4en-PINACA

The persistent availability of MDMB-4en-PINACA in Indonesian market was associated with the continued drug supply in the country. BNN investigators dismantled a clandestine MDMB-4en-PINACA laboratory in Banten in January 2026 (Figure 5). The laboratory had contributed to the increasing drug's domestic supply and its extensive distribution. In this illicit production site, MDMB-4en-PINACA was synthesized by MDMB-INACA as starting material or precursor which is purchased from online marketplace. Several chemicals and reagents were found on site, including 5-Bromo-1-pentene, dimethylformamide (DMF), methanol, ethanol, acetone, propylene glycol, and an empty white bottle labeled "Potassium Carbonate". MDMB-INACA was detected as residue on a used transparent plastic bag (Figure 6).

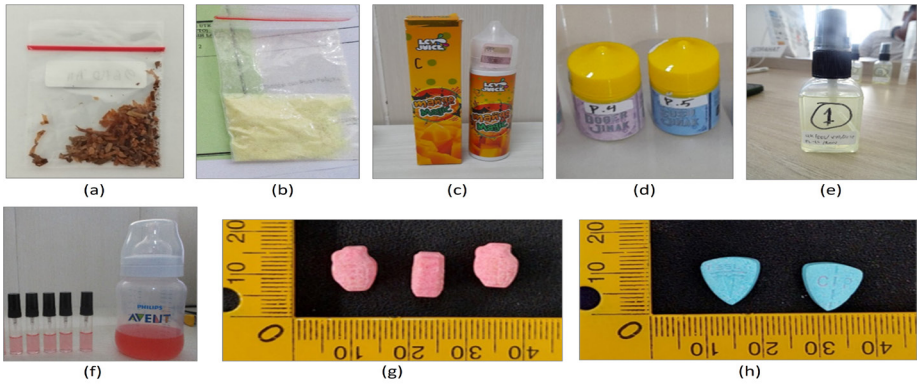


Figure 4. Products containing MDMB-4en-PINACA analyzed by BNN Laboratory:
(a) Vegetable Matter (MDMB-4en-PINACA),
(b) Powder (MDMB-4en-PINACA),
(c) e-Liquids (MDMB-4en-PINACA),
(d) e-Liquids (MDMB-4en-PINACA & MDMB-INACA),
(e) Liquid spray (MDMB-4en-PINACA),
(f) Liquid spray MDMB-4en-PINACA, MDMB-INACA, 5F-ADB, MDMB-5-Methyl-INACA,
(g) Pink Grenade Tablet (MDMA, Methamphetamine, MDMB-4en-PINACA, 5F-ADB) and
(h) Blue Tesla Tablet (Methamphetamine, MDMB-4en-PINACA, MDMB-INACA)..



Figure 5. MDMB-4en-PINACA Clandestine Laboratory.



Figure 6. Examples of chemicals and reagents found on site of a clandestine laboratory.

The synthesis process of MDMB-4en-PINACA was initially carried out by placing MDMB-INACA into a reaction vessel and heated and stirred for several hours together with dimethylformamide (DMF), potassium carbonate, and 5-bromo-1-pentene. After cooling at ambient temperature, ice water or ice was added to the mixture for the final precipitation step and yielded the paste or wet solid form. The products were then filtered to produce wet solid containing MDMB-4en-PINACA (Figure 7). Its precursor, MDMB-INACA, was also found as impurities in some incomplete reactions. Reaction conditions applied affected the degree of precursor involved in the final product [1]. The products were then dissolved in methanol, ethanol, or acetone prior to spraying to the tobacco leaves. Plant materials laced with MDMB-4en-PINACA were identified in this illicit laboratory, which led to the longer persistence of MDMB-4en-PINACA in Indonesia. I n 2023, 2024 and 2025, a total number of 1181, 2245 and 1063 seized samples containing both MDMB-4en-PINACA and MDMB-INACA have been detected in our Laboratory, respectively, which might indicate that these compounds have already been produced using the same synthesis pathway.

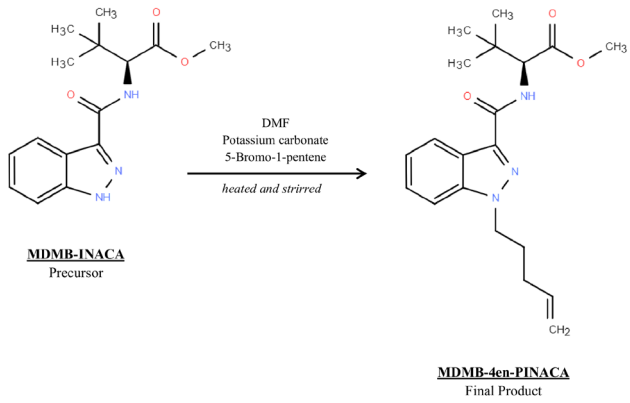


Figure 7. One-step synthesis pathway of MDMB-4en-PINACA.

2.3. Analytical workflow

Sample preparation

The analytical workflow for analysis of MDMB-4en-PINACA in BNN Laboratory is carried out based on the type of samples as shown in Figure 8. Each analytical workflow begins with sample preparation prior to drug identification.

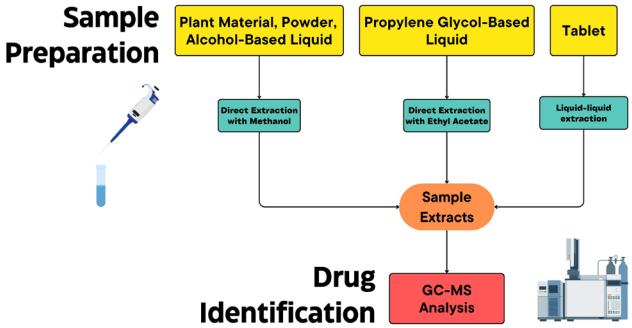


Figure 8. Workflow for MDMB-4en-PINACA analysis.

a. Direct extraction with methanol

It is applied for samples in the form of plant materials, powder, and alcohol-based liquid. An amount of samples was added by 5 mL of methanol and extracted by 1 hour sonication. After completion, the extracts were filtered prior to GC-MS identification.

b. Liquid-liquid extraction

For tablet samples suspected containing MDMB-4en-PINACA, liquid-liquid extraction is applied. First, tablets were ground into homogenous powder, then weighed approximately 80 mg and dissolved in 5 mL of distilled water. The water-based solution was added by an organic extracting solvent followed by shaking for 5 minutes and centrifugation at 3000 rpm 5 minutes. Organic layer was collected and filtered prior to GC-MS identification.

c. Direct extraction with ethyl acetate

It is applied for propylene glycol-based vape liquid samples. The liquid sample is mixed with ethyl acetate (1:1 v/v) and sonicated for approximately 1 hour. The upper layer was filtered prior to GC-MS identification.

Instrumental analysis

Qualitative analysis of MDMB-4en-PINACA was performed by GC-MS (7890B – 5977B, Agilent) equipped with an HP-5MS fused silica capillary column (30 m × 0.25 mm x 0.25 µm). Injection mode was split 1:50 and flow rate was 1.2 mL/min. Injector and ion source temperature were maintained at 300°C and 280°C, respectively. The initial column temperature was set at 80°C and held for 0.17 min followed by ramps of 30°C/min to 300°C and held for 2 min then increased to 320°C at 5°C/min and held for 3 min. The total run time was 17 min.

For liquid samples, Raman spectroscopy and Fourier Transform Infra-Red (FTIR) analysis was carried out to identify the solvent involved in the liquid samples before the sample extraction.

Interesting GC-MS profiles were observed from several samples containing MDMB-4en-PINACA whether in single or multi-compound products (Figure 9 to 11).

3. Conclusion

MDMB-4en-PINACA continues to be a growing concern in Indonesia due to its huge increase in cases, presence in many forms of illicit products, and the ease of illicit manufacture. The physiological effects themselves have been associated with a wide range of adverse reactions and may cause or contribute to death. Mixture of this drug with other substances in multi-compound products may contribute to more severe intoxication. To address the fast-evolving MDMB-4en-PINACA trend, it is necessary to tighten regulations on importation of precursors substances, especially those purchased through online marketplaces. Laboratories should develop quantitative methods to measure the content of MDMB-4en-PINACA in each analyzed sample.

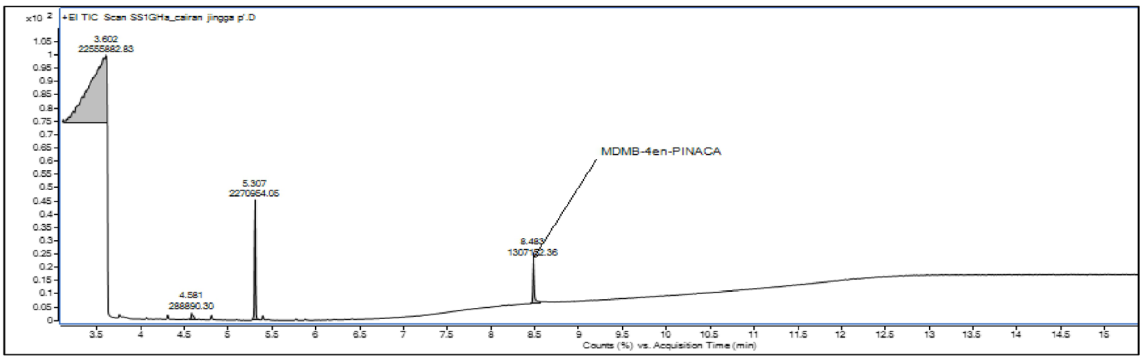


Figure 9. GC-MS chromatogram of liquid spray containing MDMB-4en-PINACA.

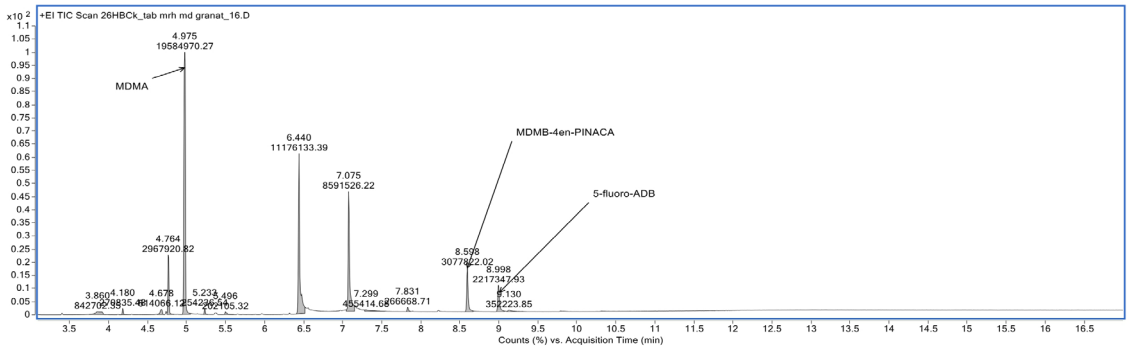


Figure 10. GC-MS chromatogram of tablet containing MDMA, MDMB-4en-PINACA and 5-fluoro-ADB.

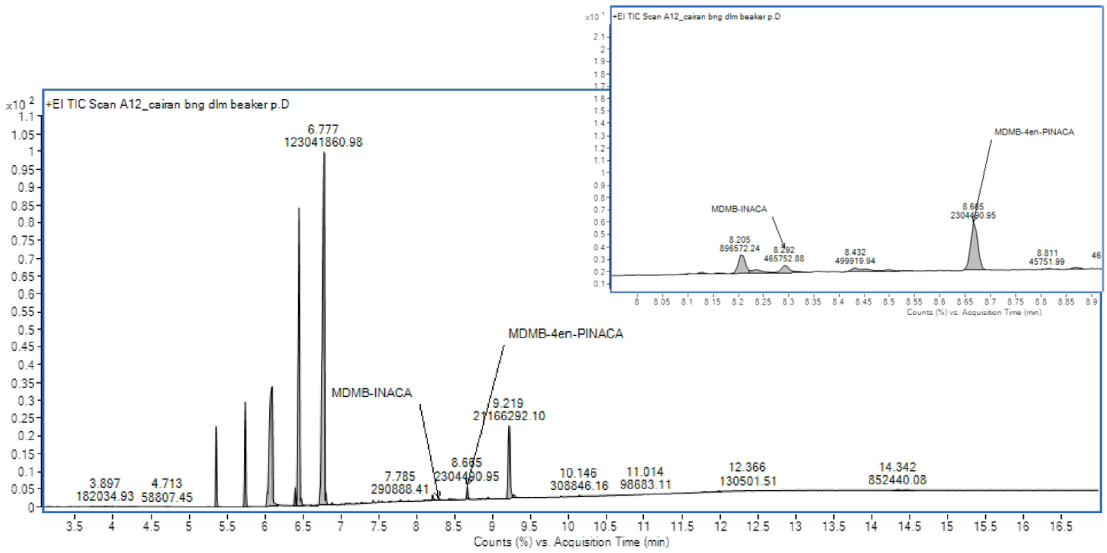


Figure 11. GC-MS chromatogram of clandestine laboratory evidence containing mixture of MDMB-4en-PINACA and its precursor, MDMB-INACA.

References

1. *Monti MC, Rautio T, Deventer MH, et al. Tail-less precursors in synthetic cannabinoid production: investigating a clandestine laboratory, seized samples, and CB1 activity. Archives of Toxicology. 2025, Sep; 99(9):3641-61.*
2. *The Center for Forensic Science Research & Education. NPS Discovery — New Drug Monograph: MDMB-INACA (2023). Https://www.cfsre.org/images/monographs/MDMB-INACA-New-Drug-Monograph-NPS-Discovery-230626.pdf, 2026 (accessed 4 April 2026).*
3. *Deventer MH, Krotulski AJ, Stove CP. "Do It Yourself" Synthetic Cannabinoid Receptor Agonist Precursors as a Ban-Evading Strategy: Comparison of the Pharmacological Characteristics of Precursors and Their Final Products. Drug Testing and Analysis. 2025, Nov; 17(11):2148-58.*
4. *Schoeder CT, Hess C, Madea B, et al. Pharmacological evaluation of new constituents of "Spice": Synthetic cannabinoids based on indole, indazole, benzimidazole and carbazole scaffolds. Forensic toxicology. 2018, April; 36(2):385-403.*
5. *World Health Organization. Critical Review Report: MDMB-4en-PINACA. Geneva: 43rd ECDD; 2020.*
6. *EMCDDA. MDMB-4en-PINACA: Risk Assessment Report. Luxembourg: Publications Office of the European Union; 2022.*
7. *Qiao Y, Shi X, Li K, et al. Assessment of abuse potential of three indazole-carboxamide synthetic cannabinoids 5F-ADB, MDMB-4en-PINACA and ADB-4en-PINACA. International Journal of Molecular Sciences. 2025, Jul 3; 26(13):6409.*
8. *Gu K, Qin S, Zhang Y, et al. Metabolic profiles and screening tactis for MDMB-4en-PINACA in human urine and serum samples. Journal of Pharmaceutical and Biomedical Analysis. 2022, October; 220:114985.*

Forensic Profiling of Synthetic Drugs in the Republic of Uzbekistan

Rakhiya Akhmedova and Elleonora Pak*
Republican Centre of Forensic Expertise named after Kh. Sulaymanova, Ministry of Justice, Uzbekistan
**Email: elleonora-pak80@mail.ru*

1. Introduction

In global expert practice, the problem of identifying drugs in complex mixtures is not new. The United Nations Office on Drugs and Crime (UNODC) provides a clear definition of the terms "bulking agents", "adulterants" and "impurities," along with their classification, [1], while lists of composition of illicit drugs and adulterants have also been reported [2].

Studies on impurities in amphetamine-type stimulants (ATS) have been presented in [3]. These extraneous substances and route-specific impurities are inevitably formed along the synthesis pathway due to the reaction involving precursors, solvents, and reagents. Consequently, thorough purification processes are critically required to remove these manufacturing by-products and obtain a high-quality product. Researchers have also identified the most common impurities found in preparations of methamphetamine (MA), 3,4-methylenedioxymethamphetamine (MDMA), amphetamine (AP), N,N-dimethylamphetamine (DMA), and p-methoxyamphetamine (PMA).

The fact that street drugs are rarely pure was highlighted in a study [4]. An analysis of more than 5,000 samples established that less than 0.1% of the preparations contained only the primary target ingredient. The remaining samples were contaminated with at least one bulking agent or impurity. As noted in the publications and UNODC annual reports [5], these impurities can be harmful when consumed and can also complicate drug identification in forensic analysis.

In the present work, the Republican Centre of Forensic Expertise named after Kh. Sulaymanova under the Ministry of Justice of the Republic of Uzbekistan analyzed samples of narcotic drugs received between 2021 and 2025, which were submitted by law enforcement agencies for forensic chemical examination. Laboratory studies were conducted using a comprehensive approach, employing both non-destructive and destructive methods. The analytical procedure included visual inspection, optical microscopy, infrared spectroscopy (IR), gas chromatography-mass spectrometry (GC-MS), and inductively coupled plasma mass spectrometry (ICP-MS). The results are presented in the form of illicit substance profiles for forensic characterization and serve as the basis for methodological recommendations for forensic experts.

The aim of this study was to develop forensic chemical profiles of illicit drug samples seized in Uzbekistan between 2021 and 2025 by integrating morphological examination with molecular and elemental analytical techniques. The study evaluated the composition of seized materials, identified characteristic bulking agents, adulterants, synthesis-related impurities, and trace elemental markers, and assessed their value for forensic profiling, comparison of exhibits, and identification of potential common manufacturing sources.

2. Materials and Methods

Reagents and Standards

All chemical reagents and standard samples specified in this work were used as received. Chemicals and solvents from Sigma-Aldrich (USA) and Merck (Germany) were of analytical reagent (AR) grade. Certified reference materials (CRMs) for narcotic substances supplied by Lipomed (Switzerland), with the assistance of the UNODC, were used as standards. Helium (Air Liquide) served as the carrier gas. For ICP-MS analysis: standard solutions included "SIGMA ALDRICH TraceCert" multielement calibration solution (23 elements) and "LabKings" multielement calibration solution (28 elements).

Sample Preparation

All experimental samples underwent a preliminary visual inspection to determine morphological characteristics (consistency, physical state, odor, color, homogeneity, and the presence of foreign inclusions). For microscopic examination and IR spectroscopy, the samples were used as received. Relatively homogeneous samples without foreign particles were dissolved in organic solvents for GC-MS analysis, in accordance with standard protocols [6].

Meanwhile, for the analysis of samples with complex matrices, a sequential transition from category C to category A methods was applied referred to SWGDRUG. This ensures comprehensive screening of the submitted exhibit (physical evidence) [7]. Figure 1 below illustrates some of the samples investigated.



Figure 1. Samples of powdered substances.

It was observed that from 2021 to 2025, the morphological characteristics of substances seized from illicit drug trafficking in the Republic of Uzbekistan have undergone notable changes. At the beginning of this period, substances submitted for examination were predominantly homogeneous white powders. Over the reporting period and up to the present, the forms and types of these narcotic substances have evolved.

Forensic examinations increasingly involve heterogeneous mixtures of powdered, granular, crystalline, and liquid substances of various colors. The statistics of these samples are presented in Figure 2. The growing diversity of physical forms in illicit substances poses challenges to comprehensive, objective, and scientifically sound investigation. Consequently, the development of advanced analytical methods tailored to these distinct physical forms is an urgent and essential necessity.

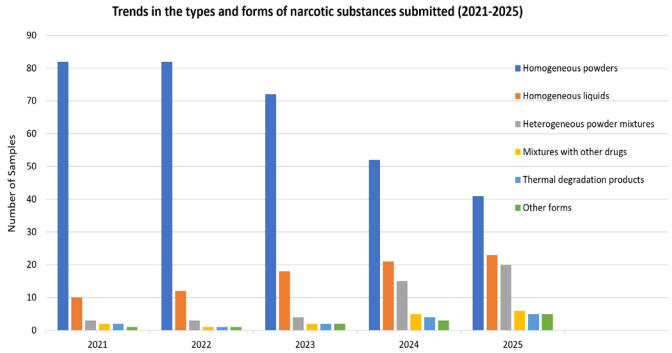


Figure 2. Trends in the types and forms of narcotic substances submitted 2021-2025.

Preliminary Analysis

The sample preparation procedure was selected based on the physical state, the presence of extraneous mechanical impurities, and the nature of the carrier object.

Preliminary microscopic examination was performed using an Olympus SZX10 optical microscope (Japan) equipped with an SD-50 digital video camera. Mechanical mixtures were separated into individual fractions of particles and granules, which were then dissolved in organic solvents. Bulking agents, adulterants (sugar, salt, baking soda, starch, flour, cereals, syrup) and certain impurities (pharmaceuticals, caffeine) were identified using qualitative chemical tests.

The preliminary chemical composition was determined using an Agilent Technologies FTIR-640 spectrometer (spectral range 4000 - 400 cm^{-1}). Homogeneous liquids were evaporated to dry residues. Substance residues were rinsed from the carrier objects using organic solvents and then concentrated to a minimum volume or evaporated to dryness.

Confirmation tests

SHIMADZU GCMS-QP2020 gas chromatograph-mass spectrometer equipped with a capillary column (30 m × 0.25 mm, 5% phenyl methyl siloxane in dimethylsiloxane) was used as the confirmation method. The analytical conditions were as follows: HP-5MS column (30 m × 0.25 mm × 0.25 µm); the oven temperature program was 150 - 280°C; the linear velocity was 56.3 cm/sec; and the system operated in split mode.

Elemental Analysis

For comparative purposes and to determine the trace elemental composition , an ICP-MS AT 7500 instrument was utilized. The presence of metal and non-metal ions may result from the inclusion of extraneous bulking agents, adulterants and impurities (e.g., salt, baking soda), as well as from contamination of raw materials, intermediates, solvents, and the target substance during organic synthesis in illicit laboratories. Analysis is feasible when a sufficient sample size is available, with a minimum required weight of 0.1 gram (g).

3. Results and Discussion

The following informative criteria were selected for the forensic characterization of the investigated samples: purity, quantitative content of the target narcotic substance, the nature of bulking agents, adulterants and impurities, and the trace element mineral composition. Based on the experimental data, a steady temporal trend has been established: the average purity of drugs (mephedrone, α-PVP, methamphetamine) decreased over the reporting period (see Figure 3).

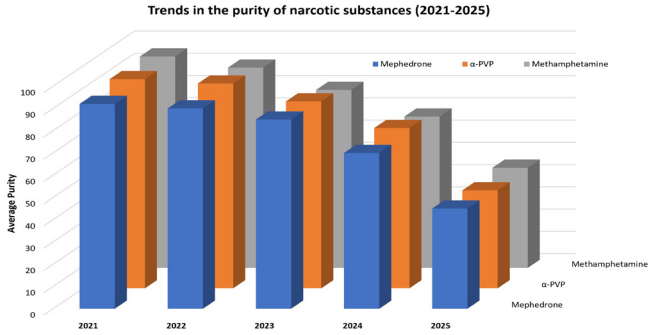


Figure.3. Trends in the purity of narcotic substances over the reporting period.

Bulking agents were detected in almost all samples, particularly those seized in 2024-2025. These included substances of household origin - salt, sugar, flour, starch, baking soda, chalk, food colorants, and semolina - as well as caffeine, nicotine, and pharmaceuticals such as diphenhydramine and paracetamol.

Cases of mixing synthetic drugs with natural substances, such as marijuana, hashish, and opium, were also noted. Impurities predominantly accompanied the main component in the samples analyzed during 2024-2025. This is attributed to the intensified activity of illicit drug laboratories within the Central Asian region, including Uzbekistan, during this period. It is probable that these inseparable contaminating impurities are unintentional by-products of drug synthesis carried out in these laboratories (Table 1).

Particular attention in this study was paid to other impurities that indicate the production of synthetic drugs in illicit laboratories. The identification and analysis (profiling) of such impurities can serve as a source of information regarding the synthesis route (method) of the substance, thereby enabling

Table 1. Forensic characteristics of impurities in synthetic drugs analyzed in the Republic of Uzbekistan, 2021–2025.

Physical Form	Detected Drugs	Adulterants	Contaminants / Impurities
Powders, Crystals, Granules, Liquids	α-PVP	Caffeine,baking soda, food coloring, caffeine, syrup, chalk, kofein, diphenhydramine, nicotine	Marijuana, hashish, opium, Synthesis by-products (pyrrolidine, pyrrolidinone-2pyrrolidine hydrobromide, pyrazines, α-PHP, α-PBP, toluene)
	Mephedrone	Salt, sugar, flour, starch, chalk, paracetamol	α-PVP, heroin, Synthesis by-products (isomephedrone, 4-aminopropiophenone,4-methyl-2-bromopropiophenone, 3-MMC, toluene, methanol)
	Methamphetamine	Plant fertilizers, fruit juice, wood treatment liquids	Tramadol, Pregabalin, Synthesis by-products (benzyl methyl ketone, NMP (N-methyl-2-pyrrolidone), methamphetamine dimers, methylamine)

the critical forensic task of linking specific street drug samples to products manufactured in an illicit laboratory.

Beyond the identification of controlled substances, forensic profiling provides valuable intelligence regarding illicit drug production and distribution. The combined evaluation of chemical composition, synthesis-related impurities, adulterants, bulking agents, and elemental signatures makes it possible to compare independent seizures, establish similarities between exhibits, and identify batches that may originate from the same clandestine laboratory or production process. Such profiling significantly expands the evidential value of forensic chemical examinations and supports intelligence-led investigations aimed at disrupting organized drug trafficking networks.

The results of ICP-MS analysis demonstrated the feasibility of studying the trace elemental composition of the samples. The presence of sodium and chlorine ions confirms the addition of salt as an adulterant in drug mixtures, while sodium and carbonate ions (qualitative chemical reactions for the carbonate ion using hydrochloric acid) indicate the presence of baking soda. Elements such as iron, manganese, molybdenum, lead, titanium, chromium, and boron are also detected in synthetic drugs seized from illicit laboratories. Selected statistical research results are presented in Figure 4.

The contamination of drugs with heavy metal ions is primarily attributed to the use of specific metal catalysts in organic synthesis, as well as potential leaching from metal equipment and their presence in raw materials, precursors, and chemical reagents. The elemental profile is therefore indispensable for confirming the presence of bulking agents within drug compositions and is useful for forensic comparation of samples.

4. Conclusion

Stricter controls over synthetic drugs have led to the emergence of masked mixtures in illicit trafficking. In Uzbekistan, a similar trend has been observed over the 2021–2025 period. The modification of synthetic compound matrices using readily accessible bulking materials – such as carbohydrates, mineral fertilizers, or industrial substrates – is a documented practice that artificially inflates total sample mass and causes a concomitant decrease in analyte purity. The inclusion of these synthetic or organic cutting agents typically reflects efforts to reduce formulation costs, mask the poor quality of the primary component, or alter the physicochemical profile and delivery characteristics of the resulting mixture.

This study highlights the effectiveness of a comprehensive analytical approach to the forensic examination of drug mixtures. Combining chemical and instrumental methods ensures target drug identification despite the presence of interfering components. The developed profiling approach extends beyond routine drug identification and provides an additional forensic intelligence tool. Comprehensive chemical profiling based on organic composition, synthesis-related impurities, adulterants, bulking agents, and trace elemental signatures enables comparative examination of seizures, supports the identification of common manufacturing sources, assists in reconstructing synthetic routes, and facilitates the detection of links between individual criminal cases. The proposed methodology has been incorporated into national forensic practice and may be adopted by laboratories involved in combating illicit drug trafficking.

References

1. *United Nations Office on Drugs and Crime. Terminology and Information on Drugs. 3rd ed. New York: United Nations Publication; 2016.*
2. *Cole C, Jones L, McVeigh J, Kicman A, Syed Q, Bellis MA. CUT: A guide to adulterants, bulking agents and other contaminants found in illicit drugs. Liverpool: Centre for Public Health, Liverpool John Moores University; 2010.*
3. *Stojanovska N, Fu S, Tahtouh M, Kelly T, Beavis A, Kirkbride KP. A review of impurity profiling and synthetic route of manufacture of methylamphetamine, 3,4-methylenedioxymethylamphetamine, amphetamine, dimethylamphetamine and p-methoxyamphetamine. ForensicSciInt.2013Jan10;224(1-3):8-26.*
4. *Zubrycka A, Kwaśnica A, Haczkiewicz M, Sipa K, Rudnicki K, Skrzypek S, et al. Illicit drugs street samples and their cutting agents. The result of the GC-MS based profiling define the guidelines for sensors development. Talanta.2022;237:122904.*
5. *United Nations Office on Drugs and Crime. World Drug Report 2023. Vienna: UNODC; 2023.*
6. *United Nations Office on Drugs and Crime. Recommended methods for the identification and analysis of synthetic cathinones in seized materials. New York: United Nations; 2016.*
7. *Scientific Working Group for the Analysis of Seized Drugs (SWGDRUG). Recommendations. Version 8.0, 2019 Jun 13. https://swgdrug.org, 2024 (accessed 24 Oct 24).*

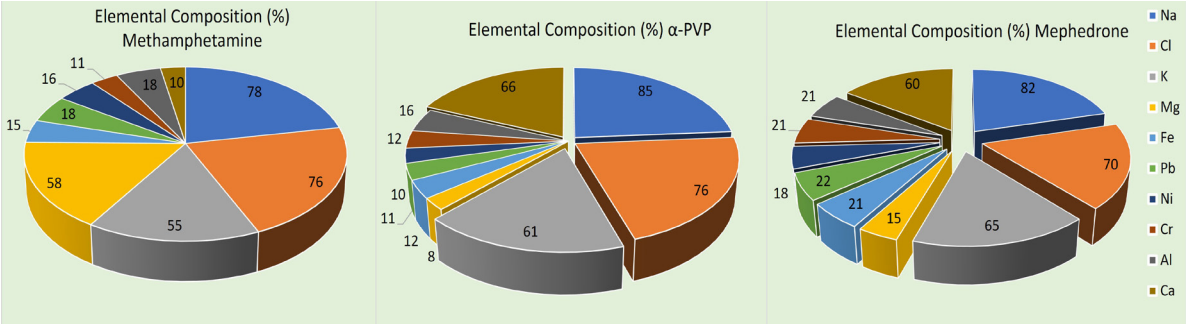


Figure 4. Average detection frequency of mineral components in samples by ICP-MS.

Cocaine Trafficking Using Counterfeit Coffee Beans: A Case Study from Hong Kong

Wing-sum Chan*, Hei-yu Maggie Tang and Shuk-mei Leung
Government Laboratory of Hong Kong Special Administrative Region, China
**Email: wschan@govtlab.gov.hk*

The global drug trafficking landscape continues to evolve, with criminal networks using increasingly sophisticated concealment and camouflage techniques to evade detection at borders and checkpoints. In the Hong Kong Special Administrative Region, the Government Laboratory (GL) is responsible for the examination of dangerous drugs seized by the Hong Kong Customs and Excise Department (C&ED) as well as the Hong Kong Police Force. This case study presents a trafficking case in which cocaine was concealed as counterfeit coffee beans.

In early 2025, GL received from C&ED a submission of brown granular solids resembling roasted coffee beans for dangerous drugs examination. A C&ED officer conducted a preliminary inspection of the solids using X-ray imaging and found a suspicious, inhomogeneous image. Visual inspection under microscope in the laboratory revealed a heterogeneous mixture containing genuine coffee beans interspersed with brown tablets meticulously crafted to mimic the size, shape, color, and surface texture of authentic beans (Figure 1). The coffee-bean-like tablets were slightly smaller than the coffee beans. In contrast, the shape and central groove of the coffee beans were more irregular, while those of the brown tablets were more consistent and uniform. Only upon close examination could the counterfeit tablets be distinguished from genuine coffee beans [Figures 2(a) and 2(b)]. The tablets were visually separated from genuine coffee beans for further laboratory examination.



Figure 1. Cocaine tablets (yellow arrows) mixing with coffee beans.



Figure 2. Photo of (a) cocaine tablets and (b) coffee beans.

Preliminary screening using the Marquis reagent, Scott reagent, and modified cobalt thiocyanate reagent – used to test for heroin (and methamphetamine), cocaine, and ketamine, respectively – showed no colour change when applied to the brown granular solids resembling coffee beans, indicating no positive presumptive results.

For further qualitative analysis for dangerous drug screening, ethanol was added to a sample of the ground brown solid. The ethanolic extract was filtered and analyzed using gas chromatography-mass spectrometry (GC-MS) (Figure 3) and high-performance liquid chromatography with diode array detection (LC-DAD) (Figure 4). The instrument conditions for GC-MS and LC-DAD are shown in Table 1 and Table 2, respectively. The GC-MS library search yielded matching scores of 99 and 96 for cocaine and caffeine, respectively.

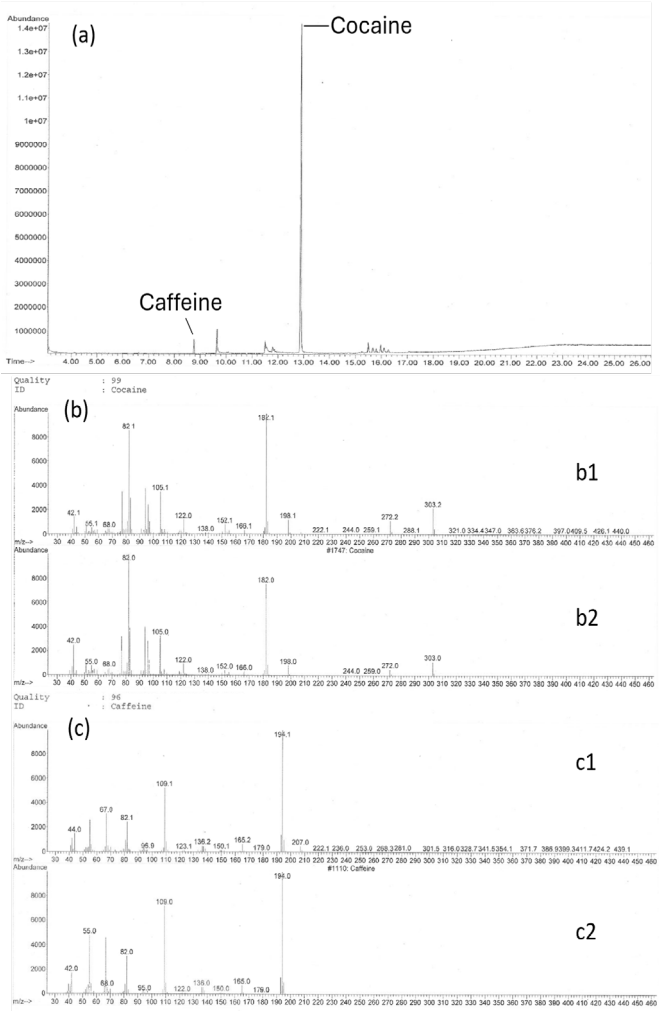


Figure 3. (a) GC-MS chromatogram of the brown tablets. (b) Library search result showing b1, sample mass spectrum at RT: 12.9min, and b2, mass spectrum of cocaine from SWGDRUG library version 3.13. (c) Library search result showing c1, sample mass spectrum at RT: 8.8min, and c2, mass spectrum of caffeine with SWGDRUG library version 3.13.

The retention time (RT) of cocaine was within 2% of that of the reference standard. In addition, the LC-DAD library search yielded matching scores of 990 and 998 for cocaine and caffeine, respectively. These analyses conclusively identified both cocaine and caffeine in the samples. Quantitative analysis by gas chromatography with flame ionization detector (GC-FID) was performed by dissolving the finely ground sample of the brown tablets in chloroform with hexacosane (C26) as internal standard (Figure 5). The operating conditions for the GC-FID are shown in Table 3. The chromatogram yielded two well-resolved peaks for cocaine and the internal standard, with no interference at their respective retention times. Cocaine content in the brown tablets was determined to be approximately 43% (w/w).

This case marked the first instance in Hong Kong where cocaine was concealed as counterfeit coffee beans deliberately mixed with authentic ones. The sophistication of this concealment highlighted traffickers' adaptation to heightened border security measures, necessitating enhanced vigilance by frontline officers trained to detect subtle inconsistencies in commodity shipments. Careful visual examination by frontline officers, supported by confirmatory laboratory analysis, is essential to detect concealed dangerous drugs. Close collaboration between the Government Laboratory and law enforcement agencies remains vital to counter increasingly sophisticated smuggling methods.

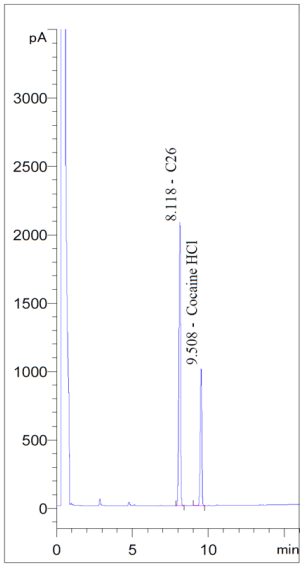


Figure 5: GC-FID chromatogram of brown tablets with C26 as internal standard.

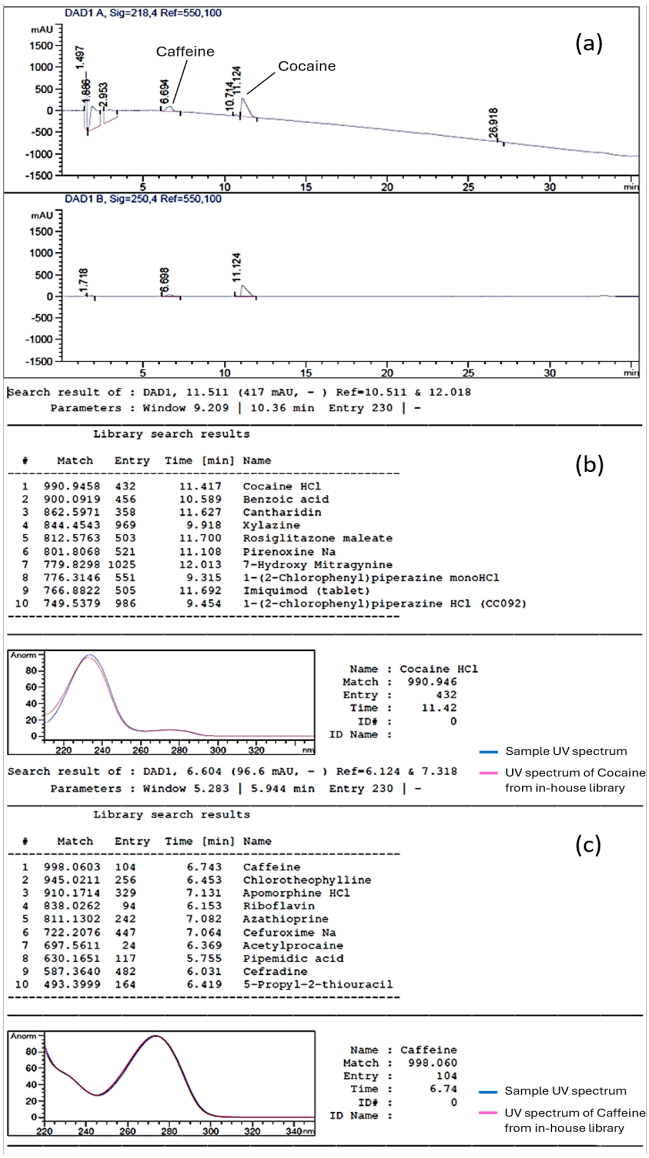


Figure 4. (a) LC-DAD signal at 218nm and 250nm respectively. (b) Library search result with overlaying spectra of sample at RT: 11.5min and cocaine from in-house library. (c) Library search result with overlaying spectra of sample at RT: 6.6min and caffeine from in-house library.

Table 1. The instrument conditions for GC-MS.

GC column:	Agilent HP-5MS-UI (30m, 250µm i.d., 0.25µm film thickness)
Carrier gas:	Helium 1mL/min
GC oven program:	i) 70°C initial and hold for 1 minute ii) 30C/min to 180°C iii) 7°C/min to 300°C iv) Hold at 300°C for 10 min
Injector temperature:	260 °C
Injector mode:	Pulsed split
Split ratio:	100 : 1
MSD setting:	
MS quad temperature:	150 °C
MS source temperature:	230 °C
Low mass:	50 amu
High mass:	450 amu

Table 2. The instrument conditions for LC-DAD.

LC column:	Agilent ZORBAX RX-C8 narrow bore RR5 µm (2.1 mm × 150 mm)
Mobile base:	Pump A: Acetonitrile Pump B: 0.01M Ammonium Formate (pH3)
LC gradient:	A : B = 10 : 90 to 80 : 20 in 30 minutes and kept for 5 minutes
Flow rate:	0.3 mL/min
Column temperature:	40 °C
DAD wavelength setting:	218 nm
Injection volume:	5 µL

Table 3. The instrument conditions for GC-FID.

Column:	HP-17, 10m × 530µm × 2.0 µm
Detector:	FID
Oven temperature:	230°C to 254°C (2°C/min)
Inlet temperature:	230°C
Detector temperature:	300°C
Injection mode:	Splitless
Carrier gas:	Hydrogen
Flow rate:	8 mL/min
Injection volume:	1 µL

Acute Cyanide Poisoning in Multiple Related and Unrelated Victims: A Seven-Case Forensic Report from Sri Lanka

Chathurika Nishani Kulasekara*, Yenali Hansika Madurawala, Ruwani Thakshila Elawelle Gedara and Lathika Sujani Hathurusinghe
Government Analyst's Department, Sri Lanka
**Email: nishi2kul@gmail.com*

1. Introduction

Cyanide is a highly potent, rapidly acting poison capable of causing death within minutes following significant exposure. Despite its well-recognized toxicity, cyanide compounds are widely used in industrial applications such as mining (particularly gold extraction), electroplating, and chemical synthesis, which increases the risk of accidental exposure as well as their involvement in suicidal and homicidal incidents [1,2]. Because of its availability and rapid lethality, cyanide continues to be a substance of toxicological and forensic importance. Exposure to cyanide most commonly occurs through ingestion of cyanide salts, such as sodium cyanide or potassium cyanide, or through inhalation of hydrogen cyanide gas, a volatile and highly toxic form. Dermal absorption is also possible. Clinical effects depend on the route, dose, and duration of exposure and range from headache and dizziness to seizures, cardiovascular collapse, and death [2,3].

The primary toxic mechanism of cyanide involves inhibition of mitochondrial respiration by binding with high affinity to the ferric ion (Fe^{3+}) in the enzyme cytochrome c oxidase, leading to cellular asphyxiation, multi-organ dysfunction, and death [1,4,5]. In forensic and clinical toxicology, blood cyanide concentration serves as a key diagnostic indicator in the assessment of suspected cyanide-related fatalities. Lethal concentrations are generally reported to range between 1–3 mg/L; however, significant interindividual variability exists, influenced by factors such as age, underlying health status, rate and route of exposure, and the timeliness of medical intervention [3,6].

2. Case History

This study presents the forensic toxicological investigation of seven suspected cyanide-related deaths in Sri Lanka, occurred between 28 December 2023 and 4 January 2024, under suspicious and potentially related circumstances. The first death was a religious male individual who was reportedly associated with advocating self-inflicted death as a means of achieving a favourable rebirth. After his funeral, four additional deaths occurred among his immediate family members. Subsequently, two additional deaths involving non-family individuals occurred. Forensic investigations and medico-legal findings of the cases indicated consistent features of acute poisoning and required a detailed toxicological investigation. Therefore, biological samples and scene materials were submitted to the Government Analyst's Department, Sri Lanka for comprehensive toxicological analysis.

Case 01 (Index case)

A 47-year-old individual, who was found deceased at his residence on 28 December 2023. From the scene investigation, two unidentified white and orange colour materials were recovered suggesting ingestion of a toxic substance.

Case 02

On 30 December 2023, four additional deaths were reported among the immediate family members of Case 01. Case 02, a 35-year-old female and spouse of Case 01, was found deceased alongside the bodies of her three children, with a white-coloured substance in close proximity. These preliminary findings suggested ingestion of a toxic substance consistent with that identified in Case 01.

Case 03-05

Cases 03, 04, and 05 involved children – a 9-year-old male, an 8-year-old male, and a 6-year-old female – who were found deceased at the same location as their mother (Case 02) and were suspected to have been poisoned by her.

Case 06

A 34-year-old male was found deceased in a lodging facility and a white substance apparently similar to that in previous cases, was recovered at the scene.

Case 07

A 21-year-old female undergraduate was found deceased at her residence. A white substance was recovered at the scene, and the circumstances were consistent with those observed in the prior cases.

3. Materials and methods

Analytical grade potassium cyanide (purity ≥96%) and sulfuric acid (purity ≥ 98%) obtained from Sigma Aldrich USA and ultra-pure water (Type I) were used to prepare standards, solutions and blank samples. For cyanide screening, benzidine–copper acetate reagent was prepared by freshly mixing equal volumes of 1% benzidine in 10% acetic acid and 3% cupric acetate solutions. Benzidine (≥98%) and acetic acid (≥99.8%) were obtained from Sigma-Aldrich, while cupric acetate (≥98%) was obtained from Loba Chemie.

Standard and working solution preparation

A stock solution of cyanide (1000 mg/L) was prepared in Type I water. A working standard solution of cyanide (100 mg/L) was then prepared by appropriate dilution of the stock solution with Type I water. From this working standard, a series of calibration standards were prepared at concentrations range of 2-40 mg/L by further dilution with Type I water.

Instrumentation

Cyanide analysis in suspected substances and biological samples was performed using an Agilent 8890 headspace-gas chromatograph coupled with an Agilent 5977B mass detector (HS-GC–MS). Separation was achieved on a GS-GASPRO column (60 m × 0.32 mm ID). Headspace oven, loop, and transfer line temperatures were set at 90°C, 92°C, and 95°C, respectively. A vial equilibration time of 10 min was employed before GC injection. Injection was conducted in

split-less mode. Helium was used as the carrier gas at a flow rate of 2.4 mL/min. The GC oven was initially held at 70°C for 2 min, then ramped at 20°C/min to 230°C and held for 8 min. The mass spectrometer was operated in electron impact (EI) mode. Elemental analysis of the orange colour substance was performed using Bruker M4 TORNADO X-ray fluorescence (XRF) scanner.

Method validation

The HS-GC–MS method for cyanide analysis was previously validated according to Eurachem guidelines for linearity, precision, limit of detection (LOD), and limit of quantification (LOQ) [7]. Selectivity and potential interference were also evaluated by analysing blank blood and blank gastric content. The same validated protocol was subsequently applied in the current investigation. A new calibration curve was established prior to analysis to verify instrument response and maintain analytical reliability.

Sample preparation

Aliquots of 1.0 mL of suspected blood samples were analysed alongside blank and cyanide-spiked blood controls. Similarly, 1.0 g portions of gastric contents were prepared and analysed with corresponding blank and spiked controls. All samples were transferred into 20 mL clear flat-bottom headspace vials (Restek, USA). Each vial was treated with 1.0 mL of 5N sulfuric acid to liberate hydrogen cyanide gas (HCN), immediately sealed with crimp caps, and then subjected to HS-GC–MS analysis. Samples yielding concentrations above the established calibration range were diluted with Type I water as necessary to ensure measurements fell within the validated analytical range.

Solid samples recovered from the scenes were initially screened for free cyanide using the Benzidine–copper acetate reagent. Presumptive positive samples were subsequently diluted with Type I water and acidified with sulfuric acid under the same conditions described above and analysed by HS-GC-MS for confirmation.

The orange-coloured solid recovered from Case 01 was further characterized using X-ray fluorescence (XRF) analysis to determine its elemental composition and support compound identification.

4. Results and discussion

Cyanide in the samples was released in the form of HCN upon the reaction with sulphuric acid in heated condition. The HCN was detected at the retention time of 8.3 min. Despite its high volatility, HCN adsorption interactions with the stationary phase, together with the extended length of the 60 m GS-GASPRO column, provided sufficient retention and separation from volatile matrix constituents. The resulting retention time of 8.3 min enabled clear resolution of HCN from potential interferences (Figure 1).

The linearity was evaluated using six calibration standards at concentrations of 2, 5, 10, 20, 30, and 40 mg/L, yielding a R^2 of 0.997. Method precision, assessed at a cyanide concentration of 10 mg/L, resulted in a RSD of 2.1%. The LOD and LOQ were determined to be 1.7 mg/L and 1.9 mg/L, respectively.

The blank blood and gastric content samples showed no peaks at the retention time corresponding to HCN, indicating the absence of matrix-related interferences. In addition to evaluation of the total ion chromatograms (TICs), extracted ion chromatograms (EICs) for the characteristic cyanide ion (m/z 27) were examined to further confirm analyte identification and method selectivity. No significant signals at m/z 27 were detected in the blank matrices, demonstrating that endogenous components of blood and gastric contents did not interfere with the detection of HCN.

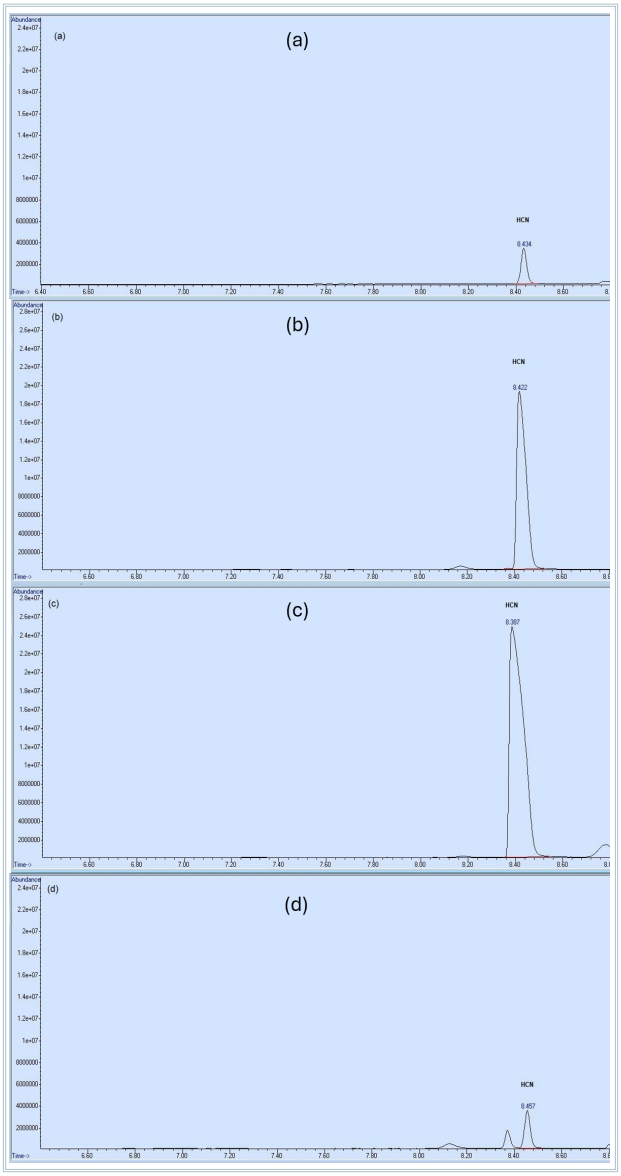


Figure 1. The total ion chromatograms of the case 02 (a) blood, (b) bile, (c) gastric contents and (d) urine.

Preliminary screening tests performed on the white solid samples collected from scenes associated with cases 01, 02, 06, and 07 yielded positive results for cyanide. These findings were subsequently confirmed using HS-GC-MS, establishing the presence of cyanogenic compounds at the respective scenes. The orange-coloured solid of case 01, released HCN upon treatment with sulfuric acid, was detected by HS-GC-MS. Elemental analysis using XRF identified potassium (K) and iron (Fe) as major constituents, indicating that the compound

is most consistent with potassium ferricyanide (Figure 2). Although relatively stable, this compound can liberate HCN under strongly acidic conditions, thereby representing a potential source of cyanide exposure.

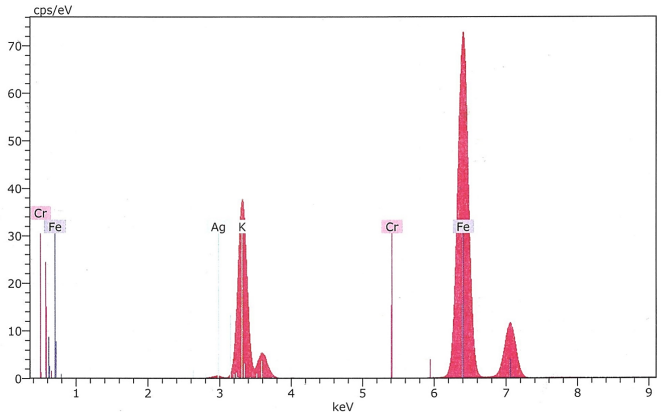


Figure 2. XRF scan spectrum of the orange colour solid found in the case 01.

Analysis of post-mortem blood samples from the seven cases revealed cyanide concentrations ranging from 3 to 161 mg/L (Table 1). According to the literature, concentrations exceeding approximately 1–3 mg/L are considered lethal, with higher levels frequently associated with rapid fatality [8]. Baselt reported that, among 32 fatal cases of cyanide ingestion, blood cyanide concentrations ranged from 0.4 to 230 mg/L, while in an additional 17 post-mortem cases, concentrations ranged from 0.6 to 185 mg/L [9]. In this context, the measured blood cyanide levels are clearly within or well above the fatal range, thereby confirming cyanide poisoning as the cause of death.

Table 1. The distribution of cyanide across different biological matrices (NA – sample not available; Detected – cyanide detected but present at a level below the LOQ).

Case No.	Blood (mg/L)	Urine (mg/L)	Bile (mg/L)	Gastric contents (mg/kg)
Case 01	161	NA	NA	NA
Case 02	14	15	155	503
Case 03	52	29	615	6068
Case 04	30	Detected	17	2027
Case 05	3	NA	NA	28
Case 06	21	Detected	Detected	428
Case 07	119	NA	8	2017

Analysis of gastric content samples from cases 02 to 07 demonstrated cyanide concentrations ranging from 28 to 6068 mg/kg. The markedly elevated concentrations in gastric contents strongly support oral ingestion as the primary route of exposure. This is further evidenced by the detection of cyanide in bile and urine in certain cases, indicating systemic absorption and distribution prior to death.

5. Conclusion

The combined chemical and toxicological findings provide consistent and compelling evidence of fatal cyanide poisoning, most likely resulting from oral ingestion of cyanogenic substances.

References

1. *Cyanide in drinking-water: background document for development of WHO guidelines. World Health Organization. Geneva: WHO; 2004.*
2. *Toxicological profile for cyanide. Agency for Toxic Substances and Disease Registry. Atlanta: ATSDR; 2006.*
3. *Cyanide: systemic agent. National Institute for Occupational Safety and Health. Cincinnati: NIOSH; 2011.*
4. *Facts about cyanide. Centers for Disease Control and Prevention. Atlanta: CDC; 2018.*
5. *Yadukul S, Venkataraghava S, Fathima T, Gaonkar VB. Fatal suicidal case of cyanide poisoning: a case report. J Forensic Toxicol Pharmacol. 2014;3(3).*
6. *Lischkova L, Pelclova D, Hlusicka J, et al . Severe suicidal self-poisoning with massive dose of potassium ferricyanide (III): hyperkalemia but not free cyanide may cause death. Monatsh Chem. 2018;149(9):1647–51.*
7. *Hathurusinghe LS, Karunarathne WDV, Priyadarshani HTT, et al. Forensic toxicological findings in death due to suspicious circumstances. TIAFT Bull. 2025;55(3):5–6.*
8. *Moffat AC, Osselton MD, Widdop B, Watts J. Clarke's analysis of drugs and poisons. 4th ed. London: Pharmaceutical Press; 2011.*
9. *Baselt RC. Disposition of toxic drugs and chemicals in man. 11th ed: Biomedical Publications, California; 2017:554-555*

92 institutions from 20 countries (as of September 2026):

Bangladesh	National Police DNA Profiling Laboratory
Brunei Darussalam	Department of Scientific Services
Cambodia	Narcotic Laboratory of Secretariat General of National Authority for Combating Drugs
China	Beijing Forensic Science Institute
	Criminal Investigation School, Southwest University of Political Science and Law (SWUPL)
	Department of Forensic Science (Department of Criminal Science and Technology), School of Investigation, People's Public Security University of China
	Drug Intelligence and Forensic Center of Ministry of Public Security
	* Forensic Appraisal Center of Zhongnan University of Economic and Law
	Forensic Science Center of Guangdong Provincial, Public Security Department
	Forensic Science Department of Judiciary Police, Macau SAR
	Forensic Science Division, Department of Fujian Provincial Public Security
	Forensic Science Division of the Government Laboratory of the Hong Kong SAR
	Gansu University of Political Science and Law, Key Laboratory of Evidence Science Techniques Research and Application
	Guangzhou Forensic Science Institute
	Identification Bureau, Hong Kong Police Force, Hong Kong SAR
	The Institute of Evidence Law and Forensic Science, China University of Political Science and Law
	Institute of Forensic Science, Fudan University
	Institute of Forensic Science, Dezhou Public Security Bureau
	Institute of Forensic Science, Hangzhou Public Security Bureau
	Institute of Forensic Science, Ministry of Public Security
	Institute of Forensic Science, Shandong Public Security Department
	Institute of Forensic Science, Shanghai Municipal Bureau of Public Security
	Institute of Forensic Science, Suzhou Public Security Department
	Institute of Forensic Science, Tianjin Public Security Bureau
	* Institute of Forensic Science of Xiamen Municipal Bureau of Public Security
	Nanjing Police University
	* Nantong Public Security Bureau Forensic Science Center, Jiangsu Province
	* Shaanxi Provincial Public Security Judicial Identification Center
India	Centre for DNA Fingerprinting and Diagnostics
	Directorate of Forensic Science, Himachal Pradesh
	Forensic Science Laboratory, Govt of NCT of Delhi
	National Forensic Sciences University, Delhi Campus
Indonesia	Centre of Indonesian Automated Fingerprint Identification System of the Indonesian National Police
	Department of Police Medicine - Centre for Medical and Health Services of Indonesian National Police
	Eijkman Institute for Molecular Biology (DNA Identification Unit)
	Forensic Laboratory Centre of Indonesian National Police Headquarters
	The Indonesian Association of Forensic Medicine-Medicolegal
	Laboratory of National Narcotics Board Republic of Indonesia
	Master Program of Forensic Science, Postgraduate School, Universitas Airlangga
Kazakhstan	Forensic Examinations Centre of the Ministry of Justice
Laos	Food and Drug Quality Control Center
Malaysia	CyberSecurity Malaysia
	Department of Chemisty Malaysia
	Forensic Investigation Unit, Enforcement Division of Royal Malaysian Customs
	Malaysian Communications and Multimedia Commission
	Malaysian Institute of Road Safety Research (MIROS)
	National Institute of Forensic Medicine, Hospital Kuala Lumpur
	Pharmacy Enforcement Division, Ministry of Health
	Royal Malaysia Police Forensic Laboratory
Mongolia	Mongolian National Institute of Forensic Science
Myanmar	Defence Services Medical Research Centre
Nepal	* National Forensic Science Laboratory
Philippines	Laboratory Service, Philippines Drug Enforcement Agency
	National Bureau of Investigation
	National Reference Laboratory for Environmental and Occupational Health, Toxicology and Micronutrient Assay, East Avenue Medical Center, Department of Health
	Natural Sciences Research Institute, University of the Philippines Diliman Quezon City
	Philippine National Police
Singapore	Corrupt Practices Investigation Bureau
	Health Sciences Authority
	Ministry of Defence
	Ministry of Home Affairs
South Korea	Daejeon Health Institute of Technology (Daejeon Health Sciences University)
	Department of Forensic Sciences, Sungkyunkwan University
	Graduate School of Forensic Science, Soon Chun Hyang University
	Institute of Forensic and Anthropological Science
	Korea Coast Guard Research Institute
	* Korea National Police University Police Advanced Institute of Science and Technology
	National Digital Forensic Center of Supreme Prosecutors' Office
	National Forensic Service
	Scientific Investigation Center of Korean National Police Agency
	Scientific Investigation Laboratory, Ministry of National Defense
	SJS Institute of Forensic Science & Medicine
Sri Lanka	Government Analyst's Department
	National Dangerous Drugs Control Board
Thailand	Central Institute of Forensic Science
	Central Police Forensic Science Division
	Department of Forensic Medicine, Faculty of Medicine Chulalongkorn University
	Department of Forensic Medicine, Faculty of Medicine, Siriraj Hospital, Mahidol University
	Division of Forensic Medicine, Thammasat University Hospital
	Department of Medical Sciences
	Faculty of Medicine, Chiang Mai University
	Human Genetics Unit, Department of Pathology, Faculty of Medicine Ramathibodi Hospital, Mahidol University
	Institute of Forensic Medicine, Police General Hospital, The Royal Thai Police
	Narcotics Analysis and Technical Service Institute Office of Narcotics Control Board
	* Forensic Medicine Department, Maharat Nakhon Ratchasima Hospital
	* Faculty of Medicine, Prince of Songkla University (PSU)
Timor-Leste	Polícia Científica de Investigação Criminal - Laboratório de Polícia Científica
Uzbekistan	Republican Scientific and Practical Center of forensic Medical Examination, Ministry of Health
	Republican Center for Forensic Examination under the Ministry of Justice
Vietnam	Forensic Medicine Center of Ho Chi Minh City
	National Institute of Forensic Medicine
	Vietnam Forensic Science Institute

* New Member Institute